Dissertations, Theses, and Masters Projects   Theses, Dissertations, & Master Projects

2024

A Methodology For The Visualization Of 3D Petroglyph Data As Applied To Rock Markings Of The Eastern United States

Matthew Owen Forcier
William & Mary - Arts & Sciences, forcier.matt@gmail.com

Follow this and additional works at: https://scholarworks.wm.edu/etd

Part of the History of Art, Architecture, and Archaeology Commons

A Methodology for the Visualization of 3D Petroglyph Data as Applied to Rock Markings of the Eastern United States

Matthew Owen Forcier

Virginia Beach, Virginia

Bachelor of Arts, College of William & Mary, 2020

A Thesis presented to the Graduate Faculty of The College of William and Mary in Virginia in Candidacy for the Degree of Master of Arts

Department of Anthropology

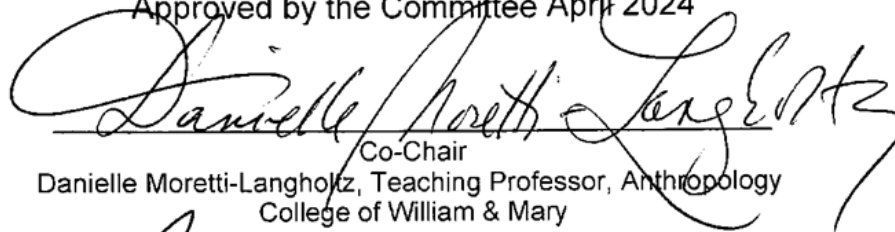The College of William and Mary in Virginia
May 2024

APPROVAL PAGE

This Thesis is submitted in partial fulfillment of
the requirements for the degree of

Master of Arts
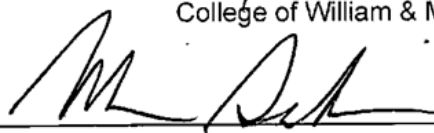
Matthew Owen Forcier

Matthew Owen Forcier

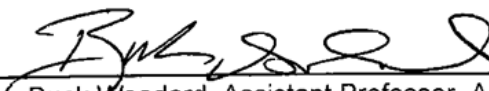Approved by the Committee April 2024

Co-Chair

Danielle Moretti-Langholtz, Teaching Professor, Anthropology
College of William & Mary

Co-Chair

Martin Gallivan, Professor, Anthropology
College of William & Mary

Buck Woodard, Assistant Professor, Anthropology
College of William & Mary

ABSTRACT

As a visual testament to the complexity of ancient peoples, rock markings have long captivated the public imagination. More recently, the archaeological field has witnessed a renaissance in rock marking scholarship as researchers increasingly recognize both the continued importance of these features to descendant communities and their potential to inform our understandings of antiquity. In the semiotic content of petroglyphs and pictographs, many archaeologists see an opportunity to access otherwise irretrievable details of past belief systems. Yet, attempts to engage with this content are complicated by the immense challenge researchers face in delineating the boundaries and details of rock markings. Sketches, charcoal rubbings, and – since the advent of photography – pictures of chalk-marked stones comprise just a few of the subjective recording methods applied to documenting these features. As a result, entirely different drawings often exist for the same petroglyphs, and from their widely divergent starting points scholars have unsurprisingly arrived at antipodal interpretations.

In the last couple decades, archaeologists have brought new technology to bear on this subject. Increasingly prevalent in the documentation of rock markings are three-dimensional recording techniques such as digital photogrammetry, LiDAR, and structured-light scanning. Despite a growing body of 3D spatial data, we still lack a comprehensive and objective methodology for making appropriate use of this new class of information. This study presents new techniques for leveraging the data potential of 3D petroglyph scans in the creation of objective visualizations of rock markings. It outlines and then demonstrates a process of uniform manipulations performed on 3D petroglyph data in CloudCompare, a free 3D modelling software, for the purpose of achieving improved visual contrast of rock carvings. It also evaluates some existing methods and tools for colorizing images on stone. The methodology offered here can contribute significantly to petroglyph research as it fulfills the need for a systematic route to increasing glyph clarity, yet does so in a more objective manner than traditional segmentation techniques. In this role, it has the capacity to make visible previously unidentified markings. The use of this process on a dataset primarily from the Eastern United States facilitated the discovery of unrecognized petroglyphs at known petroglyph sites. Moreover, this process may prove applicable to other archaeological problems, such as reading eroded gravestones.

TABLE OF CONTENTS

ACKNOWLEDGEMENTS

This work is dedicated to the countless minority communities disproportionately affected by the COVID-19 pandemic. Their inestimable loss offers a stark reminder of the inequalities we as a nation must work to correct.

LIST OF TABLES

LIST OF FIGURES

Chapter 1: Introduction to the Research

What was once a marginalized and neglected subject in mainstream archaeology is undergoing a promising resurgence. Today, tourists flock to publicly accessible rock marking sites (and at times trespass to observe private ones). Researchers the world over gather for interdisciplinary study of the same. Native nations commemorate and engage with spaces that record histories longer than written record. But if we ask an individual what they see, the answer varies depending on the person. If we ask what is truly there – where the markings begin and end – the answer becomes more complicated still. Key to any science is the ability to make accurate, empirical observations and then to accurately convey those observations to a wider audience. Simple, diagrammatic recordings of images on stone have remained elusive, however, due to both the limited technological means previously at the archaeologist's disposal and inherent complications posed by this category of feature. Erosion distorts and hides, natural features camouflage and deceive, and lighting conditions reveal or conceal. This is to say nothing of the inherent biases of the researcher which we must still contend with. All of these factors challenge the detection and adequate recording of rock markings using the most accurate and objective means until now available.

This work intervenes in the standard ways of depicting petroglyphs and offers a different path forward. This first chapter presents the background of the study, specifies the problem it addresses, describes the research design, and outlines the aims of the work. The greater portion of this chapter is then dedicated to reviewing the relevant literature. The second chapter looks at the experiments and evaluations conducted in the development of a methodology, reviews the immediate results, and applies the developed methodology to a brief case study. The third and final chapter summarizes my efforts and reflects on the findings. It additionally discusses insights from this research

as well as their implications for the field, lastly providing recommendations for future research.

Background of the Study

It would be helpful to first describe some developments in archaeological research on petroglyphs which had implications for the conceptualization of this study. This work was conducted at a time when the archaeology of rock markings is in flux. Today, a burgeoning interest and awareness of rock-borne imagery has garnered renewed attention from academia (David and Wilson 2002; Diaz-Granados and Duncan 2004; McDonald and Veth 2012; Gillette et al. 2014; Agnew et al. 2015; Stebergløkken et al. 2015; Diaz-Granados et al. 2018; Nash and Mazel 2019; Moro Abadía and Porr 2021; Davidson and Nowell 2021). The study of rock-borne imagery is increasingly being recognized for its potential to meaningfully expand our knowledge of prehistoric Indigenous cosmologies and cultural landscapes, as well as the opportunity to perform research that resonates with Native peoples and attests to both continuities and ruptures in the wake of colonial processes.

The willingness of professional archaeologists to seek out, record, and interpret images on stone still constitutes a relatively recent development in the United States, spurred on by the discoveries of avocational researchers and Section 106 work, growing recognition of the need to protect and preserve these cultural resources, and the political and cultural resurgence of Native American nations (Beaudoin and Eagle 2009; Whitley 2013; Hale 2010; Associated Press 2021; Hanson et al. 2022). Many of the latter groups have assumed archaeological responsibilities on their lands through Tribal Historic Preservation Offices and today count among their ranks Native archaeologists who are eager to reengage with ancestral places from which their communities have frequently been alienated and dispossessed (Colwell-Chanthaphonh et al. 2010; Nicholas 2014; Dring et al. 2019). In the past authors have frequently shoehorned rock markings into a

concocted binary opposition between the functional and the religious, but non-native researchers have in recent years beneficially expanded their interpretations, such as by exploring how contemporary descendant communities engage with ancestors through rock-borne imagery (Brady 2016).

Yet, the many new directions being taken in this area of study are juxtaposed by the dearth of available data, and in rushing to interpretation many authors have sought to run before we can walk. Difficulties dating, objectively recording, and even finding petroglyphs and pictographs have hampered our efforts to study them. This second point is of critical importance to any discussion of meaning. To analyze the semiotic content of glyphs, we must first establish and delineate in a scientific manner the actual boundaries of human manipulation on a stone. At many sites, the ambiguity of markings exacerbates interpretational division. Authors disagree over the actual composition of the petroglyphs and from these divergent starting points arrive at increasingly disparate interpretations.

Archaeologists are now more actively seeking out and documenting sites, and in doing so they are applying new technologies to the task. The recent use of three-dimensional scanning represents one of the most promising developments in many years for the objective baseline documentation of these features. Armed with advanced equipment like laser scanners, archaeologists daily capture millions upon millions of points of three-dimensional data. Ultra-precise and hyper-accurate, these tools generate data-rich recordings of surfaces, often paired with high resolution imagery, all in a neatly packaged container. However, even with impressive 3D models allowing us to study petroglyph sites from the comfort of our labs, the way in which we represent the petroglyphs themselves has changed little. Whether by freehand sketching in the field or digital tracing in the lab, common procedures for representing petroglyph content are still rife with subjectivity and tedious manual differentiation. Despite the growing prevalence of 3D scanning in the documentation of rock markings, still absent are established

3

methods for realizing the full potential of this data. I perceive then a clear gap in existing knowledge which may be remedied by this study, or more aptly by the product of this study: a simple, effective, and objective process for visualizing petroglyphs. The development of such a process also offers an opportunity for its inauguration on a dataset primarily from the Eastern United States. With this small contribution I hope to attend to and moreover bring attention to a neglected region in rock marking scholarship.

Statement of the Problem

Archaeologists increasingly recognize and apply 3D recording of rock markings as a best practice in documenting and managing these sites. Yet, after the work is complete and the scanners stowed away, we often lack a route to making use of the data for answering basic questions about the extent and content of images on stone. Researchers still require a means for systematically, consistently, and objectively visualizing the petroglyphs found in these recordings. In the absence of clear evidence with which to make authoritative statements about petroglyph content, professional archaeologists are hampered in their efforts to combat the pseudoscientists, conspiracy theorists, and misguided avocationalists who bend these images to their will and implicate them in revisionist histories that disproportionately harm minority communities. There exists a clear need for a method which can leverage the potential of three-dimensional spatial data in order to improve our knowledge and enhance our stewardship of such sites, as well as aid us in dispelling neocolonialist propaganda. Filling this need constitutes the primary purpose of this research.

Research Design and Goals

This study essentially engages in a form of evaluation research. It seeks to develop a new instrument which may be applied by researchers for the manipulation of three-dimensional data. More specifically, this instrument is a straightforward methodology for the colorization of petroglyphs in 3D modeling software. This work may

be best described as quasi-experimental: It attempts by trial and error to establish a cause-and-effect relationship between a series of operations and the visual contrast of petroglyphs in a 3D scan. By this means, it aims to develop, evaluate, and enhance the effectiveness of a process for achieving clear colorizations of images on stone. It also goes further in testing the developed approach on a regional dataset. The state of the field and nature of the subject however prevent the complete elimination of confounding variables. Similarly, trials could not be feasibly randomized.

Individual trials were generally conducted according to a one-group pretest-posttest research design, with the visibility of petroglyphs appraised before and after an intervention. These trials iteratively guided development to culminate in a process for maximizing petroglyph visibility. Appraising the ideal visualization of rock markings however is inherently subjective. This task is also not readily quantifiable; though a numerical category score could be applied to each visualization, this would only belie the qualitative nature of the data. Additionally, the routes to achieving visualizations traversed here produced customizable display ranges as opposed to singular images, and this complicates attempts at direct comparison of the results. Where possible, I temper this subjective assessment with comparison to what Seidl (2016:24) refers to as *the ground truth*: the expert manual segmentations generated by professional documentation of sites, which can help corroborate the markings revealed in this work. I hold the site plan or diagram, simultaneously depicting all anthropogenic features in their spatial and environmental context, as the ideal toward which we endeavor in working with 3D petroglyph data.

Overview of Petroglyph Studies

From some of the earliest colonial encounters in North America, Native American practices of pictorial communication and commemoration have attracted the attention of outside observers. Often, observers remarked upon rock markings in passing, as

curiosities, or tangentially in the context of some other purpose for writing (Beverley 1705:44; Joutel 1714:164-165; Morse 1802:672-673; Hanna 1911:179; Galbreath 1921:84-85). If and when they were recorded, it was frequently by freehand drawing that poorly reflected the reality of the imagery. The desire to accurately document rock markings grew in tandem with a fledgling preservation ethic during a period of salvage archaeology in the early twentieth century. The tools available for accurate documentation, however, had largely remained the same: sketching, tracing, frottage, and photography, the latter often preceded by the application of chalk for color contrast.

Antiquarians involved in recovering the Bald Friar petroglyphs from the Susquehanna River had noticed in 1929 that chalking petroglyphs was fraught with error. Observers obtained variable results "in accordance with their varied opinions," the cautious recording of some juxtaposed by the carefree approach of others (Anon. 1929:7). Working with the limited evidence of now obliterated sites, researchers today often take for granted that photographers were even attempting to accurately portray the carvings in their images. Some, it seems, were more interested in a photograph they would be happy with: "Others have sought only to obtain pretty pictures, and to obtain effects have added to the outlines" (7). The recognized fidelity of taking impressions from stones is undoubtedly why Baer, Cadzow, and others went to the great pains of making casts of petroglyphs which could not be removed. Smith (1926) experimented early on with making cement casts of rock markings, which not only made more durable replicas but allowed for the imitation of the rock's original color and texture by changing cement composition. While this allowed for accurate documentation of a rockface as a whole, it did little to help delimit the markings themselves.

Throughout the years this fundamental problem remained a constant thorn in the side of petroglyph scholarship. Steward (1937) recognized that rock-borne imagery, especially when highly eroded or abstract, proved extremely vulnerable to the

6

subjectivity of the observer. He enumerated the challenges in recording petroglyphs objectively, noting the mistaken identification of petroglyphs in natural features due to things like differential weathering, lichen growth, and peculiarities in the stone's composition. More importantly, he remarks on the limitations of accurately documenting even genuine petroglyphs using current technology, as the necessity of chalking to create visible contrast for a photograph "introduces a real possibility that the person will chalk so as to idealize…One tends to record what he thinks the petroglyph is intended to be, not what it really is" (1937:411). These difficulties exacerbated the interpretational malleability of images on stone, further enabling pseudoscientific claims and fringe archaeology. Steward lamented, "It is all too easy for a person bent on proving a thesis to read into [rock markings] whatever he desires and to find any shapes he seeks" (408). While practical technical limitations prevented the objective discernment of petroglyphs from natural rock, this was compounded by the absence of any real guidance on systematic recording procedures.

Recognizing limitations in recording, scholars attempted to improve methods and critically sought to standardize data collection. Fenenga (1949:2), inspired by Steward's systematic treatment of the topic, offered a form "designed to facilitate the complete and accurate recording of data" by standardizing criteria and categories and setting a minimum level of information to collect. It also prescribes the collection of necessary supplementary material, and Fenenga details steps and best practices for photographing, sketching, and tracing petroglyphs (4-5). Later authors proposed minimum recording standards according to explicit criteria. The American Committee to Advance the Study of Petroglyphs and Pictographs was formed in 1979 and, synthesizing the expertise of its roughly eighty members, weighed in on best practices for recording rock markings (Swartz 1980, 1981). Though unable to universally condone any one recording method due to the highly contextual nature of this judgment, they

disavowed chalking in any form and cautioned about the negative impacts recording can have on sites. At the same time, there were limits to the practical utility of their guidance.

The committee assumed the average archaeologist would have the knowledge and expertise to distinguish the minute differences in "wear surfaces" (i.e., different manners of petroglyph and pictograph creation) and "superpositions" (i.e., the placement of rock markings over one another) (1981:94). While apparently a simple task, accurately identifying the superpositional order of markings is often deceptively complex. Some of the committee's instructions are certainly easier said than done, such as the imperative to "avoid interpretive preconceptions" (95). Various scholars (Bain 1971; Clewlow and Wheeling 1978; Loendorf, Olson, and Conner 1988; Sanger and Meighan 1990; Bock and Bock 1991; Loendorf et al. 1998) answered the deficit of practical resources with detailed recording manuals for rock markings. While archaeologists sought to standardize and set expectations for recording, the methods of recording at their disposal remained largely the same. Researchers still lacked tools to enhance petroglyph visualizations, while basic theoretical issues like the subjectivity of the recording process went unresolved.

In the early 2000s, new techniques arrived on the scene. With the maturation of the personal computer, some were quick to seize upon the potential applications to archaeology. The digital enhancement of photographs in particular shone as a method of making rock markings more visible while crucially allowing this work to take place in the lab rather than the field. With their sensitivity to color manipulation, pictographs were often subjected to this treatment (David et al. 2001). Clogg, Díaz-Andreu, and Larkman (2000) used a threshold filter to create binary images separating paintings from their background. Almost two decades later, Wang et al. (2019) apply an essentially similar process to good effect. Yet the digital enhancement of pictographs may have reached its apex in Harman's (2005) decorrelation stretch software (DStretch), which has become

an industry standard tool for enhancing highly eroded rock paintings (McDonald et al. 2016; Simek et al. 2019). Work on further enhancing pictograph visualizations continues, such as in the application of multispectral imaging (Fredlund and Sundstrom 2007; Pereira Uzal 2015; Zainuddin et al. 2019) and other tools (Andrews and Brink 2022) alongside DStretch. Though these methods are sometimes applied to petroglyphs, they are generally not effective. Charles, Castilla, and Bodenstein (2022) have even called for portable particle accelerators to be applied to the study of rock markings and suggest paths for the development of such a device based around Particle Induced X-ray Emission (PIXE). They report that elemental mapping of the kind that revealed hidden portraits in the works of Van Gogh and Degas might offer a way of seeing pictographs which exist only in trace amounts or are obfuscated by fouling like graffiti and dust.

Work with petroglyphs has taken a slightly different route. Around the same time that digital image enhancement began gaining traction, early applications of 3D recording also appeared. Cooper (2000) demonstrated the utility of photogrammetry in cooperation with digital representation, producing not only digital outlines of petroglyphs but also colorized contour models of the three-dimensional data they generated. Darvill et al. (2000) likewise digitally traced petroglyphs after recording sites with photogrammetry and laser scanning. Since the inception of 3D scanning, it has been applied to recording rock-borne imagery with increasing frequency. While there are a few ways of capturing three-dimensional data, documentation through laser scanning (Doering and Collins 2012, 2013; Kirk 2013), photogrammetry (Simpson et al. 2004; Rowan and Hill 2014), or both (Riveiro et al. 2011) remain the most popular options. Yet, despite the 3D character of the new datasets being generated, the way that petroglyphs are depicted has remained largely the same: manual delineation. For example, Landon and Seales (2006) made use of the interactive lighting parameters available in a 3D

simulated environment, but still ultimately used this to inform the manual highlighting of the glyphs they perceived.

While the complementary integration of digital drawing and 3D data has a place in archaeology more broadly (Kimball 2016), I question whether continuing the manual creation of 2D drawings from 3D datasets (Urcia et al. 2018) truly realizes the potential of this technology. I do not intend to single out any one researcher, for this behavior is not limited to an individual. Even the most revered academics in this field are prone to dutifully collecting 3D data, only to make simple, subjective digital drawings from it (Simek, Alvarez, and Cressler 2022). Of course, any well-researched, productive petroglyph scholarship is to be encouraged; but we may still seek a better path. Lee and Hyder (2009) have discussed additionally the fallibility of tracing from photographs, advocating careful and time-consuming manual recording directly at the site. Of course, Steward's ghost will attest that this is not the panacea we seek.

Bai et al. (2023) have achieved impressive segmentation of petroglyphs without 3D data at all, instead using a Gaussian loss algorithm for machine learning on high resolution images. Seidl (2016:49-65) previously applied an automatic segmentation algorithm to photographs of petroglyphs, approaching the problem as pixel classification. Seidl pointed out, however, a key issue with the use of images which is just as applicable to Bai et al.: they are left at the mercy of their lighting. He writes that "the main disadvantage of using photos for segmentation is the dependency on the lighting situation during acquisition" (6). The appearance of petroglyphs can vary greatly depending on direction and intensity of lighting, and this is another reason to critique all of the aforementioned studies which use imagery as the primary basis for delineating rock markings.

In contrast, some scholars lean heavily into the complete command of lighting offered by 3D modelling software as a means of avoiding this problem. Zachar (2017)

gives a detailed explanation of the use of different shaders with 3D models for the visualization of detail on cultural resources. Some of the most common shading techniques include ambient occlusion and radiance scaling, often in unison with basic shading lighting. Ambient occlusion simulates general illumination and essentially replicates the shadowing caused by parts of an object blocking ambient light (2017:91). Radiance scaling is adept at revealing concavities and convexities as it modifies light intensities to correlate with surface feature variations (90). Vilas-Estevez, Vázquez-Martínez, and Carrero-Pazos (2016) specifically applied radiance scaling as an alternative to traditional petroglyph tracing, arguing that it improved both visibility and objectivity. Mark and Billo (2021) have reiterated the usefulness of this lighting technique.

Others have implemented these methods into workflows for generating pseudo-traditional tracings by applying automatic vectorization to images made with radiance scaling (Gil-Docampo, Peña-Villasenín, and Ortiz-Sanz 2020). It is no surprise then that Valdez-Tullett and Figueiredo Persson (2023:14) recently described radiance scaling as "one of the most popular rendering options for rock art visualization due to its potential to clearly and easily enhance depth variations, concavities and convexities across a 3D model." Though attempting to make better use of the models as something other than proxies for firsthand observation, these studies still ultimately limit themselves to the visual appearance of the stone. That is, while freeing themselves from the mercy of natural lighting conditions, they remain constrained by *what light can do*, even in a virtual environment.

Many have thus followed the flawed but familiar models of traditional recording methods, changing only the medium of their tracing and sketching. A growing number have exploited their ability to control the virtual environment, but few have unlocked the real power of topography in engaging with this data. Ironically, a breakthrough appeared

11

early on with the application of methods from GIS frequently used in landscape

archaeology. Trinks et al. (2005) essentially convert a 3D model of a stone bearing

petroglyphs into a Digital Elevation Model (DEM). The color at a given point is thus not

assigned by lighting conditions (real or virtual) but by a quantifiable elevation value over

a hypothetical plane. What makes this contribution even more significant is their

development of a means for showing *local* surface variation. Trinks et al. realized that

the extreme curvature of some rocks made the overall elevation poorly suited to show

petroglyph details. By homing in on the small variations at the surface level, better

visualizations could be achieved. They offer an explanation of their method:

> "The local (or relative) elevation…may be achieved by applying a spatial high-pass frequency filter to the 3D point data and removing the low frequency (long-wavelength) curvature of the natural rock surface, thereby flattening the model of the rock artificially. The surface may then be coloured according to elevation... since the remaining elevation differences are solely due to the short-wavelength, artificial markings or natural fissures in the rock surface." (2005:136)

One strength of this approach is that the only subjective input of the researcher is their

control over the color scale parameters when selecting the upper and lower limits of the

colorization. The other, more obvious strength is the exceptional visualization achieved.

This method surprisingly has not proliferated despite its effectiveness and unassailable

objectivity. Brink (2007:89-92) does similarly measure distance against a hypothetical

flat plane to create a colorization of replica petroglyphs, but settles for colorizing global

elevation, perhaps due to the stone already being relatively flat.

Jalandoni and Kottermair (2018:585) have carried on the use of GIS tools for

visualizing petroglyphs but take a different approach. They generated a DEM from their

3D model and then applied a hillshade effect to help visualize the markings. They found

however that the hillshade created an unacceptable bias due to the artificial illumination

angle. This same critique can be levelled at practically any use of real or artificial

shading to segment petroglyphs. Their more promising innovation is their approach to

capturing local elevation by way of a topographic position index (TPI) algorithm, which

operates thus:

> "The TPI compares the elevation of each pixel of a DEM to the mean elevation of
> pixels in a specific surrounding area, providing a relative position...a TPI is
> commonly used to classify a landscape into valleys, slopes, and ridges or to
> detect anomalies such as depressions..." (581)

The TPI algorithm can be applied through a simple tool in ArcMap, and with it Jalandoni

and Kottermair were able to identify almost twice the number of engravings compared to

manual tracing, as well as correct inaccuracies in the latter. Jalandoni and Taçon (2018)

apply these same methods with equal success.

Other experimental uses of algorithms for enhancing petroglyphs appear

arguably less successful. Wojcicki, Korga, and Milosz (2022) developed an algorithm

which takes cross-sections of the point cloud and progressively removes extreme points

to reveal anthropogenic depressions. At this stage in their research, however, the

product is visibly inferior to other enhancement methods covered. In response to his

critiques of segmentation algorithms using images of petroglyphs, Seidl (2016:67-83)

also attempted the automated segmentation of petroglyphs based on 3D properties. A

computational representation of a given point is extracted based on the point's

neighborhood, following a set rule, and these representations are then compared to

identify similarities and, ultimately, to classify them. This classification was done by

machine learning and classified points as either engraved or natural rock surface. The

technical nature of Seidl's work is difficult to describe and I likely oversimplify it. In any

case, Seidl found that segmentation of petroglyphs by this 3D descriptor-based method

was prone to false positives and performed much worse than expected despite

excessive computation times.

Seidl's work instead achieved its best segmentation when the machine

classification used an image-space approach with an "enhanced depth map" (2016:75-

76). The process for making this enhanced depth map is outlined in Zeppelzauer and Seidl (2015) and has since been applied in Horn, Pitman, and Potter (2019) and Horn et al. (2022). Besides Jalandoni and Kottermair's use of TPI, this colorization process is probably the most successful method currently being applied to the problem of petroglyph visualization. This success is not entirely shocking, since the process is identical in premise to the aforementioned method outlined by Trinks et al. (2005). In Zeppelzauer and Seidl's revision, they simply smooth a depth map "by convolution with a two-dimensional Gaussian-shaped filter" to approximate the global curvature and then subtract this from the original to see the microtopography in what they refer to as a "compensated depth map" (2015:2846). This is what Trinks et al. refer to as a relative elevation model. Horn et al. (2019:4) borrow from landscape archaeology in referring to this method as "local relief modelling (LRM)," but the process is the same. Horn et al.'s (2022) major contribution is the packaging of this technique in a simple software, Ratopoviz (Rock Art Topographic Visualization). I discuss this software in greater detail in the next chapter.

Beyond these studies there have been few other routes explored for improving glyph visibility. Mark (2017) outlined a "digital rubbing" method that is thankfully less traditional than it sounds, using Poisson Reconstruction on a point cloud to create a contrasting visualization against the backdrop of the original mesh. DeGayner, Rodriguez, and Moss (2019) describe a unique process involving the manual selection of points to create "a faceted surface that generally approximates what the surface would have looked like prior the creation of the petroglyph" (2019:40). They then run an algorithm to calculate the difference between their simulated, pristine rockface and the actual scan. These last two works offer a point of departure for my own research as I seek to make use of the latent potential of 3D petroglyph data. Together with popular shading filters like radiance scaling and the promising method originating with Trinks et

14

al., we have the raw material for a survey of existing colorization strategies and a

starting point for further experimentation. Moreover, we have an opportunity to explore

some of these state-of-the-art approaches with petroglyphs of the eastern United States,

where this work has not been applied.

Chapter 2: Experimentation and Results

The following section of this work discusses experiments conducted in the development of a methodology, results of the experiments, and brief analysis of those results. While somewhat unconventional, the choice to combine these discussions came organically consequent the iterative nature of the work, which caused these conversations to become inextricably intertwined. Since the aim was to develop, by trial and error, archaeological methods and workflows for the analysis of three-dimensional petroglyph data, the manner of conducting each trial and the product obtained informed the methods used in subsequent trials. Moreover, it appeared necessary to address the many possible combinations and substitutions of steps in the production of a streamlined process. This was especially true with regard to conducting a cost-benefit analysis of alternative methods which resulted in similar products.

Recognizing also the widely variable needs of researchers working in many different contexts, it became important to offer for consideration any method which proved productive. Indeed, as many different procedures generated encouraging results, the research question shifted. Rather than identifying a singular, superior process, the task evolved into identifying what processes best suited specific contexts. Of the many workable combinations of procedures, in what settings did some combinations particularly excel? Where two options initially produced the same results, did they lead to any divergence in the final product after other steps had been applied? Where the final products were the same, could one combination of steps result in an overall more efficient or less resource-intensive workflow? These factors thus complicated a compartmentalized organizational scheme, which by truncating these discussions would belie their interconnectivity.

This work employed diverse three-dimensional datasets in terms of geographical distribution of sites, data quality, and file format. More specifically, the datasets

consisted of 3D point clouds and point clouds with associated meshes in .ply, .obj, and .stl formats which were generated by TLS and photogrammetry. The petroglyph sites represented in these files are CHOH-3 and CHOH-26 (or by its state trinomial, 18MO0134) of the Chesapeake and Ohio Canal National Historical Park, the Pimmit Run Petroglyph (44FX3079) of the George Washington Memorial Parkway, the Octoraro Creek Petroglyphs (18CE0398), Dighton Rock (BRK.902), and Judaculla Rock (31JK0003). The high-resolution 3D models of the CHOH and GWMP petroglyphs and the scans from which they are derived were created by a team from the University of South Florida using a Surphaser 25HSX laser scanner for sub-millimeter accurate recording (Doering and Collins 2012; 2013). The remaining files are publicly available online and are more variable in their resolution and accuracy.

The model of a boulder bearing petroglyphs from Octoraro Creek and two scans of Judaculla Rock were found submitted by their various creators to a community-based, 3D model webhosting service called Sketchfab. While found hosted on the website of a frequently pseudoscientific avocational archaeology group, the partial scan of Dighton Rock was originally produced in 2015 by Stephen Wilkes, former Director of 3D Services and current Chief Innovation Officer at Feldman Geospatial, a reputable land surveying company. Regardless of who created it, sourcing data from pseudoscientists elicits reasonable concern about validity and provenience. This predicament, however, highlights an unfortunately frequent issue in petroglyph research: neglected by professional archaeology, valuable data is instead gathered or hosted by enthusiasts who at times occupy fringe positions. Out of necessity, archaeologists employ the work of and even at times ally themselves with these groups and risk legitimizing unscientific interpretations. The decision to include such data was therefore carefully weighed against the potential research benefits.

With regard to how detailed the 3D models are, the juxtaposition between meshes is made apparent in **Table 1**, which gives a summary of the files involved in this investigation and some of their relevant statistics. All of these files are 3D models with associated point clouds. The point clouds can be thought of as a raw material created during the scanning process, consisting of a 'cloud' of points in space. What we call a 3D model is a mesh created from these points. This mesh is a solid surface made up of triangles, with each of the triangles formed by grouping three points. In their role creating the triangles and thus the geometry of a mesh, these points are called vertices. A key consideration for working with rock markings then is not only the *accuracy* of each point recorded (i.e., how trustworthy is the scanner's measurement) but also the *number* of points recorded, since fewer points mean larger gaps in our information about a surface, fewer triangles to reconstruct that surface, and thus less detailed reconstructions.

While file size and the number of vertices and triangles are generally good indicators of the resolution of the scan, a perhaps more useful metric would be the point density relative to actual square footage of rock represented. This would offer a comparable statistic for appraising the quality of large and small area scans, which must be considered in concert with measurement accuracy. It was initially not feasible to provide such a metric here, however, given limited site documentation and uncertainties in the conversion of 3D model distances to a real-world unit of measurement. In any case, the compiled dataset offered a range of precision levels to experiment with, including two scans from the same site with a striking contrast in recording specificity. A mesh may also have a texture attached to it, referred to in the table as a 'skin,' which is simply an image that is mapped onto the mesh surface. Most of the meshes used here include a texture, giving us photorealistic representations of the glyphs. Many 3D scanners today include high definition image capture and texture creation as a standard part of the recording process.

Table 1. 3D Scans of Petroglyph Sites Employed in the First Portion of This Study[1]

Name	Site No.	Location	Source	Triangles	Vertices	Skin	Size	File	Equipment
CHOH-3	None	[Withheld]	Doering and Collins 2012, 2013	48,029,049	24,241,975	1	942.0 mb	.ply	Surphaser 25HSX (TLS)
CHOH-26	18MO0134	Montgomery County Maryland	Doering and Collins 2012, 2013	4,550,717	2,280,258	1	120.0 mb	.ply	Surphaser 25HSX (TLS)
Pimmit Run Petroglyph	44FX3079	Fairfax County, Virginia	Doering and Collins 2012, 2013	2,846,539	1,433,999	0	135.0 mb	.stl	Surphaser 25HSX (TLS)
Octoraro Creek Petroglyphs	18CE0398	Cecil County, Maryland	Brooks 2017 [sketchfab.com]	1,000,000	502,307	1	46.7 mb	.ply	[Not given]
Dighton Rock	BRK.902[2]	Bristol County, Massachusetts	Wilkes 2015 [neara.org]	441,402	221,739	0	21.0 mb	.stl	FARO [model not given] (TLS)
Judaculla Rock	31JK0003	Jackson County, North Carolina	RLA Archaeology 2017 [sketchfab.com]	15,134	7,802	1	2.7 mb	.obj	[Not given]
Judaculla Rock	31JK0003	Jackson County, North Carolina	Loubser and Logan 2017 [sketchfab.com]	2,165,669	1,086,538	1	123.0 mb	.obj	iPhone 6 Plus (Photogram.)

[1]Triangles, vertices, and file sizes given reflect the values after scans have been cleaned of any erroneous or irrelevant points (e.g., debris).
[2] Massachusetts Historical Commission Property ID; unknown if the stone or its original location possess an archaeological site designation.

While still becoming acquainted with the selected datasets and developing a familiarity with 3D modeling software, the author fortuitously stumbled upon a relevant project conducted for Pecos National Park which was detailed in a post to the park's social media. Archaeologists for the park had recorded a petroglyph panel using structured-light 3D scanning methods and then manipulated the resulting 3D model so as to enhance the petroglyphs' visibility. This work was previously published in *Archaeology Southwest* (DeGayner, Rodriguez, and Moss 2019) but the particular details of the enhancement process are omitted. After an inquiry to Pecos National Park, I received more details from the archaeologists involved (DeGayner and Moss 2022, pers. comm.), who graciously outlined their exact process. DeGayner described their methodology thus:

> "1. Define points on the surrounding bedrock that do not appear to be recessed as a result of creating the glyph. This process is somewhat subjective, but the more points you create, the better the approximation of the original unaltered surface will be.
> 2. Create a mesh surface using these points. You can think of this as a low-resolution model of the original unaltered surface.
> 3. Run a distance computation process against the scanned model and the mesh from Step 2 [….]
> 4. Adjust color ramp [of scalar field] to achieve optimal visualization of the glyph depths."

DeGayner reports using a free program called CloudCompare to complete this work, but notes that "many other scanning-oriented software platforms" are equally capable of performing these operations. He also recommends one such program, called MeshLab, for the use of built-in shaders which can be easily applied and reveal minute details on surfaces. I had been using MeshLab and experimenting with these shaders prior to being introduced to the CloudCompare program, and will briefly describe my findings before returning to DeGayner's method.

In contrast to CloudCompare, I found MeshLab highly responsive when maneuvering meshes of all sizes without 'stuttering' or lagging. Combined with its

lighting controls, MeshLab proves extremely useful for close, preliminary investigation of a rock surface. While in CloudCompare users can also achieve fine control of lighting with the custom light (toggled with F7), the controls for doing so are not as smooth. In CloudCompare, the user must hold CTRL+right click to drag the light source to a different position; otherwise, the light source will rotate with the mesh itself. In MeshLab on the other hand, the light source will by default stay in a fixed position independent of mesh rotation, which is done simply by left clicking and dragging. Manipulating shading in this manner feels quite intuitive, akin to angling a worn coin in the light to make out faint lines. The user can therefore tease out small or eroded glyph details by applying different lighting angles with greater ease and fluidity.
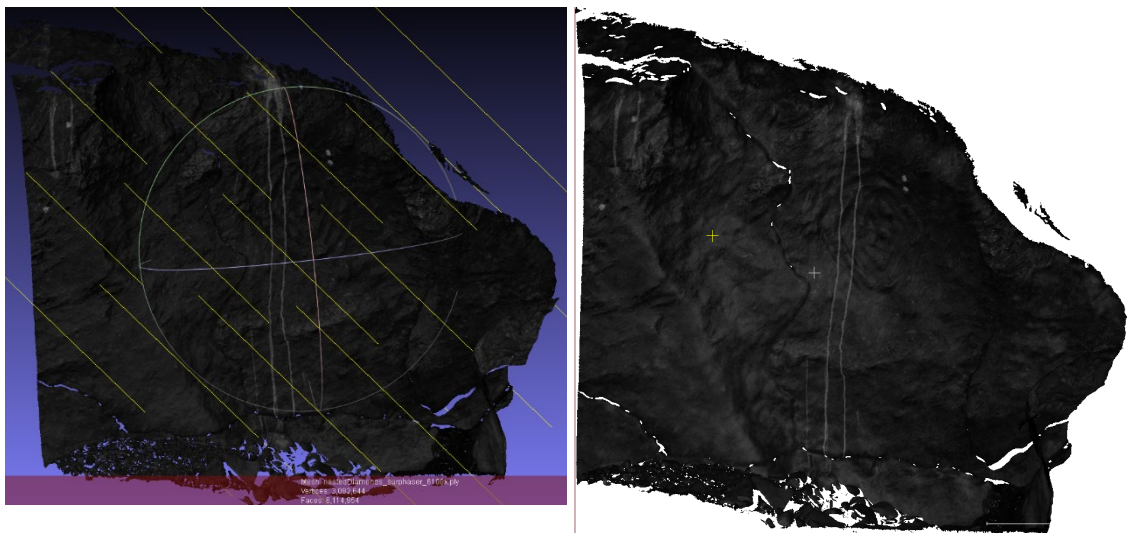
Figure 1: 3D light positioning comparison. Whereas light source positioning is indicated with a small yellow plus symbol that is easily lost in CloudCompare (right), it is intuitively and clearly illustrated with parallel 'light rays' in MeshLab (left).

Moreover, lighting can still be repositioned while the mesh remains static, as in CloudCompare, and this can be useful for taking a series of screenshots from a consistent viewpoint but different lighting angles. The controls and feedback to the user are improved in MeshLab, however: CTRL+shift+left click and drag moves the single light position, and gives a series of parallel lines illustrating the exact orientation of the light source. In CloudCompare, the source of the light is not as clearly indicated. In

summary, for achieving the seamless movement of a light source to inspect the characteristics of a surface, as in an RTI viewer, MeshLab offers a more fluid and user-friendly experience.

Shaders are, in layman's terms, preconfigured instructions for how light, shadow, and color should interact with the surface of an object. The information about the object is rendered into a visual representation according to these instructions. The potential implications of controlling these factors for visualizing petroglyphs are obvious. With a mesh opened in MeshLab, shaders can be applied by accessing the toolbar and following the path Render>Shaders. From here a drop-down list offers a default of twenty different shaders. Many of the shaders themselves are somewhat lackluster, however. While the shaders can be quite useful for acquainting oneself with the surface of the mesh and to some degree for outlining glyphs in binary color, they offer little in the way of advancing objectivity. Moreover, to the uninitiated the plethora of shaders, lacking description of their function, can act as a hindrance rather than help. While some appear to enhance glyph legibility, it tends to detract from our confidence in the results if the researcher cannot explain how or why a specific shader improved visibility, much less what the shader does.

Nonetheless, shaders can be quickly applied and some stood out as useful additions to our toolkit. Good results came from applying the radiance scaling shader (*Figs. 3-4*), especially with its ability to inverse its results. This gave similar outlining to more complicated procedures later done with CloudCompare. Some shaders were more useful when applied in unconvential ways. The effect created by the dimple shader, for example, is not desirable; however, with dimpling effectively turned off the shader becomes useful as a simple way of reproducably quantifying adjustments to the light source position (*Fig. 5*). Other shaders offer the same means of adjusting light position and can be helpful when used as intended (*Fig. 6*).

Figure 2 (top): Shader selection in MeshLab
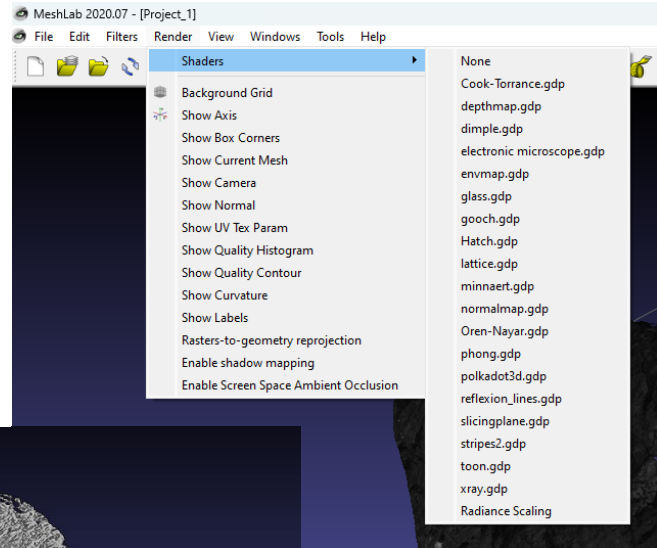
Figure 3 (middle): Radiance scaling shader (Grey Descriptor) applied to CHOH-26. Note previously unidentified carving to the left of the concentric diamonds.
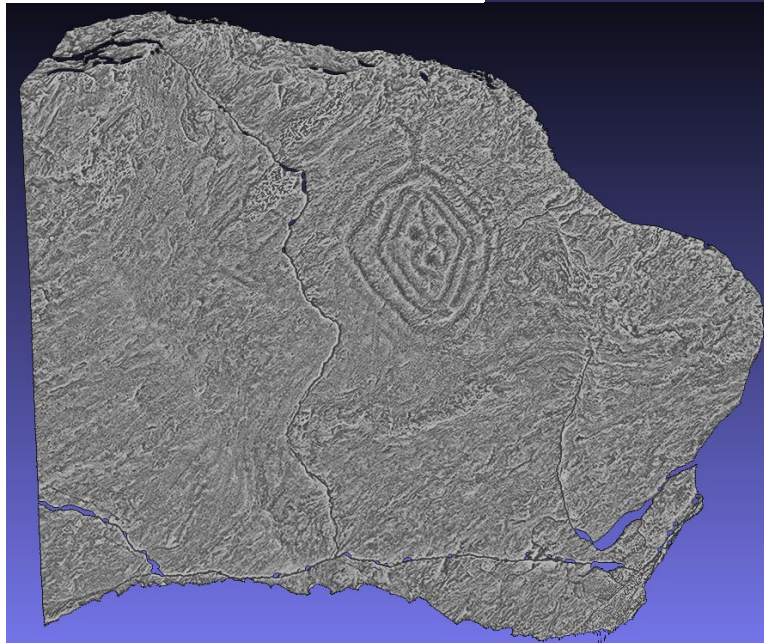
Figure 4 (bottom): Radiance scaling shader (Lambertian) applied to CHOH-26, viewed from an oblique angle with lighting from below
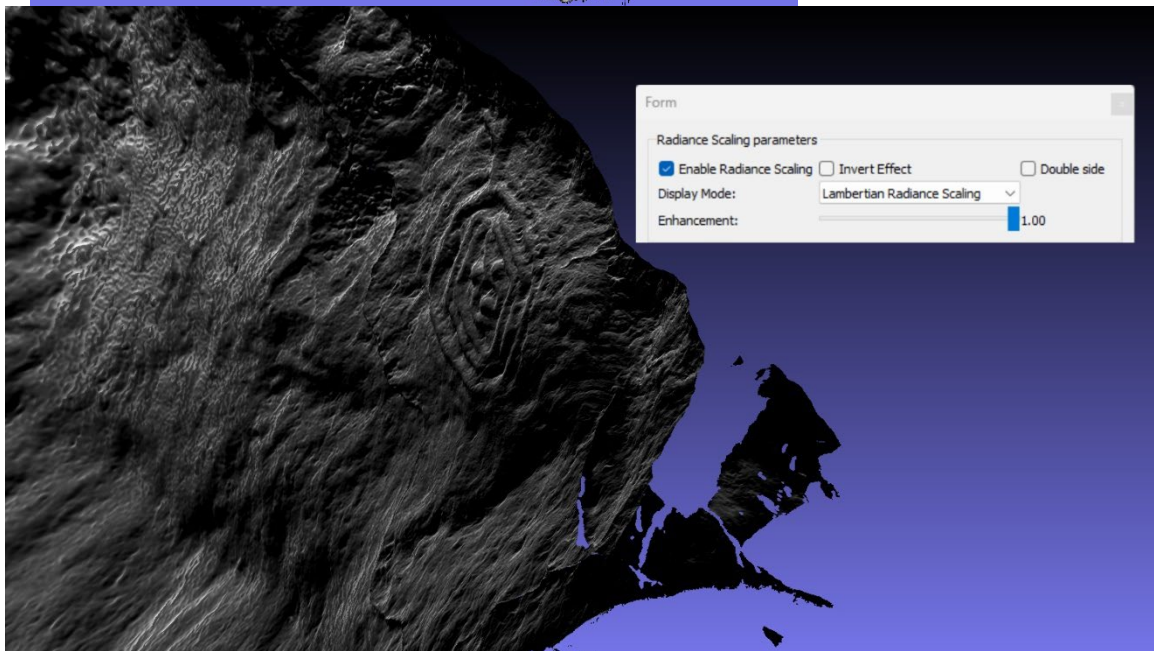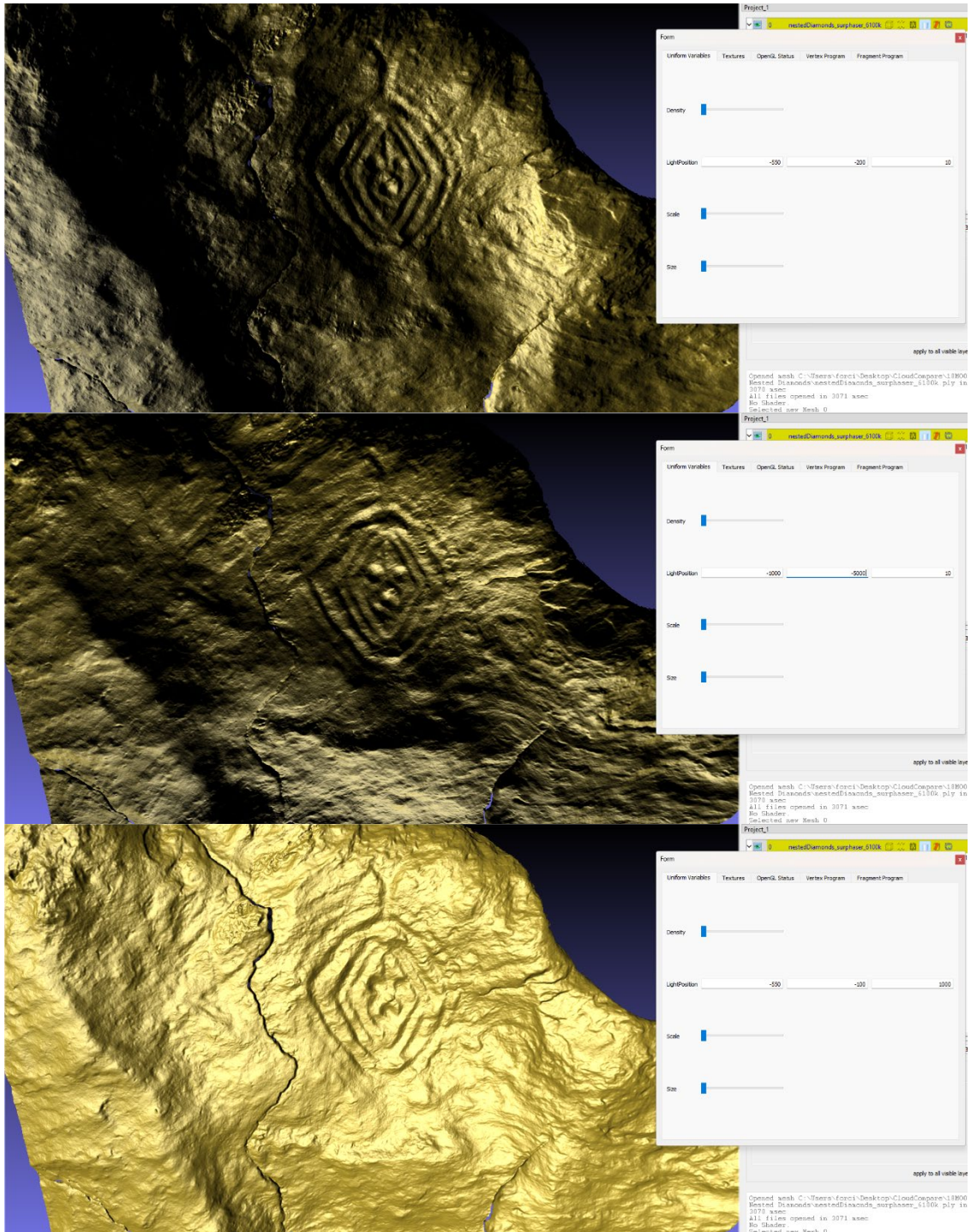
Figure 5: Three views of CHOH-26 with the dimple shader used to precisely set unique light source positions; the dimpling effect itself has been turned off.
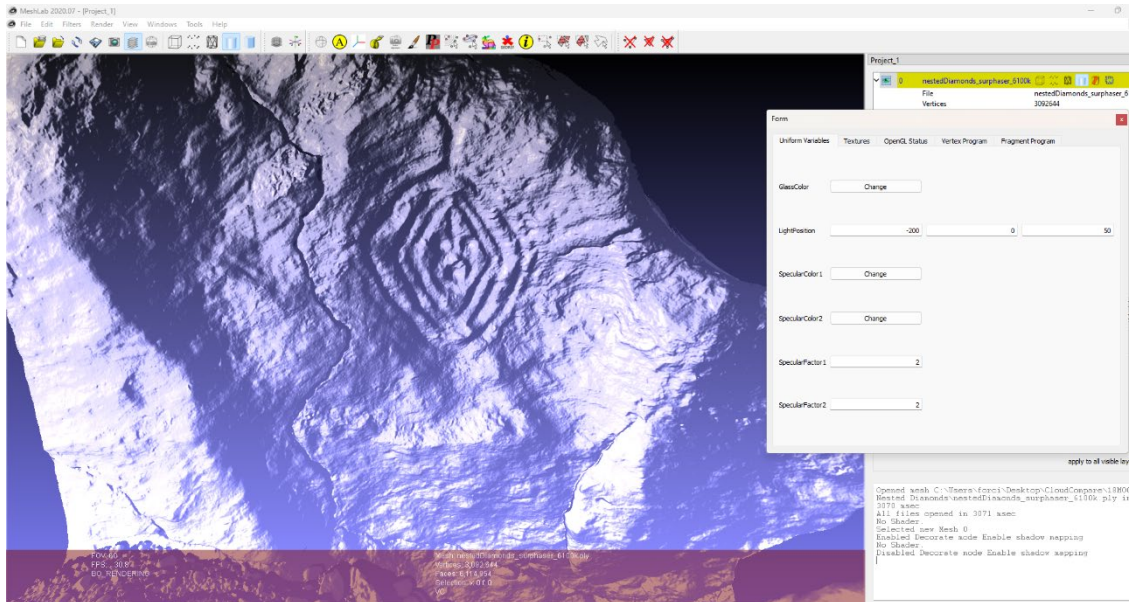
Figure 6: Glass shader applied to CHOH-26. The light source can be adjusted via the LightPosition setting as with the dimple shader. Unlike the dimpling effect of the latter, however, the 'glass' effect can be potentially useful in its own right for improving rock marking visibility.

Exploring MeshLab's capabilities also introduced me to options for colorizing mesh curvature, and these appeared more promising than shaders as a route to developing objective research methodologies. I was particularly impressed with the algebraic point set surfaces (APSS) variant of the 'Colorize Curvature' filter (***Fig. 7***). Preconfigured shaders and manual manipulation of shading prove inherently sensitive to small changes in lighting-to-mesh position, and they can rarely elicit all of the details of a rock carving simultaneously. Moreover, these strategies can rarely be extended for comparable results elsewhere, since the specific lighting angles that make carvings most apparent are highly specific to each petroglyph site. Non-shading based colorization methods, in contrast, reify the information ingrained in the mesh (e.g., the curvature of the triangles, the relationships between points, their distance to an imaginary plane, etc.) independent of lighting conditions, doing so in a repeatable manner that can be standardized across datasets.

Figures 9-11 show the APSS filter applied with the same settings (**Fig. 8**) to three petroglyph sites. Different visualizations can be achieved by adjusting the filter settings. Inputting different filter parameters sometimes further accentuated the details of the carvings; overall, however, this tool and others like it did not achieve much greater clarity than what has been pictured. Furthermore, these filters took some time to process and required significant computational resources. I therefore sought an improved approach which would similarly eschew reliance on shading and enable standardization while increasing speed, performance, and petroglyph discernment.
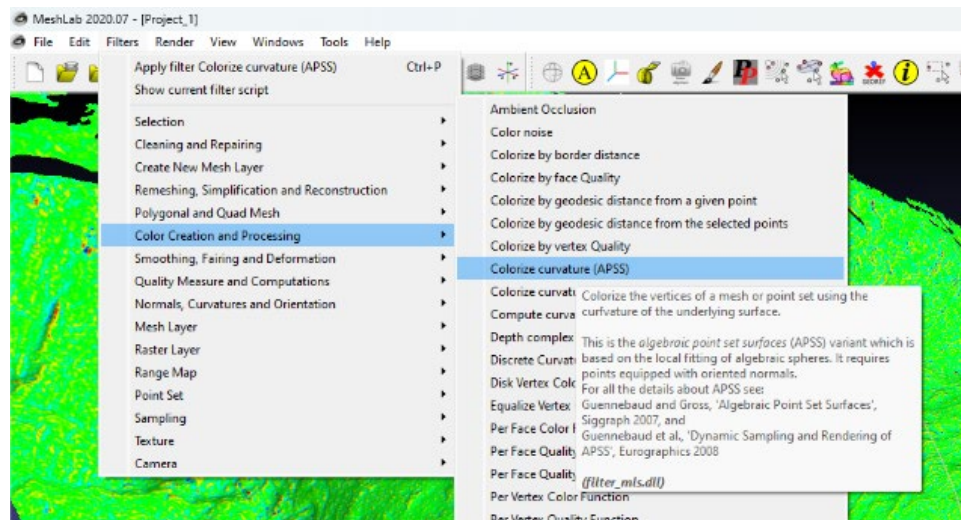
Figure 7: Location of the 'Colorize Curvature' (APSS) filter

The CloudCompare software and process suggested by DeGayner served as a point of departure for developing a refined approach. Applying the steps enumerated by DeGayner to CHOH-26 (**Fig. 12**), I began by selecting points that did not appear to be recessed by human activity. As DeGayner mentions, this process is somewhat subjective, but I found it easier to distinguish the raised areas of unaltered stone by turning off the material texture and instead viewing the mesh as a solid color (light gray) that contrasted well with normals shading (**Fig. 13**). I then used the Point List Picking
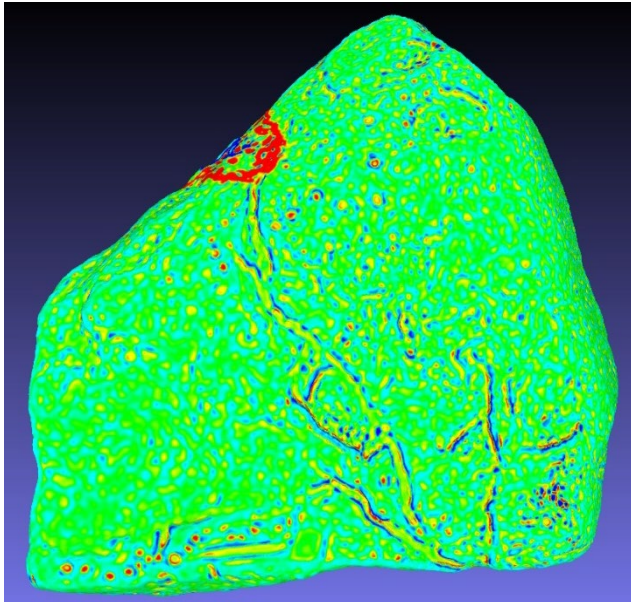
Colorize curvature (APSS)

Colorize the vertices of a mesh or point set using the curfvature of the underlying surface.

This is the algebraic point set surfaces (APSS) variant which is based on the local fitting of algebraic spheres. It requires points equipped with oriented normals.
For all the details about APSS see:
Guennebaud and Gross, 'Algebraic Point Set Surfaces', Siggraph 2007, and
Guennebaud et al., 'Dynamic Sampling and Rendering of APSS', Eurographics 2008

☐ Selection only

MLS - Filter scale	10
Projection - Accuracy (adv)	0.9
Projection - Max iterations (adv)	10
MLS - Spherical parameter	10
Curvature type	Mean
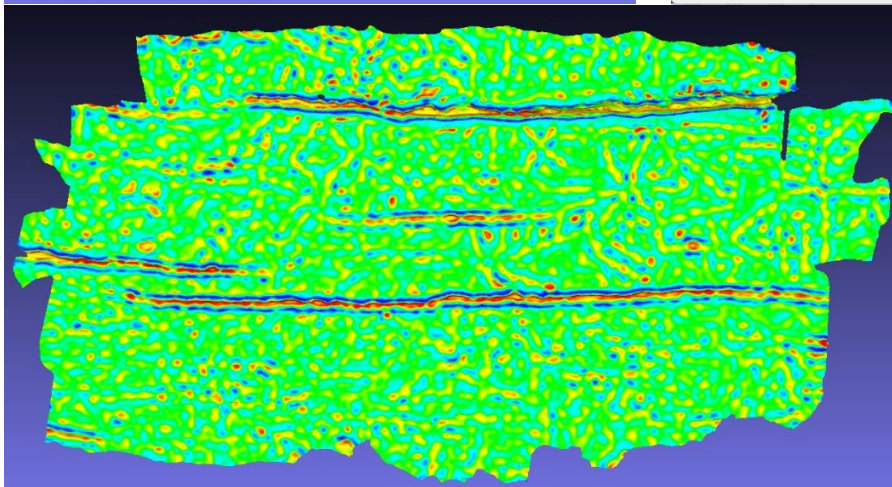
(Counterclock-wise from top right):

Figure 8: APSS filter settings applied to the 3D models in Figs. 9-11

Figure 9: Octoraro Creek petroglyphs with colorized curvature

Figure 10: Dighton Rock with colorized curvature

Figure 11: CHOH-26 with colorized curvature

27
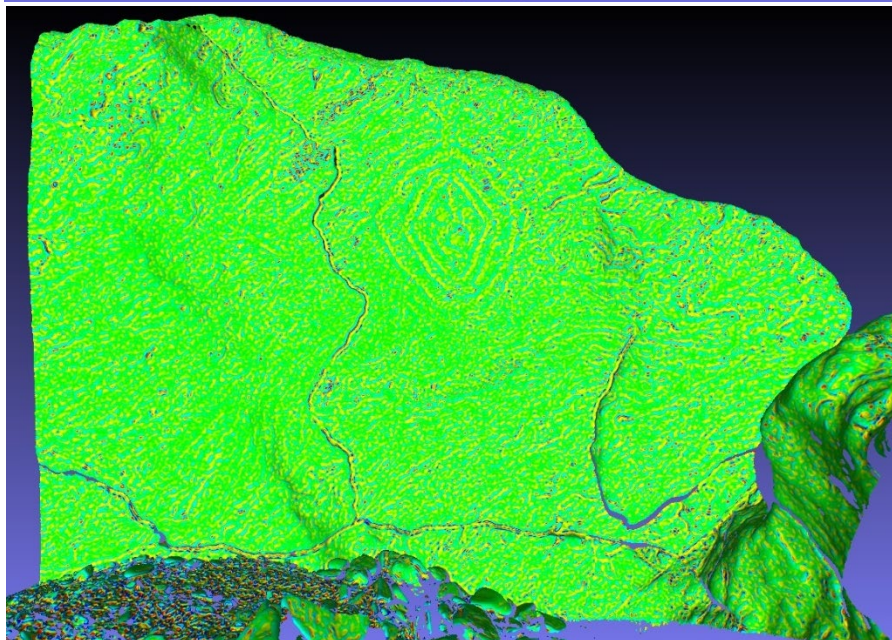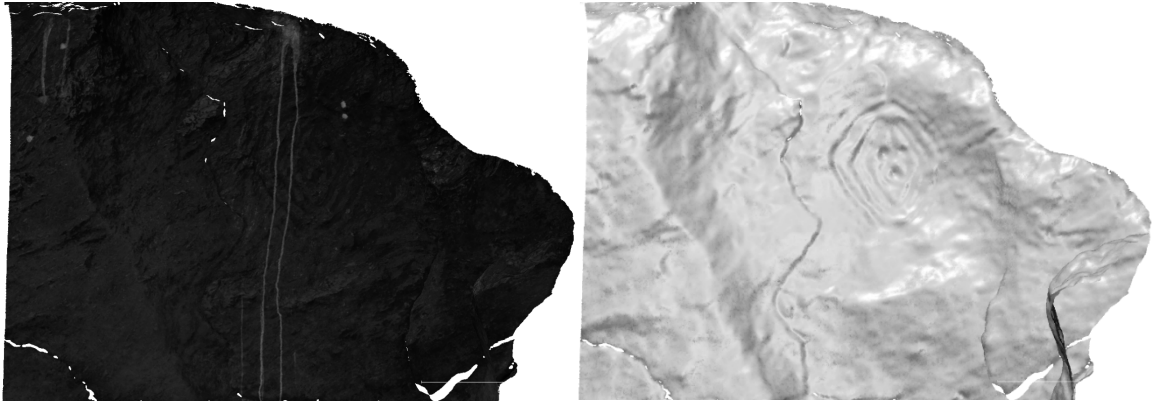
Figure 12 (left): CHOH-26 with material texture (or 'skin') and normals
Figure 13 (right): CHOH-26 with normals only

tool to sample a total of 541 points where the rock appeared unaltered, taking care to get

a good selection of points around areas that had been heavily worked (***Fig. 14***). This

produced a PickingList of the selected points, which I then exported to a new point cloud

by selecting "new cloud" from a drop-down list of options for saving the PickingList (***Fig.***

15). The resulting cloud is pictured in ***Figure 16***.

Proceeding to DeGayner's second step, there are a few methods of generating a

mesh from this new point cloud, and I employed three in testing. The first two are

through the mesh tool (Edit>Mesh) and apply Delaunay triangulation to the point cloud.

The first option, Delaunay 2.5D (XY Plane), projects the point cloud in two dimensions

onto the XY plane prior to applying triangulation and translating this triangulation back

into three-dimensional space. This mesh was therefore immediately eliminated since it

only produces usable results when the cloud has been properly oriented to the Z-axis.

The second option, Delaunay 2.5D (best fitting plane), works the same way but without

relying on any prior orientation of the cloud, as it projects instead onto a plane fit to the

cloud itself. The other tool used was the Poisson Surface Reconstruction

(PoissonRecon) plugin. In perhaps oversimplified terms, this plugin poses mesh

reconstruction as a mathematical Poisson problem: the location of the points and their

orientation are included in the problem, and the reconstructed mesh is the function that
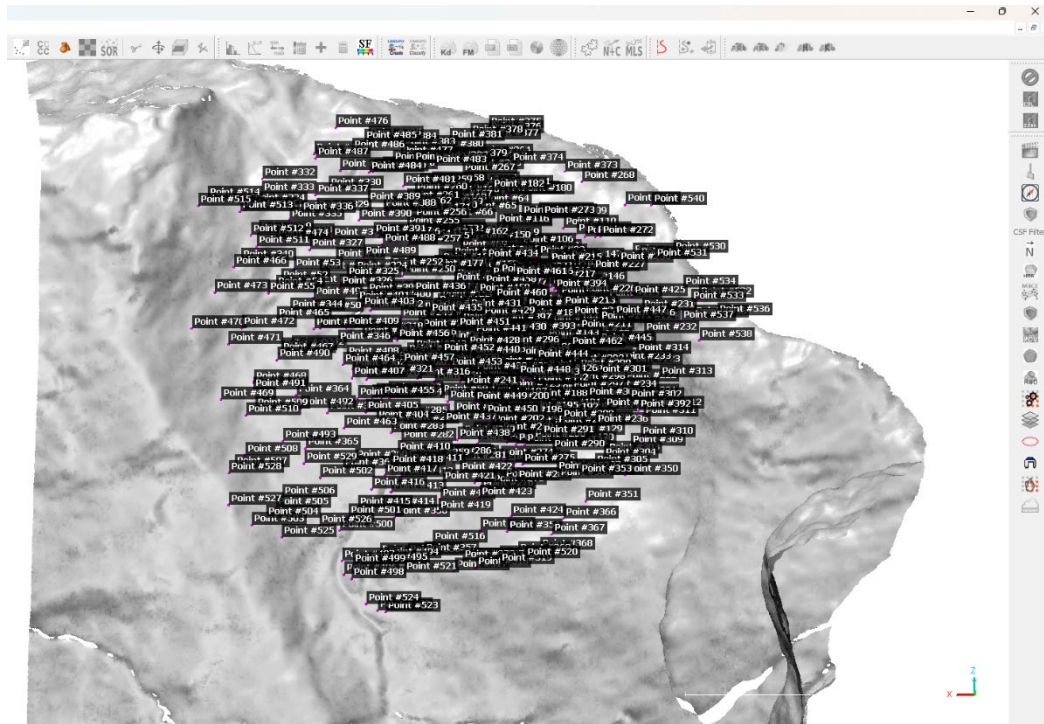
Figure 14 (top): CHOH-26 with points of unaltered stone selected as a sample.

Figure 15 (middle): Creating a new cloud from PickingList.

Figure 16 (bottom): CHOH-26 sampled points exported as a new point cloud.

best solves this problem (Kazhdan, Bolitho, and Hoppe 2006). Though the meshes made using Delaunay 2.5D (best fitting plane) (*Fig. 17a*) and PoissonRecon (*Fig. 18a*) both performed well in succeeding steps, Delaunay may be preferable given the tendency for PoissonRecon to fill the entire bounding box when it generates a mesh.

Using the two successful meshes I proceeded to DeGayner's third step and performed a total of four colorizations by distance computation. Selecting the original, unaltered and unsampled cloud for CHOH-26 and the Delaunay reconstructed mesh, I applied the "Compute Cloud/Mesh Distance" tool to perform the first distance computation, resulting in a colorized scalar field (*Fig. 17b*). I repeated these steps for the second distance computation against the PoissonRecon mesh (*Fig. 18b*). I performed two more distance computations to evaluate potential improvements to the colorization. In the first (*Fig. 19b*), the mesh generated using Delaunay 2.5D (best fitting plane) was smoothed using Laplacian smoothing prior to the distance computation (*Fig. 19a*). Smoothing by twenty iterations at a smoothing factor of 0.2 helped level the extreme points of this low-resolution mesh, and I hypothesized that this might help to negate any skew introduced by preconceptual bias in point selection.

In the second distance computation (*Fig. 20*), the original point cloud for CHOH-26 was trimmed to the area of our Delaunay 2.5D (best fitting plane) mesh so as to remove the noise introduced by points that were not reconstructed (i.e., points in the unaltered cloud that had no comparand in our low-resolution mesh). I hypothesized that this would allow us to more finely tune the scalar field and thereby elicit finer details. For all of the aforementioned computations, as well as later ones, I made certain to select the original cloud (or a copy of it) as the 'Compared,' while the downsampled mesh, cloud, or flat plane that we create was selected as the 'Reference' (*Fig. 21*). This ensures that the scalar field produced by the Compute Distance tool is attached to the original, unaltered cloud and its associated mesh. Colorizations thus remain comparable
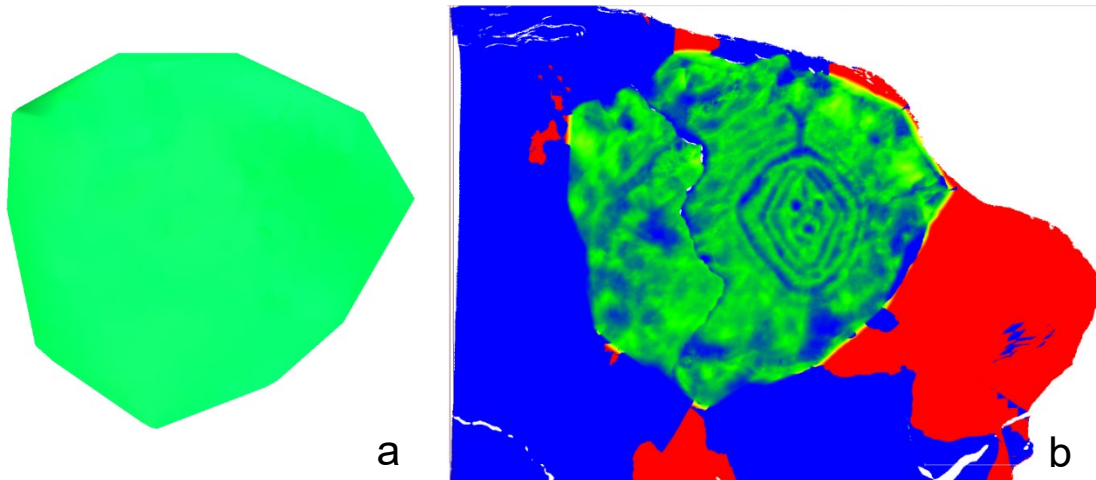
Figure 17: a) CHOH-26 mesh generated from point cloud in Fig. 16 using Delaunay 2.5D (best fitting plane); b) Distance computed to the Master Cloud.
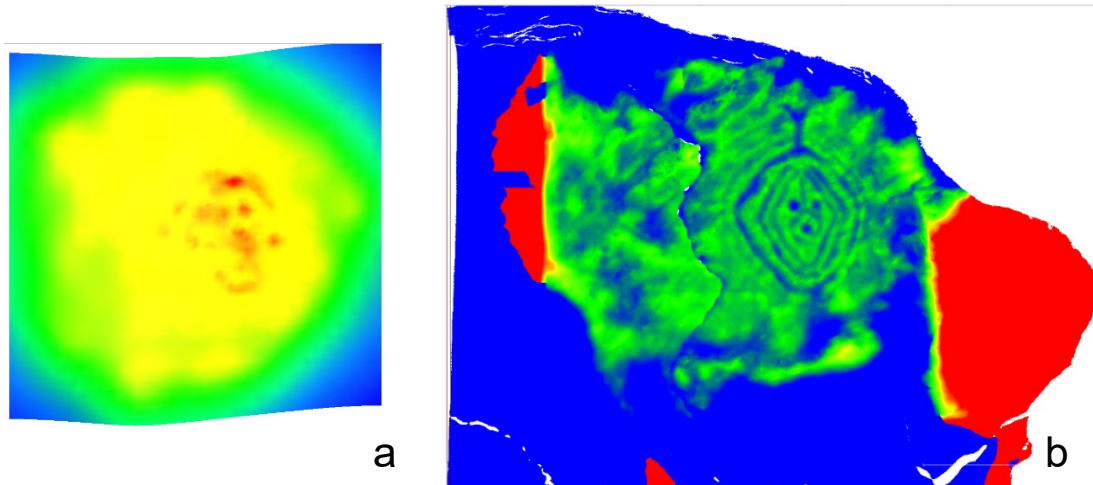
Figure 18: a) CHOH-26 mesh generated from point cloud in Fig. 16 using PoissonRecon (Octree level 8); b) Distance computed to the Master Cloud.
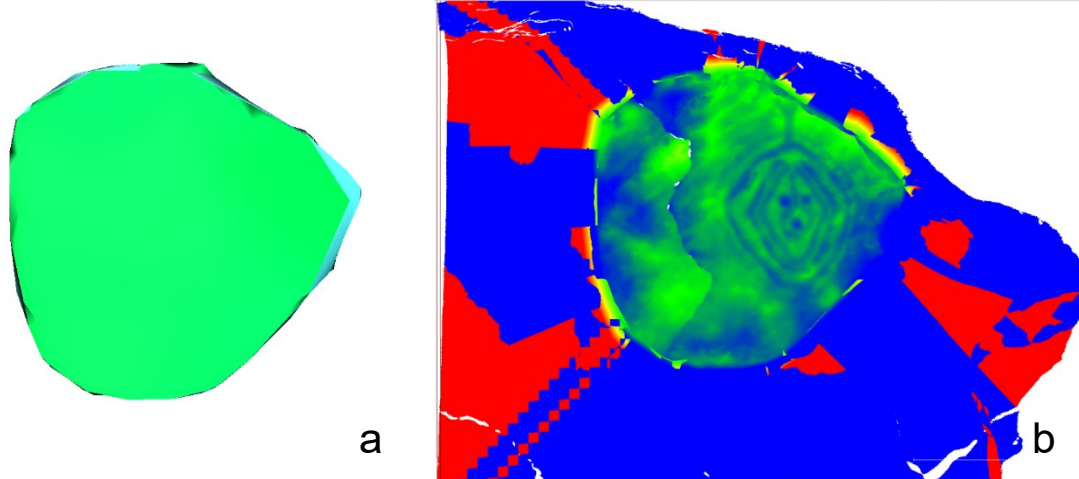
Figure 19: a) CHOH-26 mesh generated from point cloud in Fig. 16 using Delaunay 2.5D (best fitting plane) after smoothing 20 iterations at 0.2 smoothing factor; b) Distance computed to the Master Cloud.

and undistorted by operations like smoothing of the low-resolution mesh, since the final

product is solely a recolored clone of the original scan.
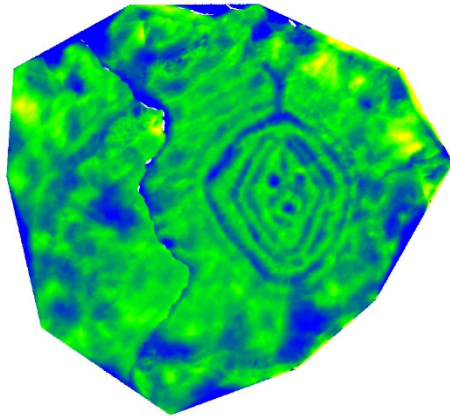
Figure 20: CHOH-26, distance computed between mesh generated with Delaunay 2.5D (best fitting plane) [Fig. 17a] and the Master Cloud trimmed to the size of its comparand
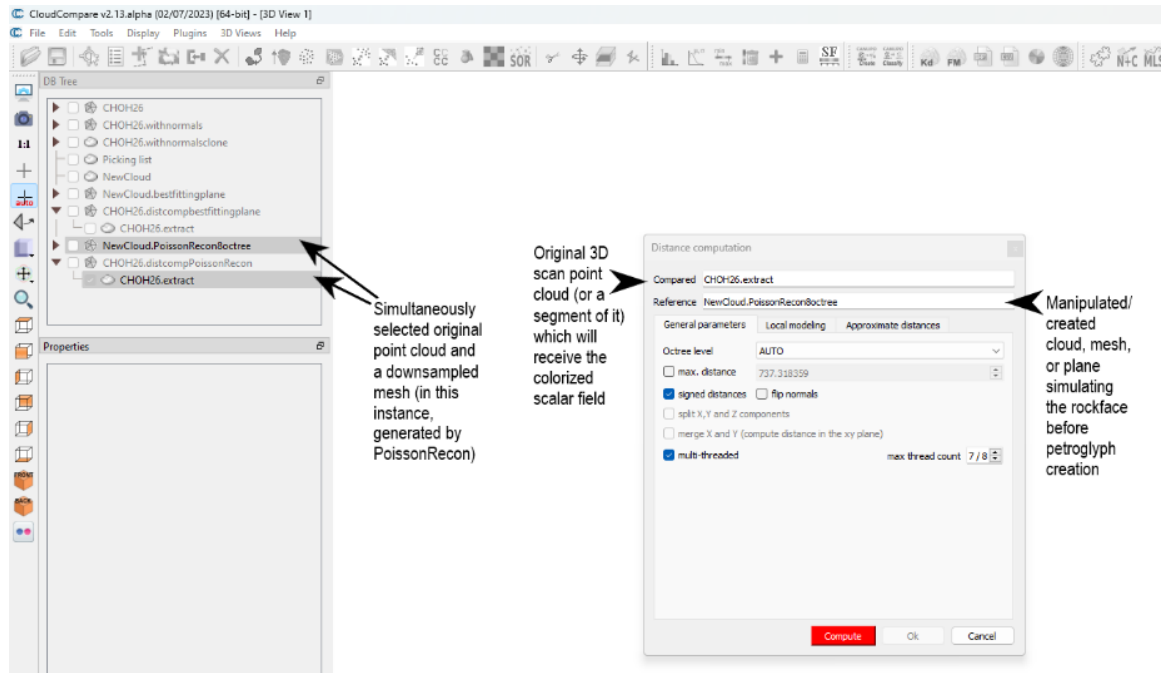
Figure 21: Selection of compared and reference entities. Selection is important for leaving the scalar field on the original, unaltered cloud and mesh.

The distance computation in ***Figure 17b*** against the Delaunay 2.5D (best fitting

plane) mesh resulted in a particularly good colorization of glyph details, with clear

distinction of the deeply incised areas and nuanced color variation showing faint details.

This scalar field also shows consistent colorization up to the edges of the sampled point

cloud since the reconstructed mesh (***Fig. 17a***) did not expand beyond the actual data

points. The distance computation to the PoissonRecon mesh (*Fig. 18b*) produced

decent results which are largely similar to the colorization in *Figure 17b*. However, while

there appear to be no perceptible improvements in the details revealed, there are clear

areas of obfuscation compared to the previous computation. Particularly at the edges of

the colorized areas, large blotches of solid color obscure details which were clearly

visible in *Figure 17b*, and this is attributable to the extension of the PoissonRecon

reconstruction beyond the sampled point cloud. In fitting the reconstructed mesh to the

bounding box rather than the limits of the 541 sampled points, the PoissonRecon mesh

fills in areas of no data at its edges. PoissonRecon also by default allows the

reconstructed mesh to exclude points (*Fig. 22*) unless adjustments are made in the

'Advanced Settings' tab, and even then the results are far from ideal.

Together these problems create an inaccurate approximation of the curvature of

the rock, leading to greater discrepancies in the distance computation at the edges of

the reconstructed mesh and thus distortion or loss of detail. The colorization (*Fig. 19b*)

resulting from first smoothing the Delaunay mesh before computing distance apparently

offered no benefit; the result was clearly an inferior colorization, being a 'fuzzier' version

of the colorization in *Figure 17b*. It is worth noting, however, that this does not

necessarily invalidate the usefulness of this method elsewhere. I suggest later that

smoothing is an important step, but one ill-suited to the low-resolution mesh generated

from such a sparse point cloud (541 points being quite a small sample relative to the

millions of points comprising some scans). In *Figure 20* on the other hand, we see a

more positive if not drastic difference from *Figure 17b*. Segmenting the original cloud to

the bounds of the reproduced mesh did offer better control over scalar field adjustments.

Irrelevant points from the original cloud which lacked a comparand in our simulated,

unaltered rockface were removed and thus did not skew the colorization. The greater

ease of scalar field adjustments is visible in the greater width of the scalar field display

parameter chart. Otherwise, there is no difference, and the accessibility of adjustments to the colorization is the only benefit. I conclude on the basis of simplicity, repeatability, and quality of colorization that a simple distance computation (*Fig. 17b*) to a Delaunay 2.5 (best fitting plane) mesh (*Fig. 17a*) presents the optimal choice when following DeGayner's process.
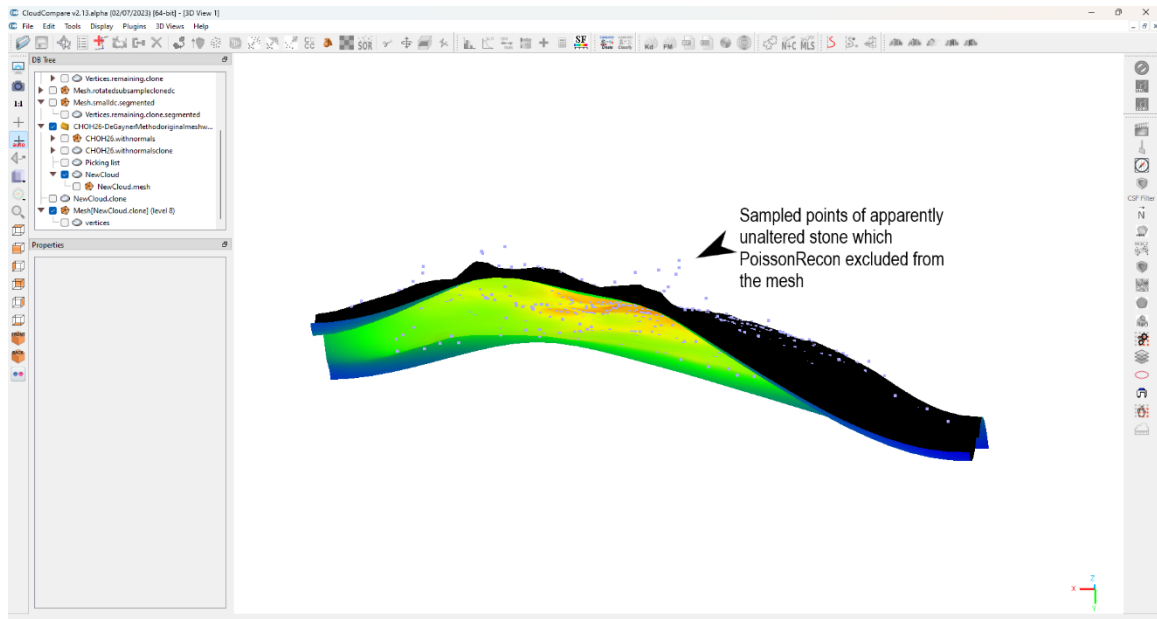
Figure 22: PoissonRecon reconstructed mesh, showing sampled points which were excluded by the plugin.

Having established a clear and effective sequence of steps, I sought to refine or rework them. Even with the 541 points we manually selected to use in our mesh, the divergence of our simulated 'pristine' rockface from reality lead to many natural features appearing in the colorization. As DeGayner noted regarding the simulation of a stone prior to petroglyph creation, "the more points you create, the better the approximation of the original unaltered surface will be." Taking this premise to its logical conclusion, the ideal form of this process would involve selecting every single point where the stone is unaltered and excluding every single point evincing human action. That is, we would achieve a perfect manual segmentation separating anthropogenic and natural features.

34

An obvious bottleneck occurs in the process if the researcher manually selects, point by point, what can amount to thousands if not millions of points. One potential solution appears in pivoting instead to *exclusion* of points: rather than manually picking points for our simulacrum, we clone the point cloud and manually remove the points showing evidence of carving, pecking, or the like. This is feasible since the markings themselves tend to comprise only a fraction of the surface area of a rock, and points can quickly and easily be segmented and deleted in CloudCompare. The result is a new point cloud which is denser by magnitudes compared to the measly 541 points we selected for inclusion previously. I hypothesized that the areas in which the point cloud is fully retained would appear as a solid color since the distance computation would return zero values.

I enacted the alternative sampling method. **Figure 23a** shows the removal of some – but not all – carved areas from a clone of the CHOH-26 mesh. Numerous obvious areas of incising were not segmented out as a sort of control, in order to see if they would also become visible or disappear into the background. **Figure 23b** shows the resulting mesh reconstructed with Delaunay 2.5D (best fitting plane). Finally, **Figure 24a** shows the colorization pursuant a distance computation between the original cloud and the mesh in **Figure 23b**. I regard this colorization as a failure, and its failure illustrates a key theoretical failing in the process. Its flaw stems from two unanswered questions: Does the manual selection of the point cloud perceptibly skew the colorization, and is the presence of distortion influenced by the percentage of the original point cloud we sample?

The reconstruction of the mesh in this manner guarantees, as hypothesized, that our distance computation will only return different values in the areas that have been segmented out. That is, the only highlighted areas are the areas we cut out of the scan. This would be acceptable if our manual segmentation of the culturally modified areas

35

was perfect, but it is not. Indeed, the entire purpose of the colorization is to make clear the details that we cannot see or only perceive with difficulty. Not only do our control areas of known incising become invisible, but the rough segmentation I performed commands the colorization. Note, for example, the odd curvature of the fork situated above the nested diamonds in *Figure 24a*; the colorization follows my imperfect cutout rather than the reality of the carving, which is more of a perfect 'Y' shape (*cf.* the same area in *Figure 20*). We may deduce that part of the reason that taking DeGayner's method to its logical conclusion fails is because, in his original method, the extremely low resolution of the mesh significantly mitigated the bias in our selection while doing the 'heavy lifting' in the colorization. The mediating role of the downscaling is illustrated in *Figures 24b-d*, which show the same colorization performed in *Figure 24a* but with progressive smoothing of the mesh prior to computing distance. As the smoothness of the mesh is increased, the real details of the carvings begin to appear regardless of our segmentation.
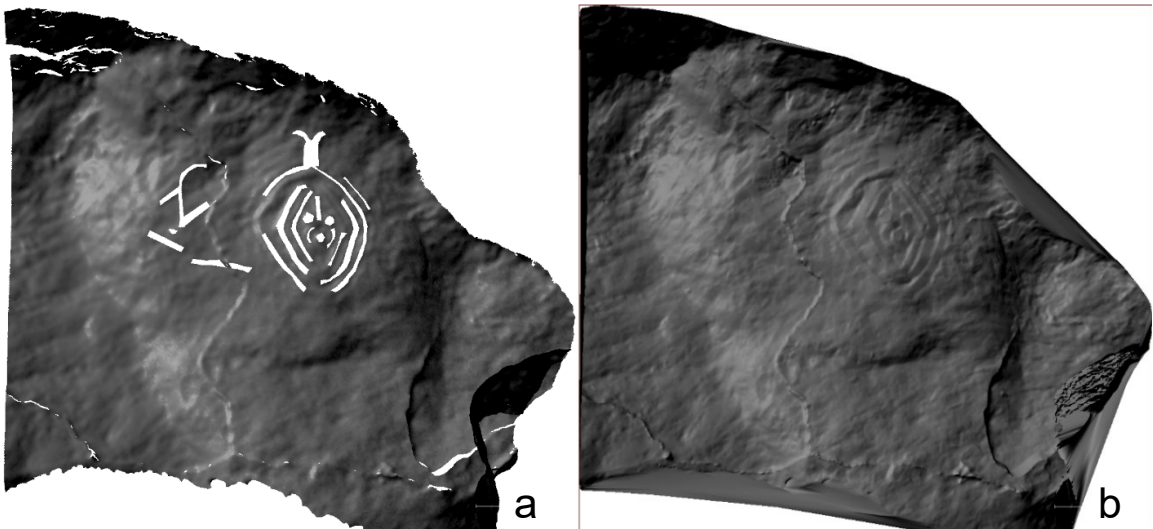
Figure 23: a) DeGayner revised method, mesh with segmented out material; b) DeGayner revised method, reconstructed mesh (best fitting plane)
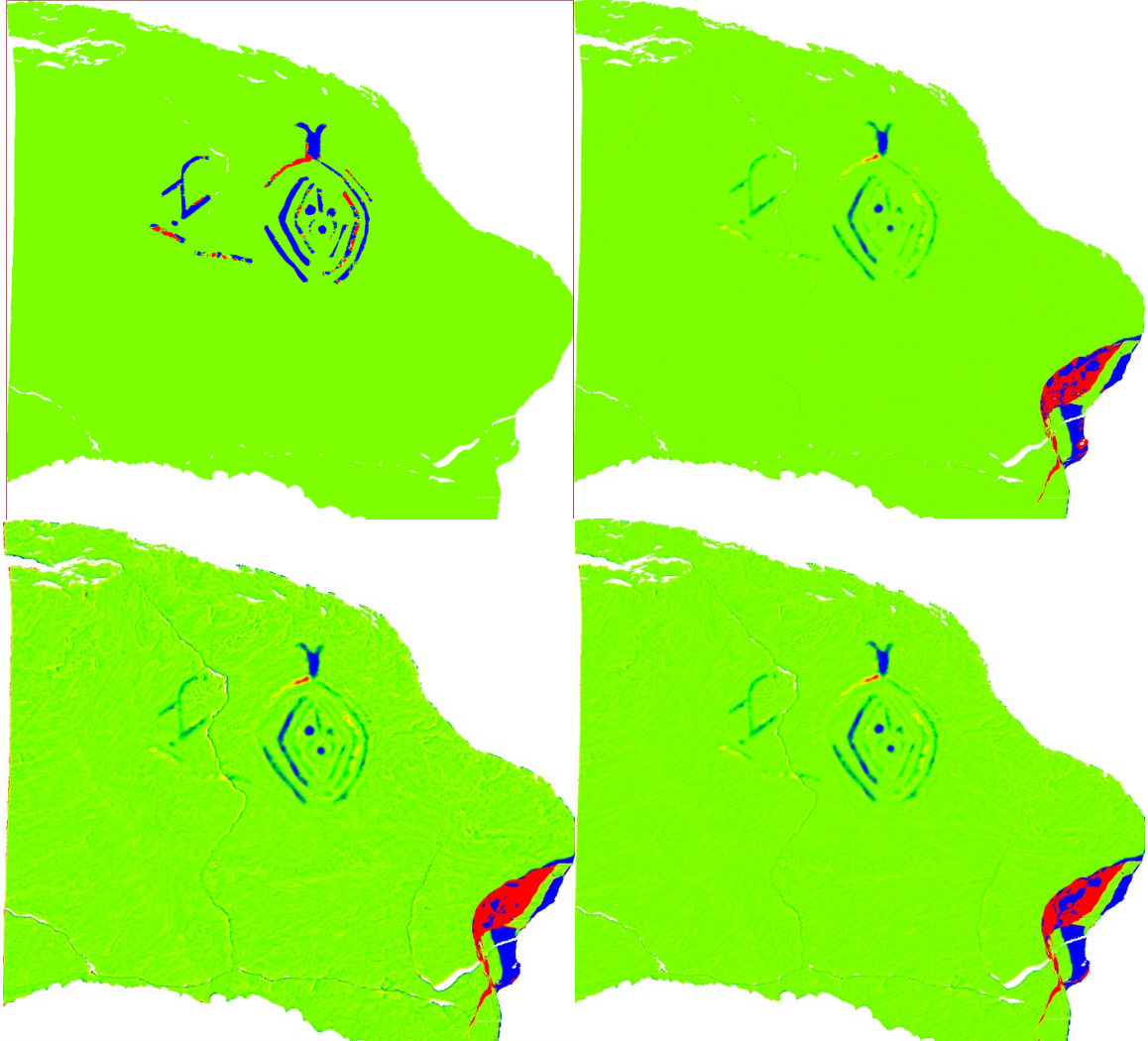
Figure 24: DeGayner revised method, distance computations with progressive increase in Laplacian smoothing of mesh in Fig. 23b; (clockwise from top left) no smoothing, some smoothing, more smoothing, most smoothing.

Summarized in simple terms, the point selection process in DeGayner's method plays only a small role in the method's success. It may even be said that the method works *in spite of* the point selection process rather than because of it. What is really happening is that a person is unlikely to select but a small fraction of the overall points to create their own mesh. In the case of CHOH-26, we could manually select over 22,000 points of apparently unaltered rock and still have selected only 1% of the points in the original point cloud. The mesh we reconstruct is thus of such a low resolution that our point selection does not significantly matter. What matters is that the global curvature of

the stone has been captured in broad strokes, and thus this curvature is accounted for in the distance computation and effectively eliminated from the colorization. The product is a scalar field that colorizes the extreme values: high and low points, both natural and cultural. The creation of difference in the simulacrum is therefore essential to creating a decent colorization. This makes the number of sampled points a key concern since as more points are included, fewer differences exist to create a colorization. Specific choice of points is less important but can still skew the colorization – especially with higher point retention – by changing the distribution of difference.

The relative insignificance of point selection in driving the colorization process is corroborated by an experiment illustrated in *Figures 25-29*. I roughly segmented a clone of the original mesh (*Fig. 25*) to the area covered in our first point selection process (*Figs. 14-17*). Then, I again selected 541 points from this bounded space, but this time by random subsample rather than meticulously selecting areas that appeared unaltered. I repeated this process three times for three different subsampled clouds comprised of 541 points each (*Figs. 26a, 27a, 28a*). I then continued with DeGayner's method as normal, generating meshes from these clouds (*Figs. 26b, 27b, 28b*) and lastly performing distance computations between the meshes and the master point cloud (*Figs. 26c, 27c, 28c*). The positive results seen in these colorizations evince the minor importance of manual point selection. The scalar fields created are on par with the ones we made through the careful, manual selection of unaltered points despite being selected completely at random.

As the slight variations in our scalar fields show, however, randomness of the point selection is not entirely immaterial. I therefore thought to mitigate the issue by averaging the scalar fields we produced via scalar field calculations (*Fig. 29*), and this gave a clearly more consistent and accurate colorization. I conclude that replacing manual point selection with random subsampling of the point cloud provides a more

objective and systematic approach to colorizing three-dimensional petroglyph data, especially when conducted in multiple trials and the results are averaged. The random subsampling method requires no more effort and generally less time while offering results of comparable quality and superior objectivity. Yet, before forsaking manual point selection on these grounds alone, I also conducted another experiment aimed at appraising the danger of interpretive preconception in manually selecting points.
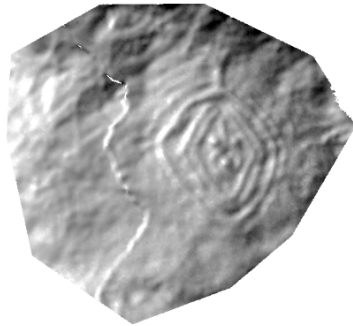
Figure 25: Clone of CHOH-26 mesh roughly segmented to the area covered by the previous point selection of 541 points.
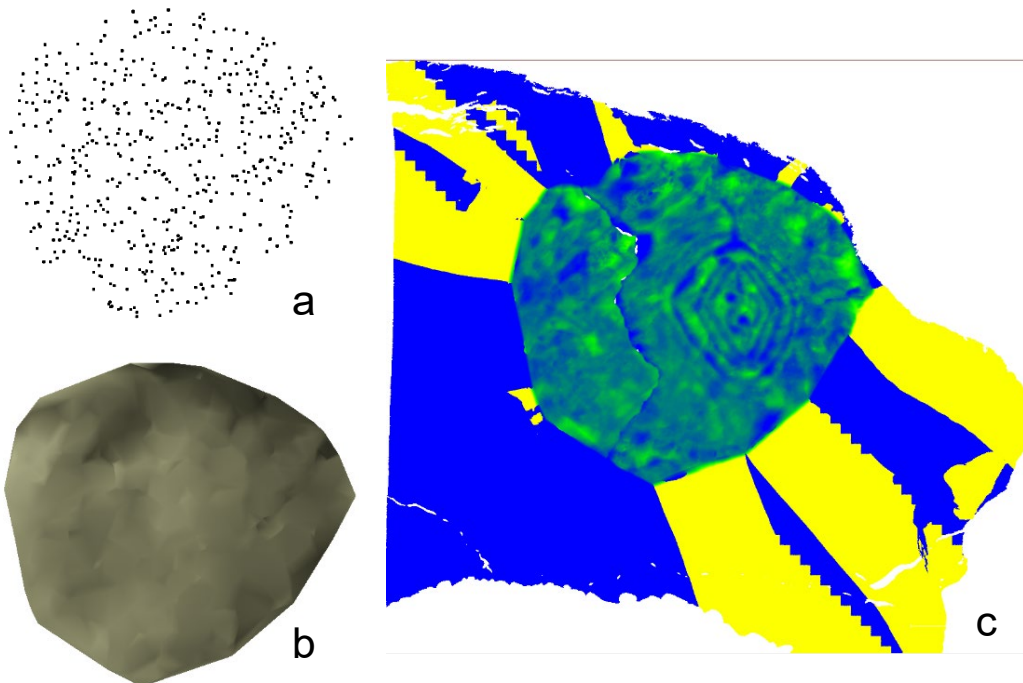
Figure 26: a) First random subsample of 541 points from area in Fig. 25; b) Mesh generated from point cloud in Fig. 26a; c) Resulting scalar field from distance computation between Fig. 26b and original mesh.
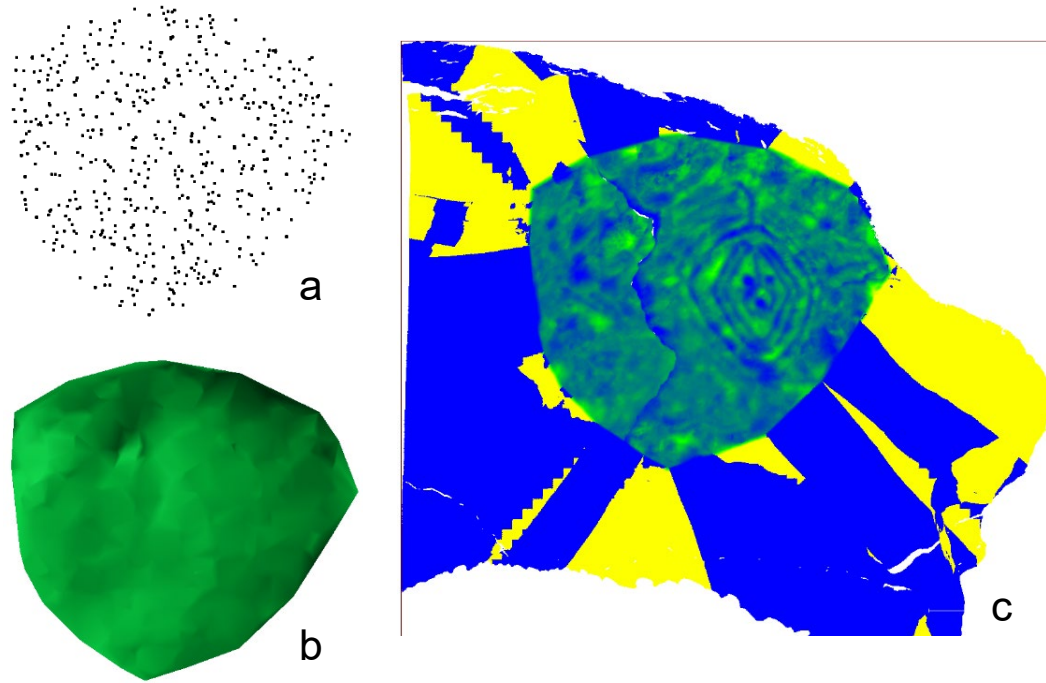
Figure 27: a) Second random subsample of 541 points from area in Fig. 25; b) Mesh generated from point cloud in Fig. 27a; c) Resulting scalar field from distance computation between Fig. 27b and original mesh.
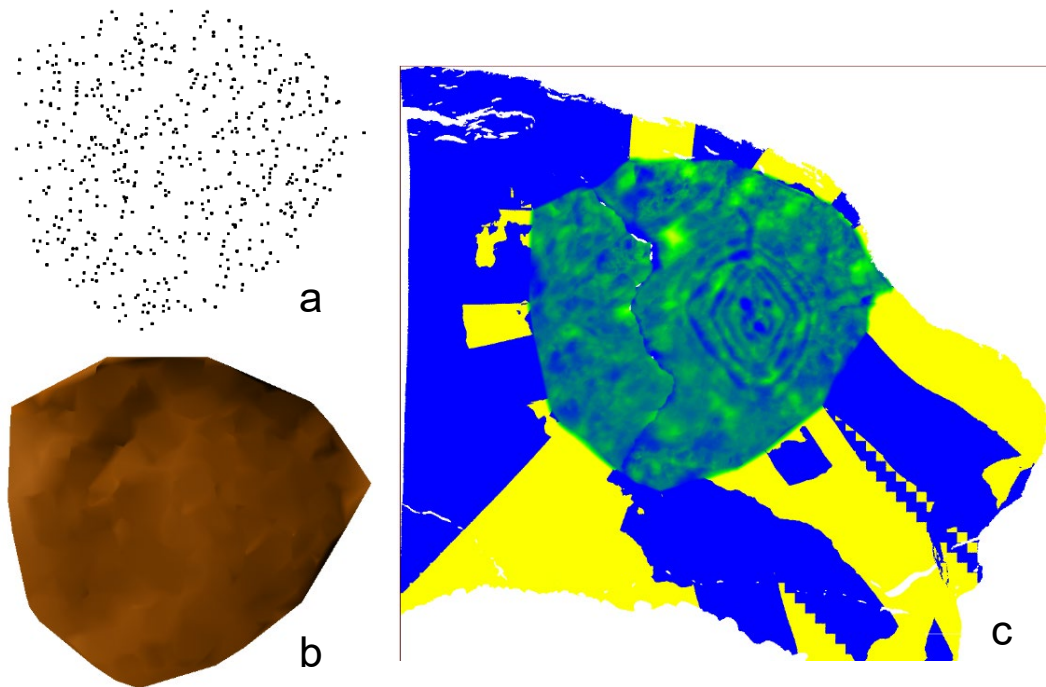
Figure 28: a) Third random subsample of 541 points from area in Fig. 25; b) Mesh generated from point cloud in Fig. 28a; c) Resulting scalar field from distance computation between Fig. 28b and original mesh.
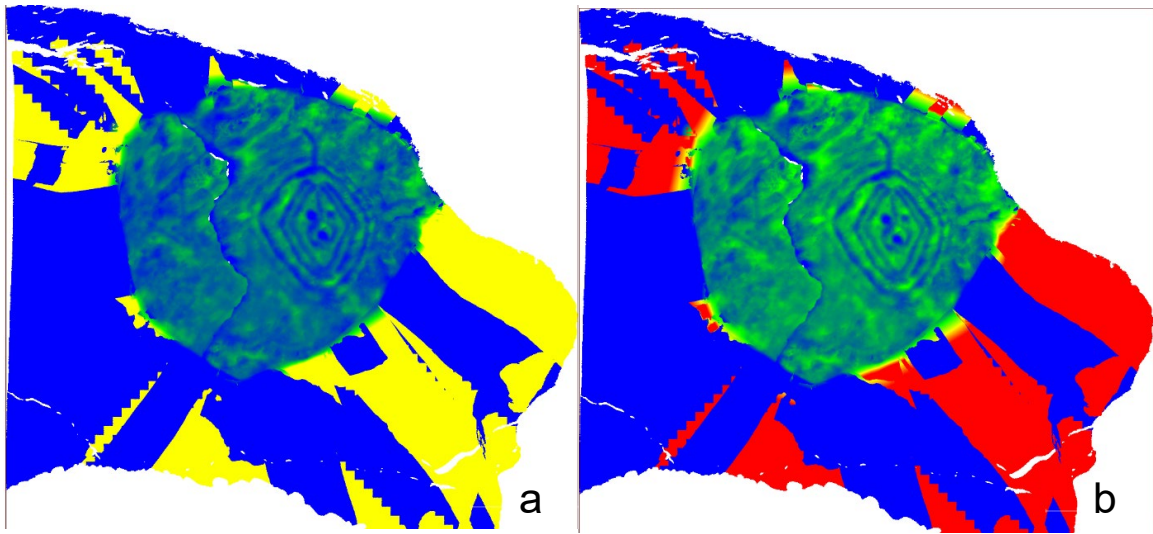
Figure 29: a) Combined scalar fields from Figs. 26-28; b) Averaged scalar fields from Figs. 26-28.

To determine the potential for misuse or inadvertent imposition of subjective interpretation onto the glyph content, I enacted a scenario in which a researcher is mistaken as to what they see. In this hypothetical setting, I pretended to see the word 'hello' in the glyphs on Dighton Rock. I applied this misinterpretation to the selection of points for our simulacrum, generating a total of five meshes: four which applied DeGayner's method at varying levels of specificity and one which followed the failed 'revised' method previously described. The meshes were generated in the following manner. I first arbitrarily segmented out the word 'hello' in all capital letters from the center of the original point cloud. No other points were removed. The many obvious, real petroglyphs were therefore 'mistaken' for natural rock and left alone. This simple segmentation was then used to make a mesh in accordance with the revised method I have described, labeled Sample A (*Fig. 30a*).

To make the other four meshes, I next used the segmented cloud to expediently simulate the manual selection of points per DeGayner's normal method. I randomly subsampled the cloud to 10%, 1%, and 0.1% of the points in the master point cloud to create Samples B through D (*Figs. 31a, 32a, 33a*, respectively). Finally, to best replicate

41

DeGayner's method as it would likely be used by a researcher, I manually selected

3,514 points around the imagined 'hello' glyphs (**Fig. 34**), then joined this cloud to a

clone of Sample D to achieve coverage of the entire stone (**Fig. 35a**). I then completed

the remaining steps to generate a colorized scalar field from each sample.

Table 2. List of Dighton Rock Point Clouds

Name	Description	Points	% of Master Cloud
Master Cloud	Master point cloud	221,739	100.00 %
Sample A	Master cloud minus points comprising the word 'hello'	216,676	97.72 %
Sample B	Random subsample of Sample A	22,170	10.00 %
Sample C	Random subsample of Sample A	2,217	1.00 %
Sample D	Random subsample of Sample A	222	0.10 %
Sample E	Sample D plus 3,514 points manually selected from around the word 'hello'	3,736	1.68 %

In the resulting scalar fields, we see the impact of our selection especially with

the clouds retaining the most points. In **Figure 30b**, the only difference to be found

between Sample A and our Master Cloud came from our point selection, resulting in the

apparent corroboration of entirely fictitious petroglyphs. The colorizations derived from

Sample B (**Fig. 31b**), Sample C (**Fig. 32b**), and Sample D (**Fig. 33b**) continue in the

same pattern, demonstrating the direct relationship between the density of the sample

and the bias introduced by our sampling. That is, the more points we retain from the

Master Cloud, the more heavily this sampling strategy will distort our colorization.
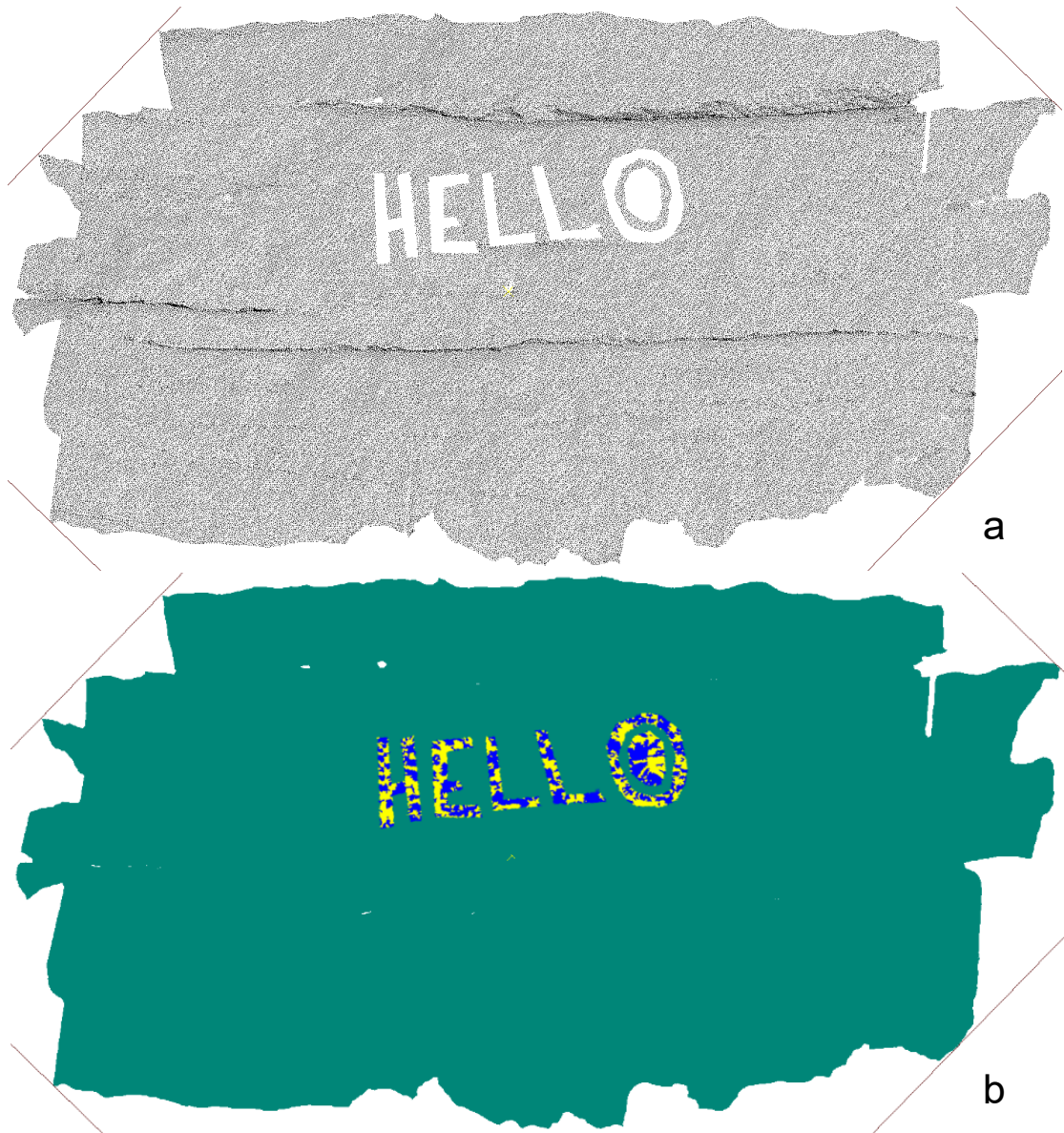
Figure 30: a) Sample A; b) Resulting scalar field from distance computation between Sample A and Master Cloud
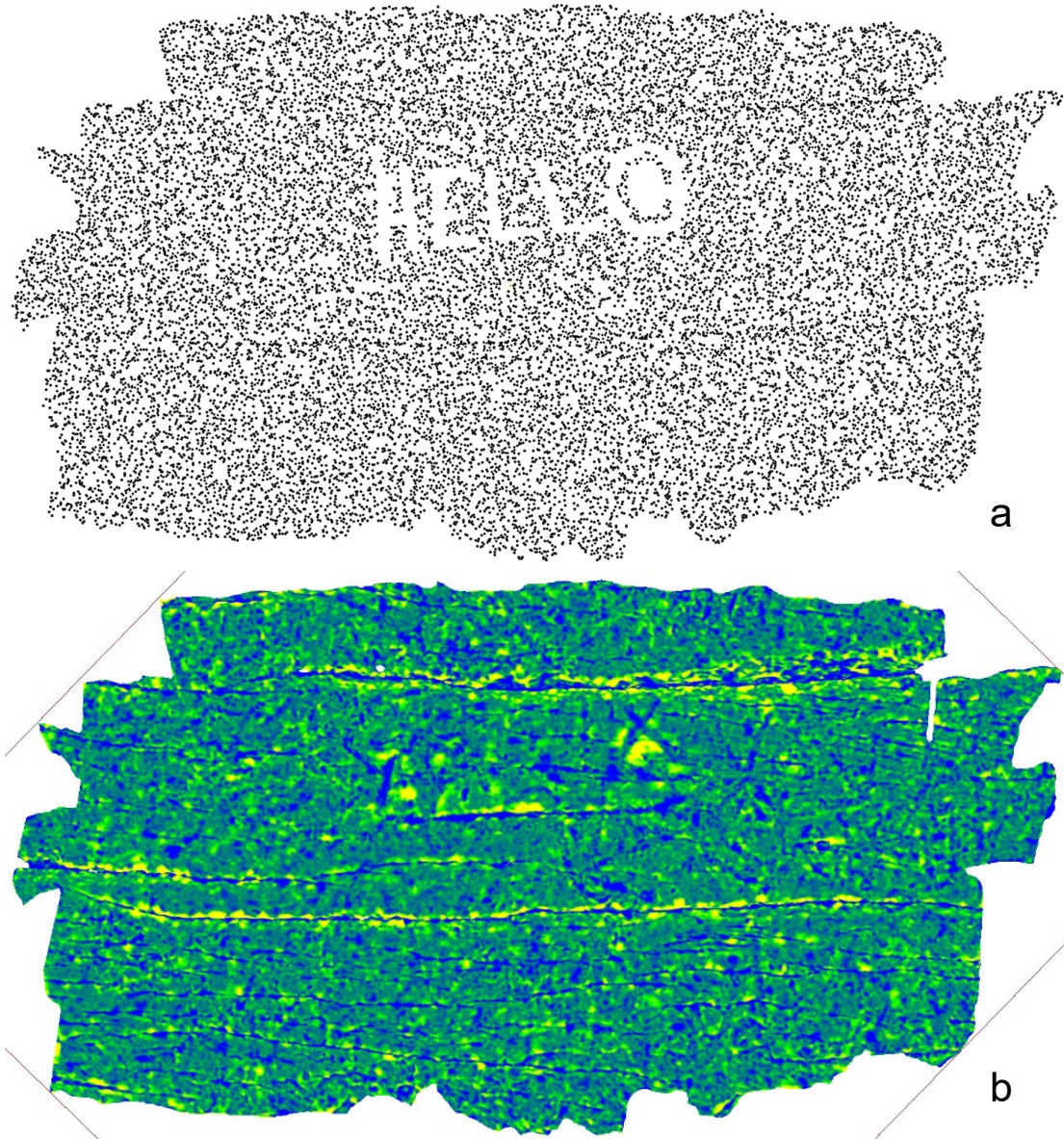
Figure 31: a) Sample B; b) Resulting scalar field from distance computation between Sample B and Master Cloud
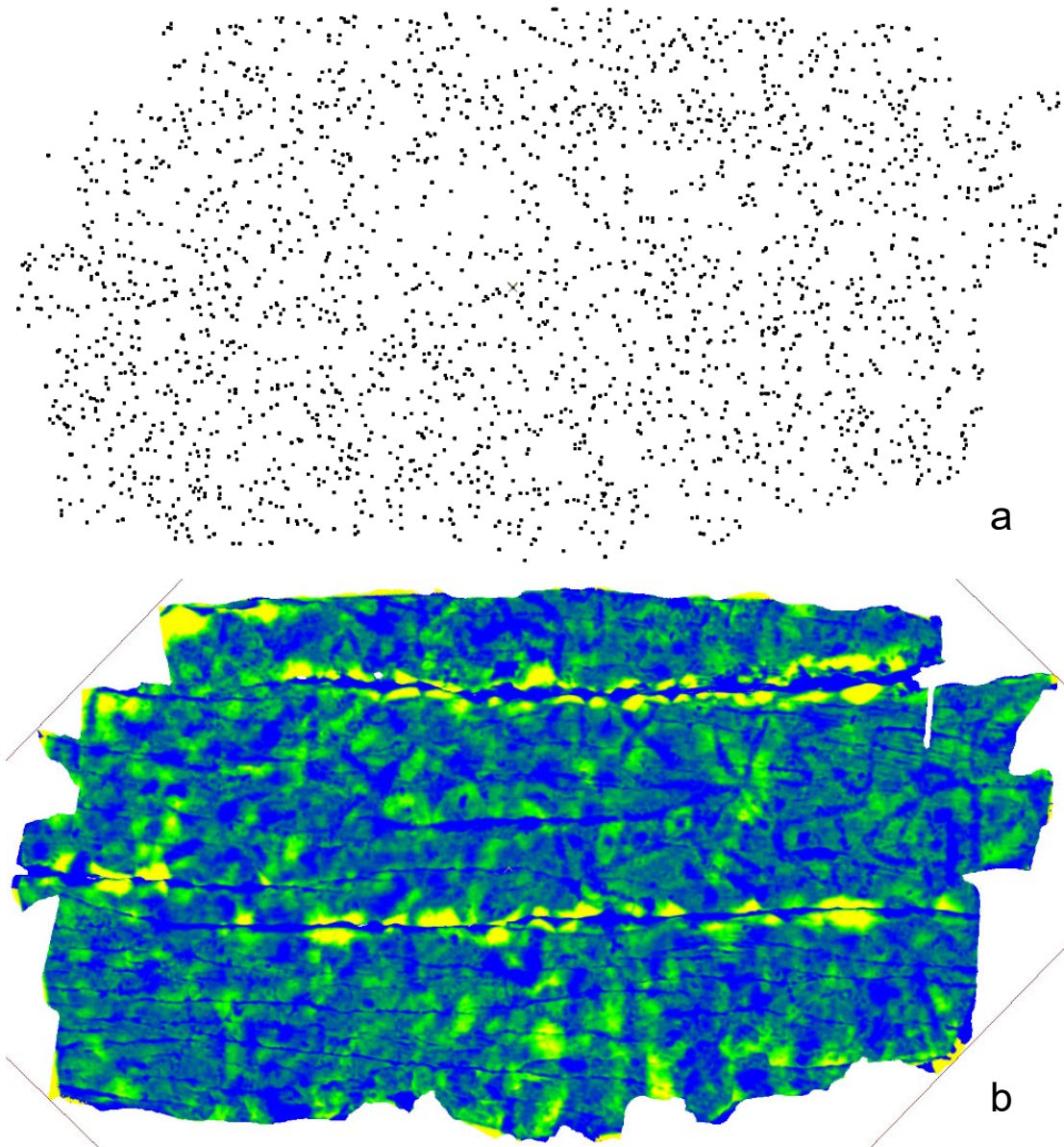
Figure 32: a) Sample C; b) Resulting scalar field from distance computation between Sample C and Master Cloud
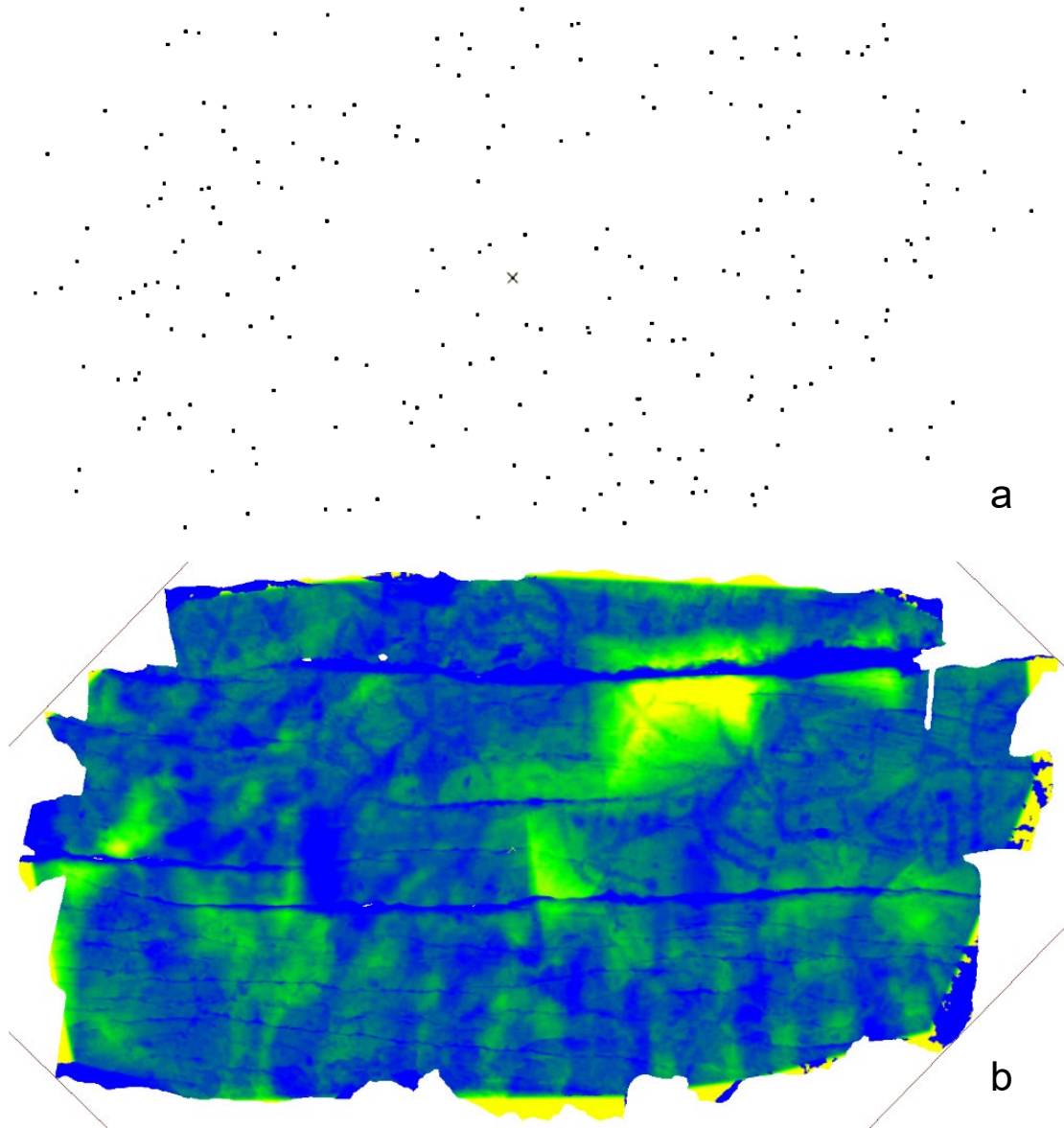
Figure 33: a) Sample D; b) Resulting scalar field from distance computation between Sample D and Master Cloud

Figure 34: Points added to Sample D to form Sample E

a

b
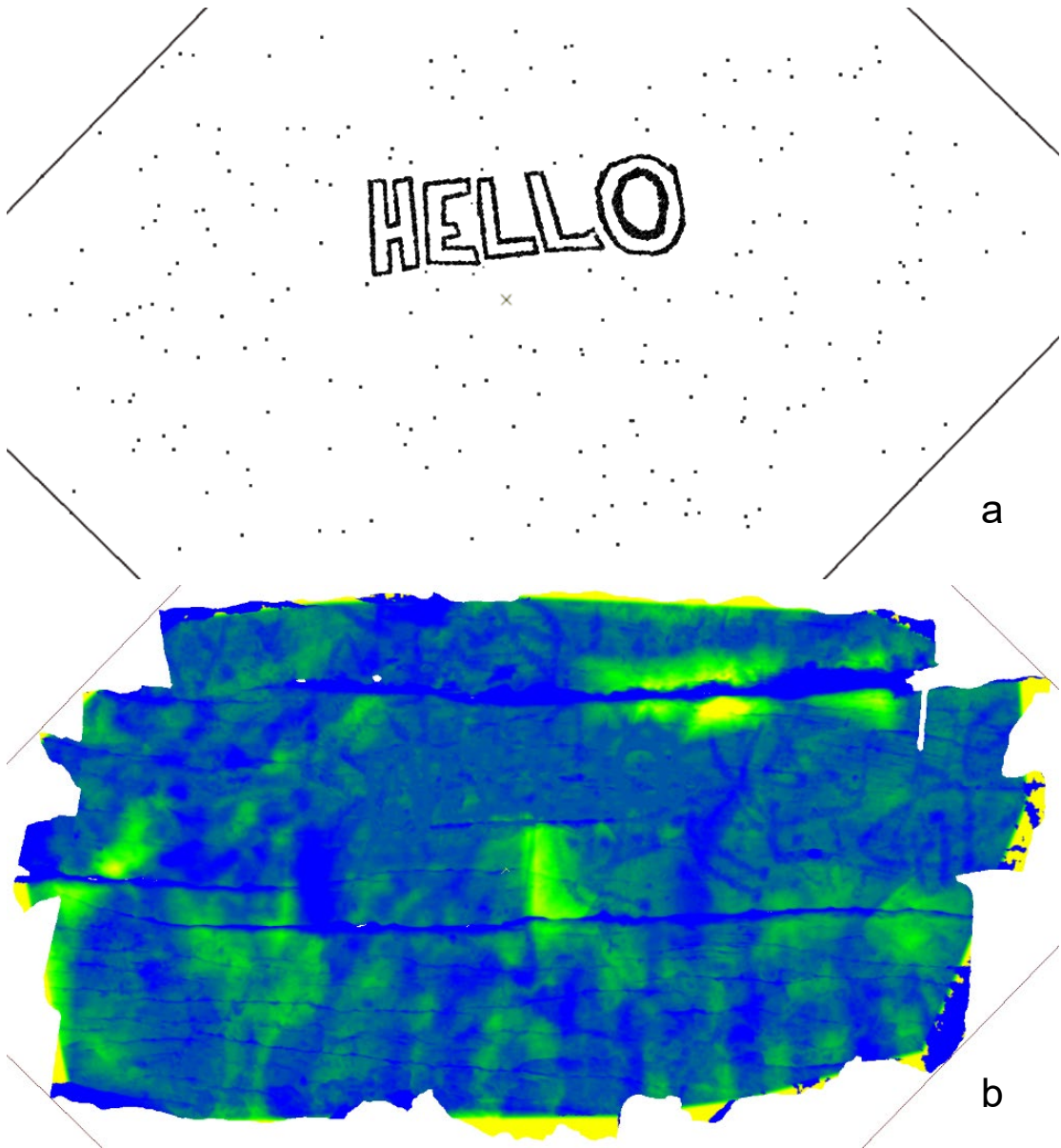
Figure 35: a) Sample E; b) Resulting scalar field from distance computation between Sample E and Master Cloud

At first glance, the results of Sample E (***Fig. 35b***) would therefore appear anomalous. The word 'hello' is even more visible than in the colorization derived from Sample B despite a smaller point cloud (1.68% as opposed to 10.00% of the Master Cloud). Upon further inspection, however, this may be explained by the difference in sample distribution at the microscale. Whereas Samples B through D were randomly subsampled and therefore relatively uniform in point density, in Sample E we gathered a majority of our points from the area of interest where we believe the glyphs to occur. The result, illustrated in ***Figure 36***, is that a small area around 'hello' where the distortion is strongest retained 3,521 out of 15,826 points, or 22.25% of the Master Cloud.

Figure 36: Sample E analysis. The sampled points [neon green] inside the inner rectangle [orange; 15,826 points] comprise 22.25% of the Master Cloud, whereas outside of this area [teal; 205,913 points] the remaining sampled points [215] amount to only 0.10% of the Master Cloud.

The surrounding area, in contrast, comprised 215 out of a possible 205,913 points, or 0.10% of the Master Cloud. This is why the colorization outside of the small area around 'hello' is virtually identical to the results of Sample D. This is significant particularly because it is how a researcher is likely to actually sample the cloud, taking

the most time to select points around areas they believe contain petroglyphs. I am compelled therefore to reject a colorization method based around manual point selection, since our findings are not only biased by the subjectivity of the process but by the natural tendency to select an irregular distribution of points. That the bias errs towards confirmation of the researcher's preconceptions and does so in a way that is difficult to detect heightens the danger it poses.

I adopted an open-minded approach to brainstorming objective alternatives, operating on the premise that uniform manipulations and sampling strategies offer fewer opportunities for the introduction of distortion and bias to the colorizations. While later continuing to experiment with downsampled clones of the Master Cloud as a route to visualizing petroglyphs, this brainstorming also led me to novel approaches. I began by experimenting with more basic methods, computing distance against a flat plane. This enabled the creation of colorizations without any alteration or manipulation of the master cloud but came at the expense of eliminating global curvature as a source of distortion. The conceptual basis for measuring against a flat plane is illustrated in *Figure 37*. In contrast to colorizations derived from a clone of the master cloud, as in *Figure 38*, we can see the failure to account for global curvature in the final product. This approach can nonetheless prove useful, is achievable by several different methods, and may be integrated into several different workflows.

One of the better methods for colorizing planar distance is also perhaps the simplest. With a mesh or cloud selected, the user navigates to the toolbar and selects Tools>Fit>Plane. CloudCompare then automatically applies a least-squares fitting algorithm to determine a plane of best fit for the cloud or mesh. Then we simultaneously select the master cloud and the plane before computing primitive distance (*Fig. 41*),

which will create a scalar field. *Figure 42* shows the results of this process applied to Loubser and Logan's (2017) scan of Judaculla Rock, with and without a corresponding texture. Though the stone is relatively flat, the dips and high points of the rock dominate the colorization. Other apparently 'flat' scans fare no better: In a colorization of Dighton Rock (*Fig. 39*) generated by the same operation, the global curvature of the rock again obfuscates glyph details so that they cannot be viewed simultaneously, regardless of changes to scalar field display parameters. The distortion is predictably greater on stones with greater curvature, as shown in a colorization of the Octoraro Creek petroglyphs (*Fig. 40*). Despite the shortcomings of this method, it does enable us to reveal some otherwise invisible glyph details by way of manipulations to the scalar field display parameters, especially on relatively flat stones.
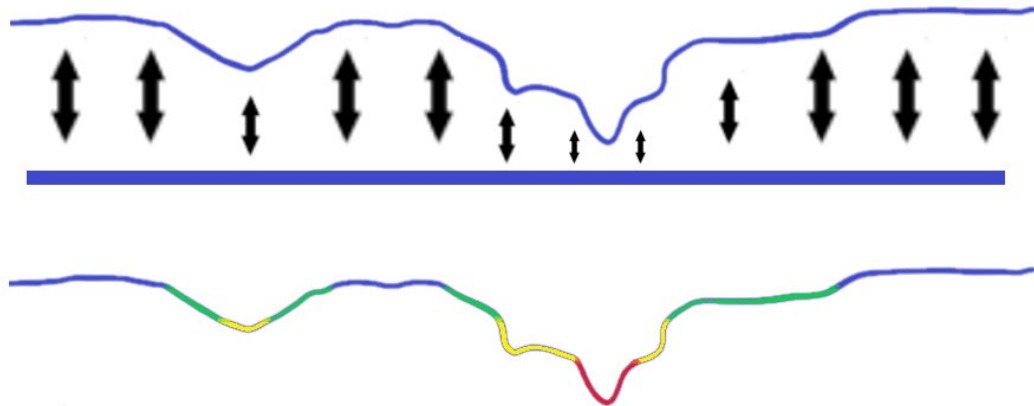
Figure 37: Cutaway section drawing illustrating the premise of the colorization process with a flat plane.
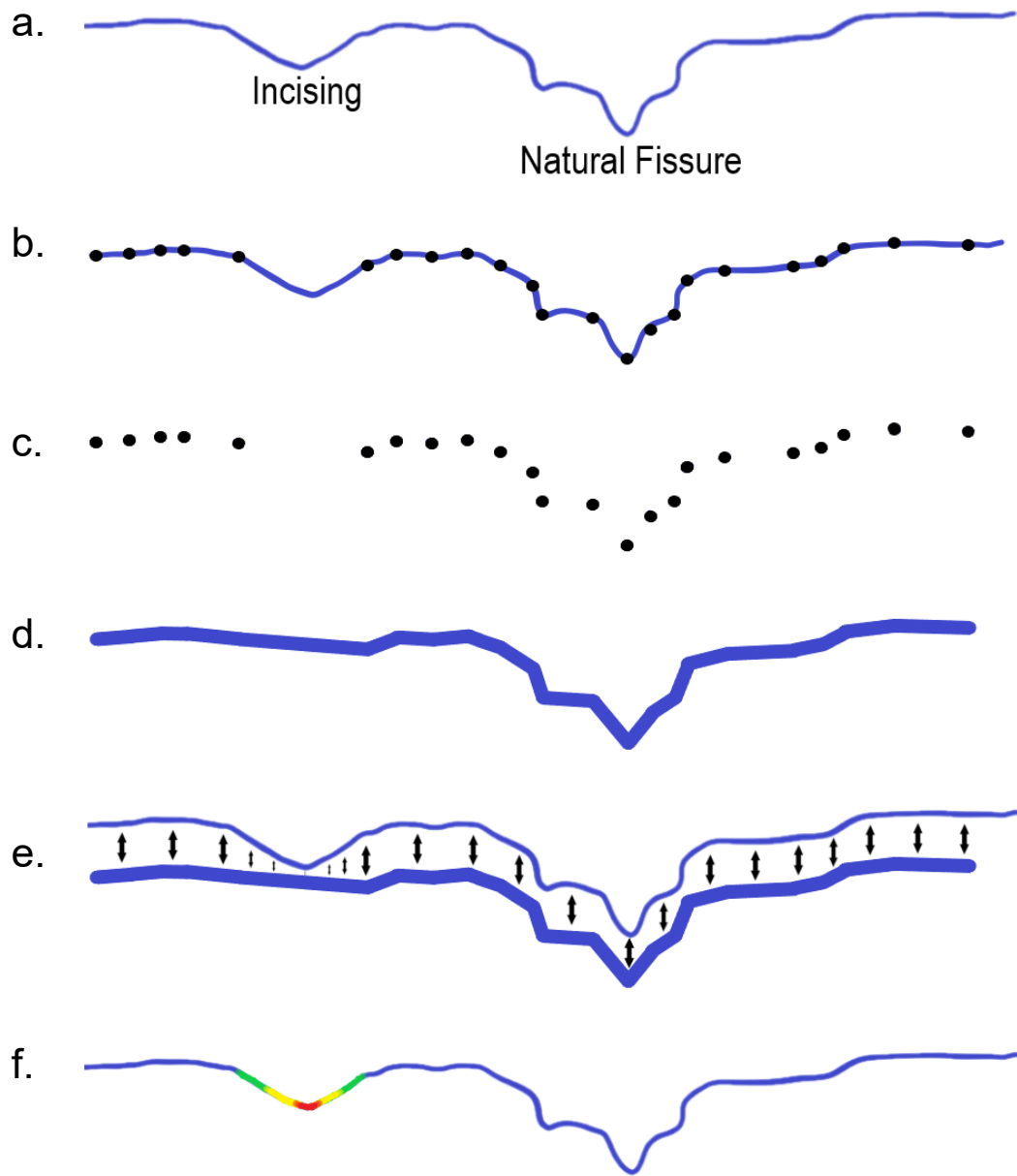
Figure 38: Cutaway section drawing illustrating the premise of DeGayner's colorization process. *a) 3D scan of rockface with petroglyphs and natural geological features, annotated; b) Point selection of unaltered rock; c) Sample of selected points (b) exported as a new point cloud; d) Low-resolution mesh reconstructed from new point cloud (c) approximating the original petroglyph-free stone – note the absence of incising; e) Distance computation between original point cloud (a) and reconstructed mesh (d); f) Colorized scalar field produced by distance computation, applied to the original point cloud or mesh.*
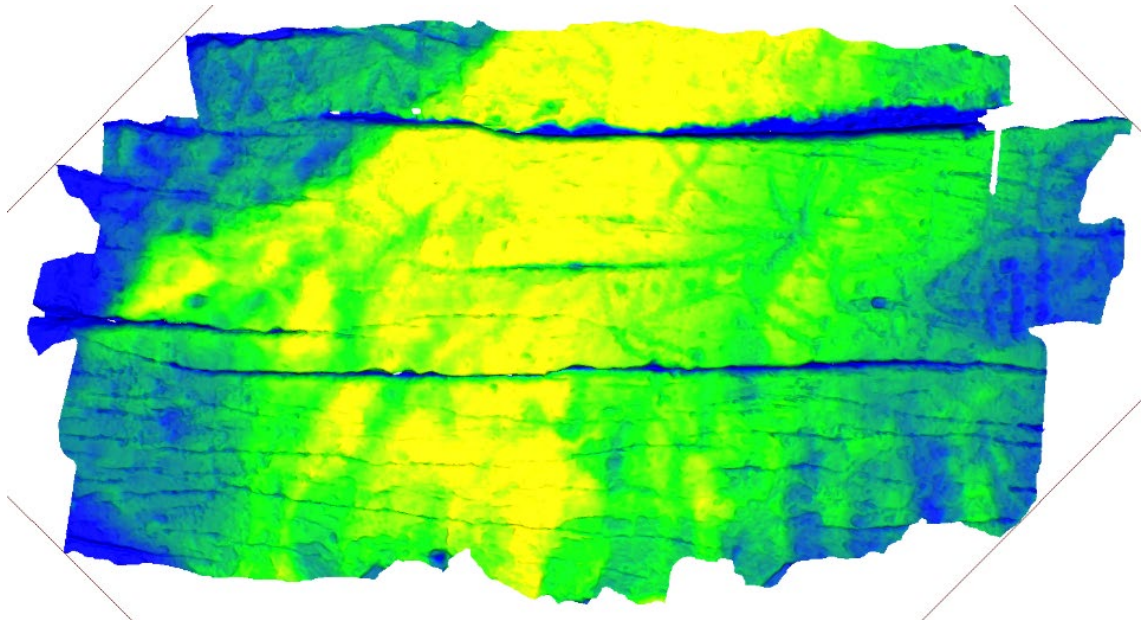
Figure 39: Dighton Rock distance computed to a fit plane.
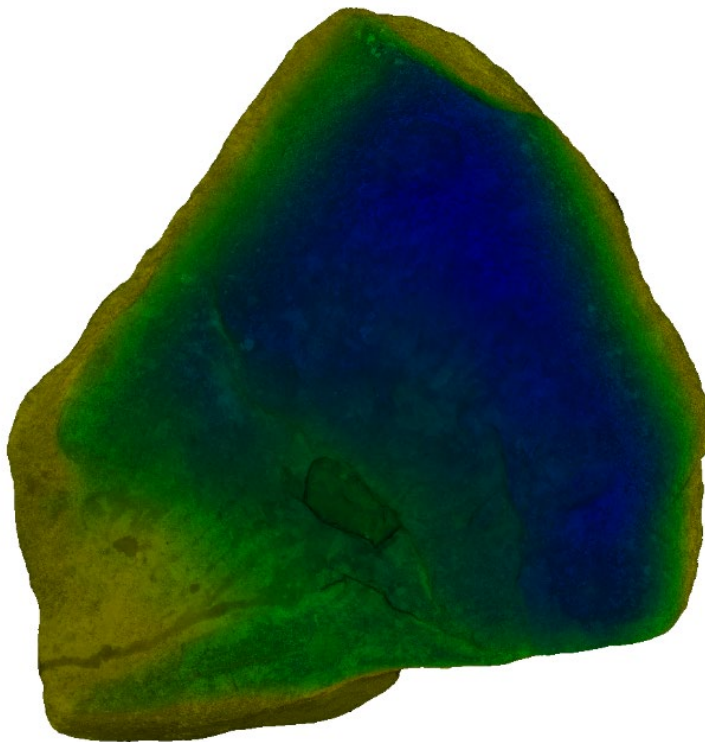
*Figure 40: Octoraro Creek Petroglyph distance computed to a fit plane. Note the
absence of identifiable petroglyphs.*
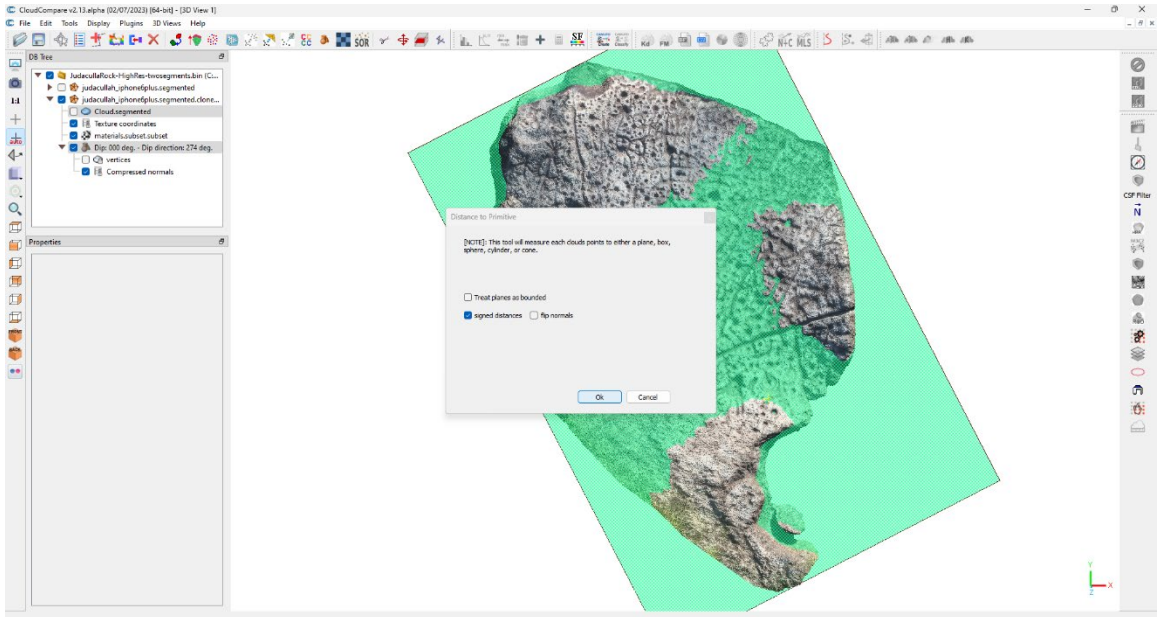
Figure 41: Judaculla Rock, measuring primitive distance to a fit plane.
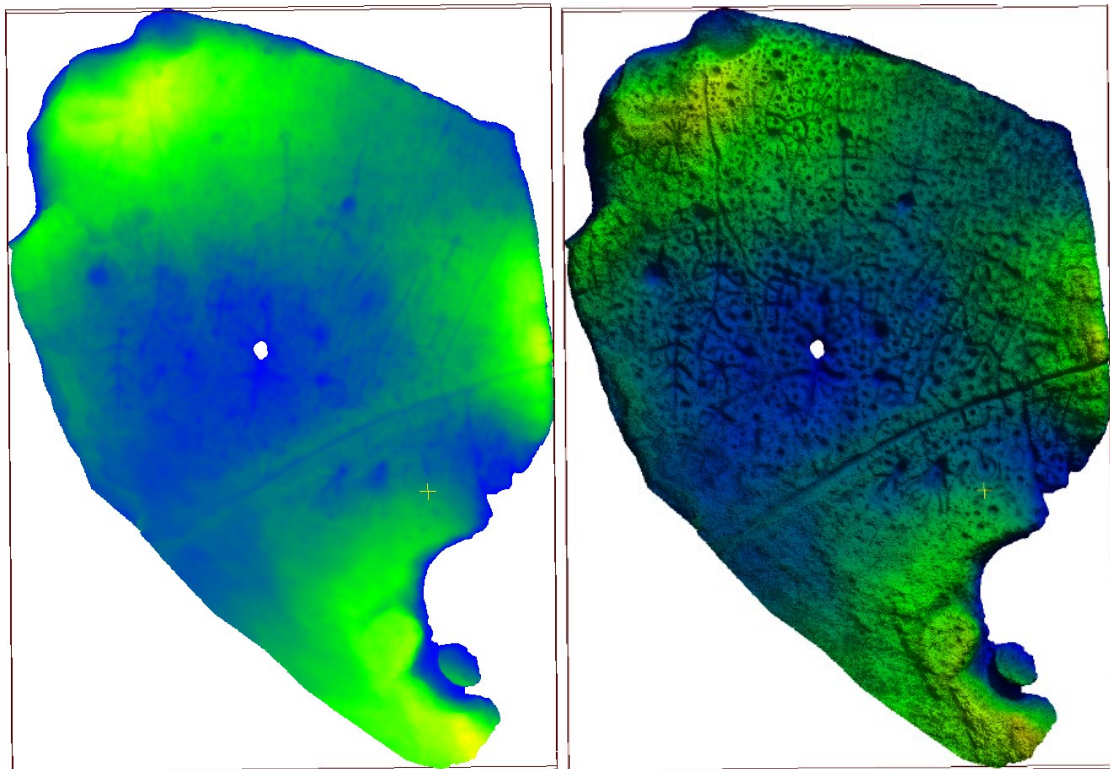
*Figure 42: Judaculla Rock distance computed to a fit plane. (left) without texture;
(right) with texture.*

While measurement against a flat plane therefore improved the objectivity of the process, pursuing an idealized schematic view would clearly require a method which eliminates global curvature. During the course of this research I learned of a relatively new tool aimed at solving our exact problem. TVT, or Topography Visualisation Toolbox, formerly known as Ratopoviz (Rock Art Topographic Visualization), is a software developed at the University of Gothenburg, Department of Historical Studies and Centre for Digital Humanities, which is designed to enhance the visibility of petroglyphs in 3D scans. TVT essentially debuted with Horn, Pitman, and Potter (2019), who outline a process in which they apply the toolkit of landscape archaeology, converting 3D petroglyph data to DEMs that may then be used to improve visualization of fine details.

Horn et al. (2022) refined this concept and created a program to automate the process. This program was made freely available to researchers as Ratopoviz but has since been renamed the Topography Visualisation Toolbox. TVT version 2.1, the latest version available at the time of writing, was used for the work presented here. TVT is comprised of two tools: a "Topographic Visualisation" tool and a "Digital Frottage" tool. Topographic Visualisation converts 3D scans into 2D raster images; in this form, it outputs depth maps, topographic maps, and normal maps among various blended versions of the same. This tool therefore produces images that are largely similar to our distance computations against a flat plane.

Topographic Visualisation also provides point cloud data (.pcd) files which may be used in the Digital Frottage tool. The Digital Frottage tool produces something more aligned with our goals as it attempts to enhance glyph details rather than merely visualize topography. The manner in which the program enhances the visibility of petroglyphs is essentially thus: 3D data is projected onto a two-dimensional plane, the image is "defocused" through Gaussian blurring, and then the pixel values of this defocused image are subtracted from the original, thereby effectively eliminating the

global curvature from the image and retaining only the fine details (Horn, Pitman, and Potter 2019:4-5; Horn et al. 2022:193-196). I applied TVT to several of the scans in our dataset and received mixed results.

Predictably, the depth and topographic maps generated by the Topographic Visualisation tool were generally dominated by the global curvature of the stone. Some of these results made the petroglyphs clearer than when measured against a flat plane, however. Moreover, the texture maps and normal maps gave useful visualizations even if they do not enhance faint markings at all. Some of the images generated had such poor contrast that they were rendered useless. While generally on par or surpassing simple measurement against a flat plane in CloudCompare, the images created by this tool lack the customizability of scalar field display parameters, while lacking the clarity and scalable image resolution also possible with scalar fields.

Applying the Digital Frottage tool presents its own problems. Though the program includes a basic user manual, it is still not entirely clear how certain parameters set by the user impact the program's operation. Additionally, the manual does not clearly enumerate how the multiple files that are produced correspond to the operations conducted by the tool. By systematic, iterative changes to the input parameters I found combinations that produced usable visualizations of the petroglyphs in our dataset, but many other combinations did not. Ultimately, I found that increasing the "Neighbourhood Size" parameter in the "Noise Reduction Settings" was necessary in order to make the petroglyphs clearly visible. With otherwise default parameters, I processed most of my dataset using the .pcd files previously generated by the Topographic Visualisation tool. This successfully eliminated most of the curvature from the visualizations (***Figs. 43-47***). Nonetheless, the images comprising ***Figures 43-47*** generally needed adjustments to brightness and contrast in order to view the petroglyphs.
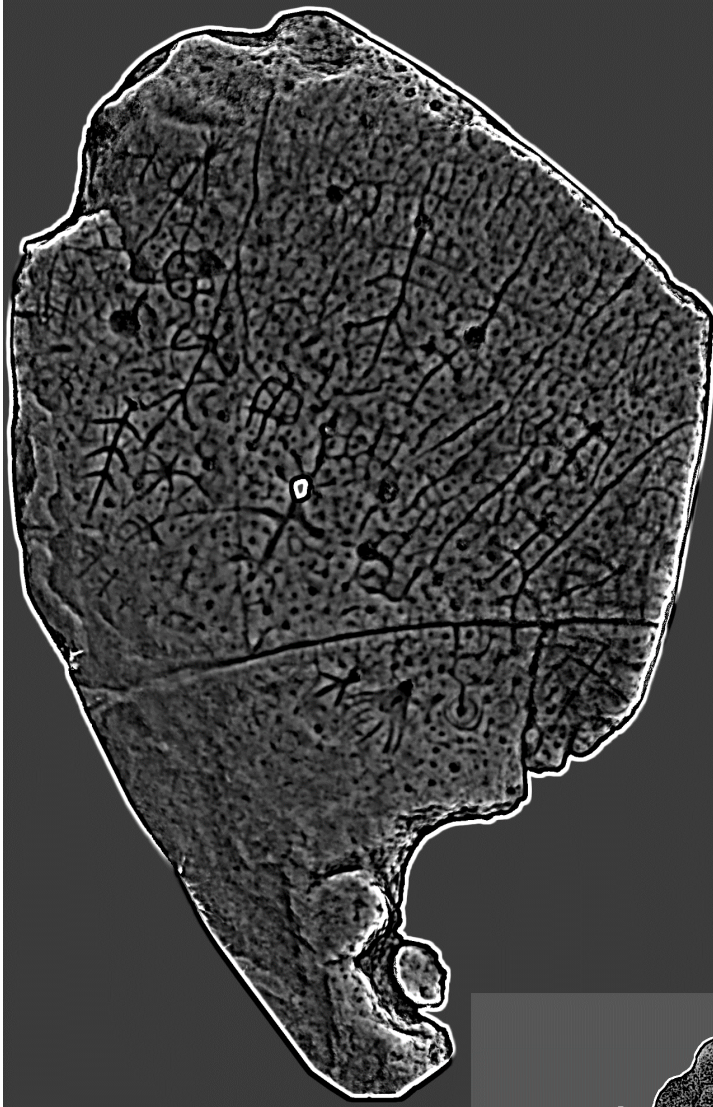
Figure 43: Judaculla Rock colorization produced by TVT.

Figure 44: Pimmit Run Petroglyph colorization produced by TVT (rotated differently from previous depictions).
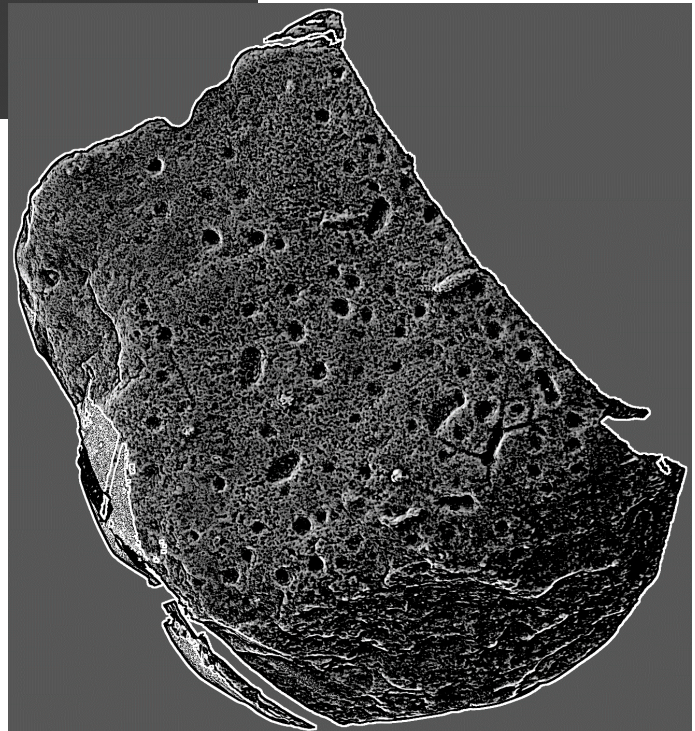
Figure 45: CHOH-26 colorization produced by TVT.
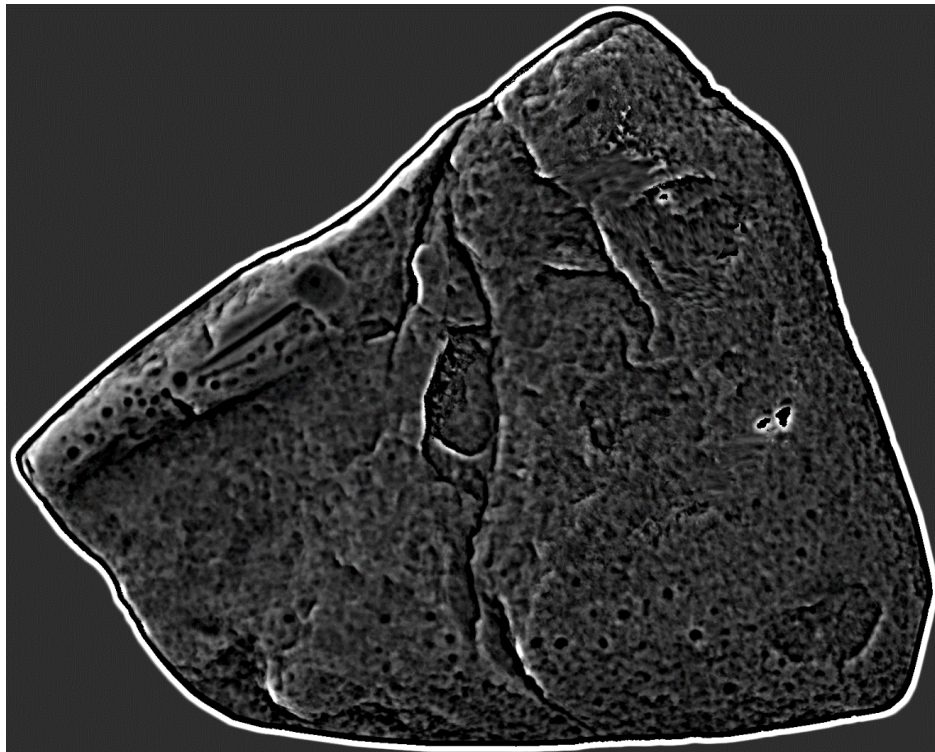
Figure 46: Octoraro Creek Petroglyphs colorization produced by TVT (rotated differently from previous depictions).

Figure 47: Dighton Rock colorization produced by TVT.

Like its sister tool, Digital Frottage suffers from several drawbacks. The Digital

Frottage tool required an excessive amount of time to complete its operation on CHOH-

26, likely due to the comparatively large size of the file. Topographic Visualisation

outputs an 'original.pcd' and a 'transformed.pcd,' and of these two the latter was

preferable as our input for Digital Frottage. The original.pcd file sometimes is not

properly oriented for use, so the tool processes the point cloud on the wrong axis.

Transformed.pcd is a transformation of the point cloud which will ensure proper

orientation in Digital Frottage; however, this may still produce an incorrect or undesired

rotation of the final image. This can especially pose a problem because image rotation is

generally a 'lossy' transformation (i.e., one that reduces image quality), although this

depends on method and degree of rotation.

Digital Frottage outputs both .tiff and .png images, and while the .tiff images are

of a higher quality, they are more difficult to work with and can display differently

depending on what program is used to view them. As previously mentioned, the tool is

somewhat difficult to control with regard to finding ideal parameters. Repeated operation

of the tool is needed to see how different input parameters change the visualization, inhibiting timely feedback to the user. Repetition is also required to change the symbology to different color ramps. For example, to view an otherwise identical image on a blue-green-red spectrum rather than a simple black-white gradient requires two operations of the tool. Contrast this with the instantaneous feedback provided by changing scalar field display parameters in CloudCompare, as well as the ease of switching between the many different color ramp options. Moreover, CloudCompare allows the creation of custom color ramps.

These issues also relate to problems common to both tools in TVT. While the toolbox automates complex processes and thereby saves users a great deal of effort, these tools still take time to run. The trial-and-error required to find ideal input parameters and the necessary repetitions to get desired visualizations compound with the time the tools take to operate. Lacking a pre-made .pcd or DEM file, applying Topographic Visualisation to a petroglyph scan represents the most sensible workflow for obtaining a .pcd file compatible with Digital Frottage. The time to operate Topographic Visualisation can therefore be included in the time it takes to run Digital Frottage. TVT additionally works entirely on the computer's central processing unit (CPU), and the authors warn about the toolset's high memory usage. This processor-intensive operation can make the performance of other tasks at the same workstation impracticable while either tool is running.

Yet, the biggest issue I identify is one of image resolution and scalability. The quality even of the higher resolution .tiff images produced by TVT cannot compare to the image resolution possible when working directly with a scan in software such as CloudCompare. With a scalar field, for example, color is assigned to each of potentially millions of points. Many images may therefore be taken at many different scales without loss of detail. In contrast, TVT offers only images of the entire scan. To see a small

detail on Judaculla Rock, for example, one could crop an image output by TVT but this image will be visibly pixelated (*Fig. 48*). One would need to crop the 3D scan itself and repeat the use of TVT in order to see the same area in the greatest possible resolution. In contrast, *Figure 49* shows the same area, with a comparable black-white color ramp achieved in CloudCompare. The file size of the latter is 2,323 times that of the cropped TVT image and contains almost 465 times the number of pixels. Moreover, this is but one of countless options for rendering the CloudCompare display. CloudCompare allows one to customize the output for a larger or smaller image, giving complete control over final resolution and scale.

The aforementioned problems are in large part a circumstantial product of our differing goals. Horn, Pittman, and Potter (2019:4-5) identify the large file sizes of 3D models as a barrier to the dissemination of petroglyph research and therefore view the significantly reduced file sizes of TVT's products as a virtue. Objective depictions of petroglyphs can be made and then easily hosted online, reproduced in print, and accessed without regard for computing power. Likewise, the limitations to user control over visualizations are a cost of simplicity and ease of use, for 3D modeling softwares can require "technical skill which potentially restricts their non-specialist use" (6). Contrary to the goals of Horn's team, this work is rather focused on developing the means to analyze 3D petroglyph data and sharing these methods with researchers so that they too can analyze petroglyph data *as specialists*. These methods do not preclude researchers from presenting their work via 2D imagery but rather expand the options for customizing presentation. I emphasize, however, the need for a process which applies colorization to three-dimensional space on an unaltered model, exhausting the capabilities of 3D data while remaining accessible to the average archaeologist. While it is clear that TVT is not a substitute for the work pursued here, it does offer us a conceptual basis for moving forward: using blurring or smoothing and subsequent

60

Figure 48: Crop of Fig. 43, created using TVT, zooming in on a specific glyph on Judaculla Rock. This image is in .png format; 42.7kb; 293x191 pixels.
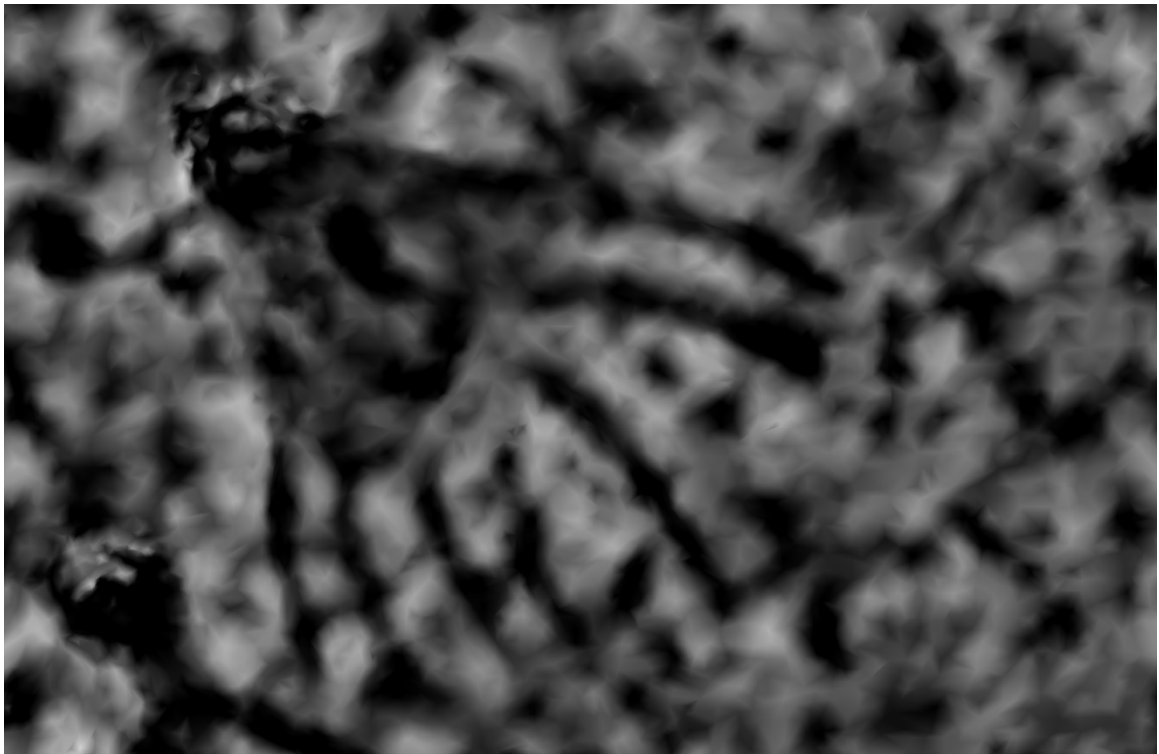
Figure 49: Visualization of Judaculla Rock in CloudCompare, zoomed to the same area presented in Fig. 48. This image is in .bmp format; 99,200kb (or 99.2mb); 6313x4121 pixels.

subtraction of a defocused simulacrum as a means of eliminating global curvature. There are multiple ways in which I suggest we might apply this concept.

The first method employed is conceptually identical to that pioneered by Trinks et al. (2005). This same concept has been reinvigorated by Zeppelzauer and Seidl (2015) and adapted by Horn et al. (2022). The approach I describe thus follows closely the procedure performed by TVT, but it is done entirely within the CloudCompare software. It therefore differs from these works in keeping the colorization process within 3D space: it does not involve 2D image projection and the final product is a colorized 3D model. We return to a distance computation against a flat plane but with the addition of procedures to eliminate curvature. The steps are as follows:

1) Fit a plane to the mesh or cloud. [With the Master Cloud or mesh selected, Tools>Fit>Plane]
2) Compute distance between the plane and Master Cloud. [With both the plane and point cloud selected, Tools>Distances>Cloud/Primitive Dist]
3) Apply a Gaussian filter to the created scalar field; the default sigma value offered by CloudCompare generally works well. [With the Master Cloud or mesh selected, Edit>Scalar Fields>Gaussian Filter>(selected sigma value)]
4) Subtract the blurred scalar field from the original scalar field [Edit>Scalar Fields>Arithmetic>(SF1 minus SF2)]

The scalar field produced by this process works very well at revealing small details in the mesh and, unlike measurement against a flat plane alone, succeeds at making them simultaneously visible. This is because the distance measurements against the plane may be characterized as the *total curvature* of the stone, including both minor and global variation in the surface. A Gaussian filter applied to the scalar field containing these distance values eliminates minute curvature and approximates the *global curvature*. Subtracting the Gauss-filtered (global) from the unfiltered (total) leaves us only with the minute curvature of the surface. Another way of framing this is to say that the final scalar field only manifests the small surface details obfuscated by Gaussian blurring.

One benefit of this approach is that, by doing the bulk of these calculations on pixel values, we save time by avoiding taxing computer operations like cloning,
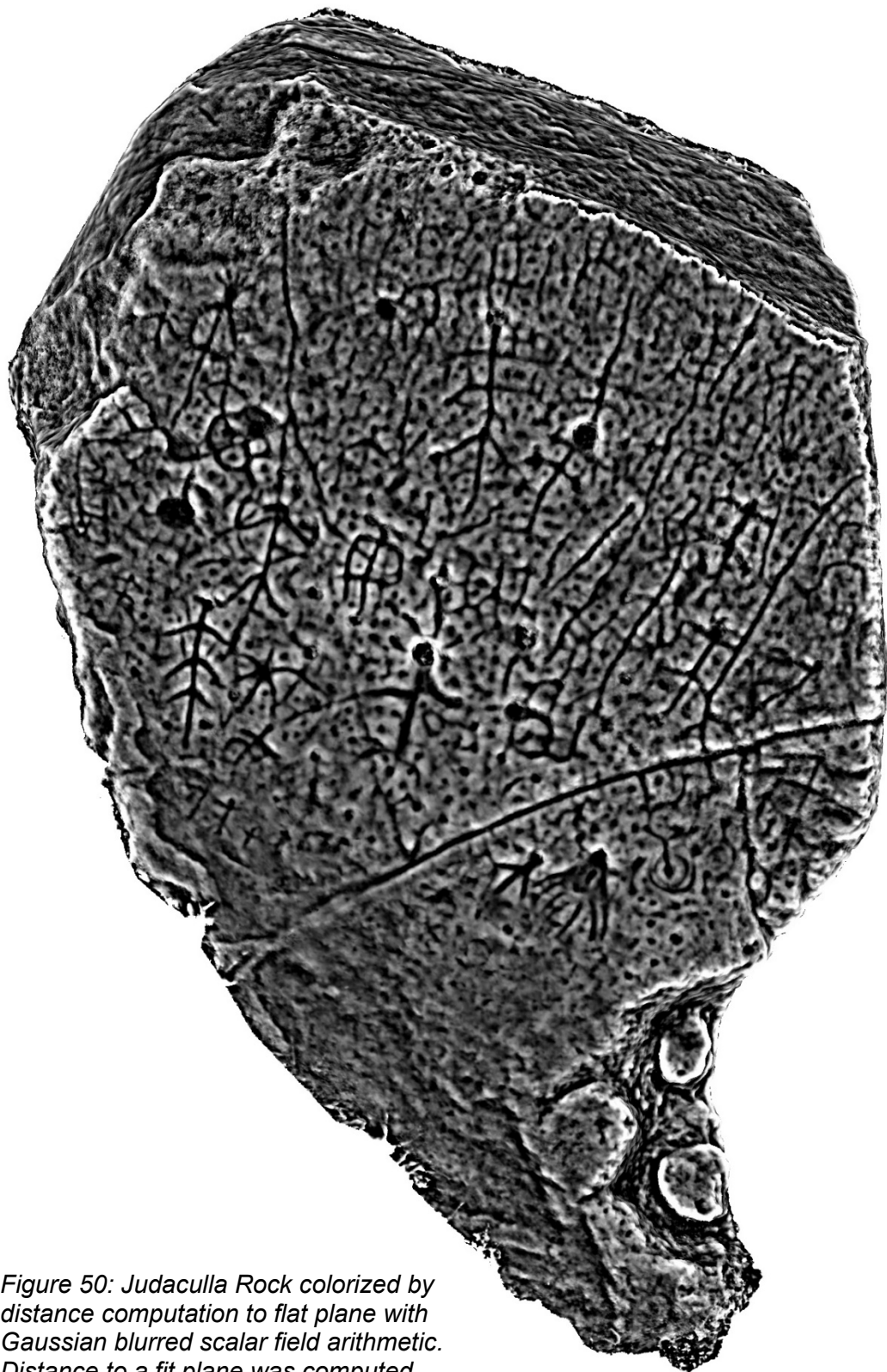
Figure 50: Judaculla Rock colorized by distance computation to flat plane with Gaussian blurred scalar field arithmetic. Distance to a fit plane was computed, then scalar field was then subjected to Gaussian blurring at 0.02925856 sigma. This scalar field was then subtracted from the original, unblurred scalar field.

manipulating, and reconstructing the original 3D scan. There are also problems with this

approach, however. As previously outlined, CloudCompare utilizes a least-squares fitting

algorithm to pair a best-fit plane to the cloud or mesh. Anywhere that the mesh is

perpendicular to the fit plane, the distance measurements will not properly capture

surface variation. This can be seen on Judaculla Rock, for example, where the

colorization of the sides is little more than meaningless noise. Thus, this method is not

capable of illuminating the entirety of any mesh with right angles. In the same vein,

performance drops off with increasingly oblique angles as the mesh moves away from

parallel to the fit plane. A laborious but serviceable workaround is to segment out such

areas, individually fitting a plane to them and repeating the process.
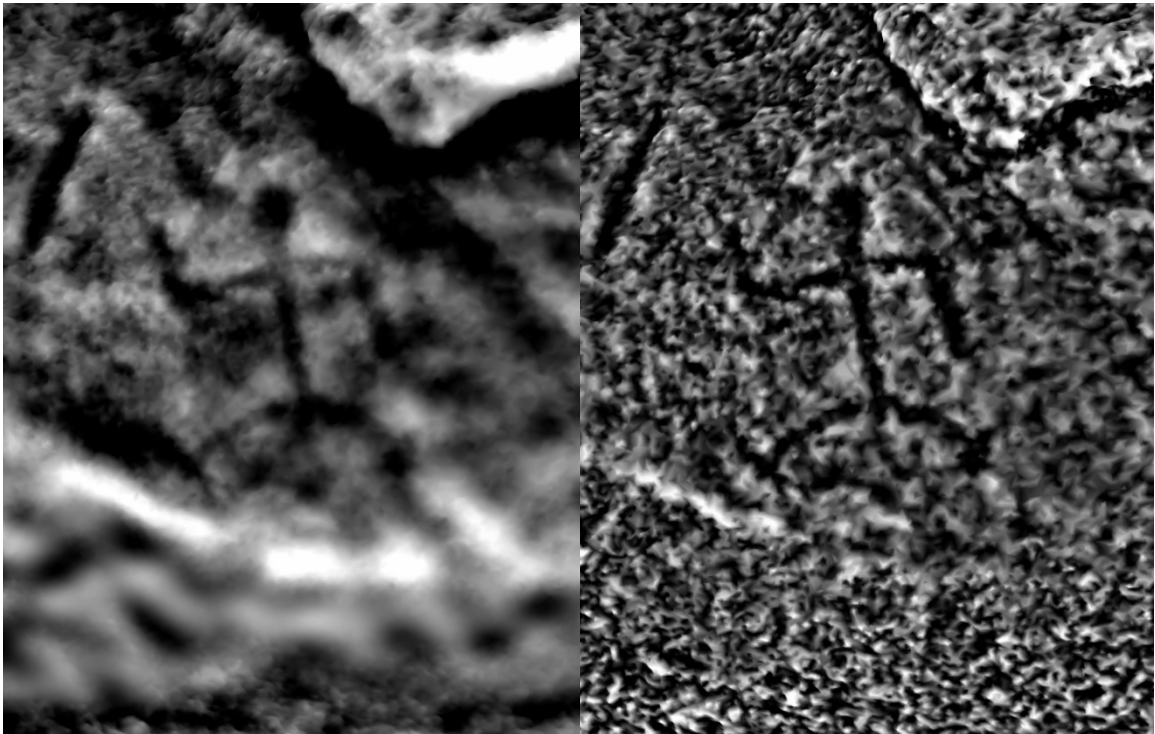
Figure 51: Detail of one side of Judaculla Rock, showing an anthropomorph. On the left (a), the colorization derived from a fit plane devolves as the mesh curves perpendicular to the plane. On the right (b), a different colorization method shows the obscured details.
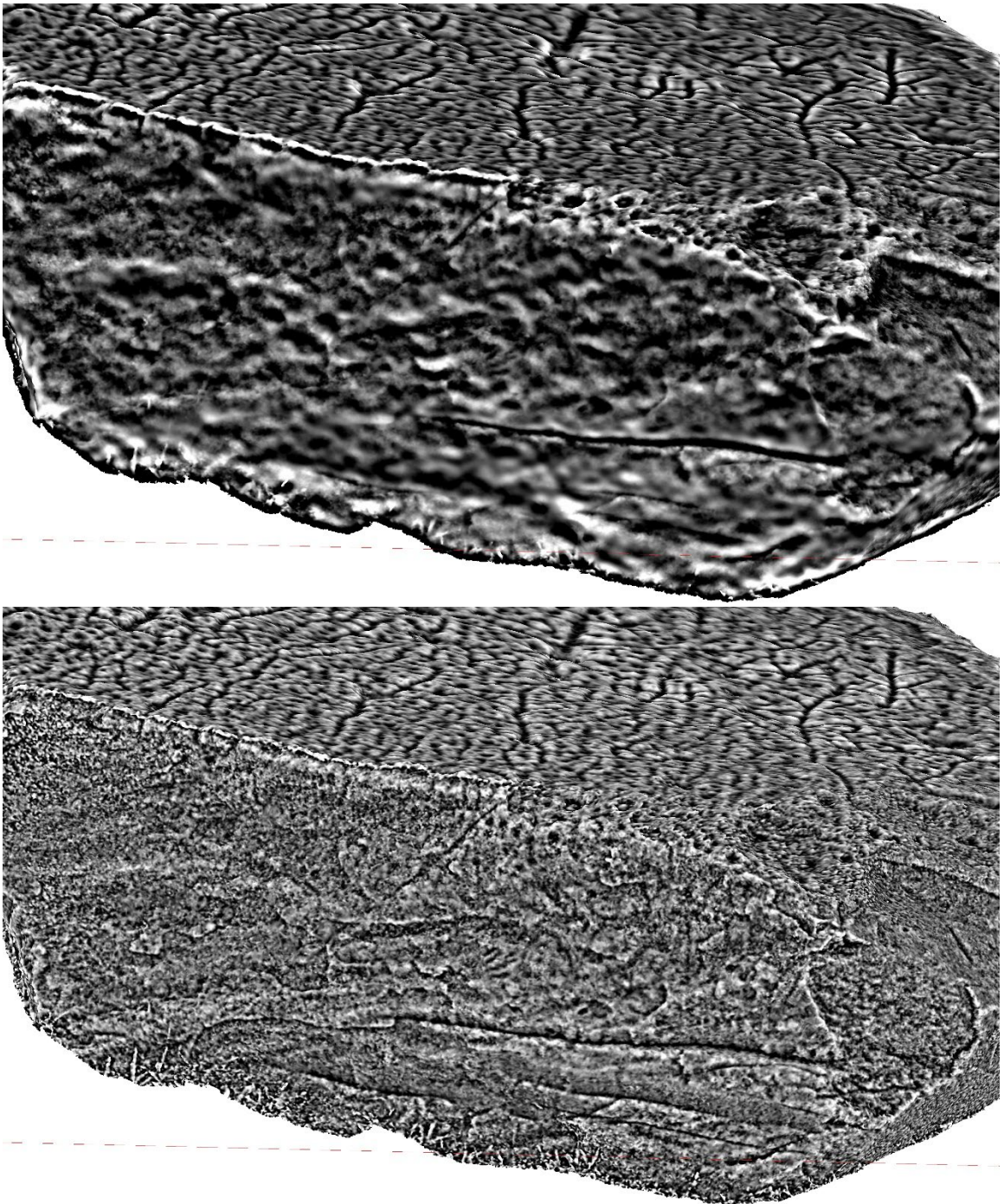
Figure 52: Another side of Judaculla Rock. On top (a), the colorization derived from a fit plane is distorted by meaningless noise. This is due to the perpendicularity of this side of Judaculla Rock to the fit plane. Below (b), a different colorization method shows the obscured details, including cupules and lines.

Another simple manner of achieving a colorization is outlined by Mark (2017). Mark exports a dense point cloud from a 3D model and opens it in CloudCompare, applies the E.D.L. shader, and finally applies the PoissonRecon plugin to the point cloud to generate a new mesh. Recognizing that "a generalized surface is fitted to the points" by PoissonRecon, Mark suggests that the "display of the points below the surface" is creating the visualization. Mark's instructions demonstrate some confusion as to the reasons for the successful colorization and also include unnecessary steps. His instructions additionally omit key details. Shading is largely immaterial to this operation. Much more important are the normals enabling shading. The cloud must have computed normals in order to use Poisson reconstruction, which generates a new mesh. It is the imperfect fit of the Poisson reconstructed mesh to the original point cloud that makes details visible, as the reconstructed mesh 'bleeds through' in areas with incising or natural depressions. The key requirements of Mark's 'digital rubbing' process then are a cloud with normals to use with the PoissonRecon tool, a different color assigned to the mesh and the original point cloud, and their simultaneous display.

By eliminating the unnecessary shader, turning off normals (which eliminates any shading at all), and using the original mesh for a backdrop rather than a dense point cloud, we get something more akin to a genuine rubbing (*Fig. 53b*) than if we follow Mark's procedures exactly (*Fig. 53a*). Though arguably producing a noisier visualization, fewer details are obscured. The benefits of these changes are more apparent with a lower resolution mesh, such as Dighton Rock (*Fig. 54*). Mark's method still produces a less than ideal visualization partly because of the aforementioned problems with using Poisson reconstruction for the simulacrum. I therefore reinvent this process through the use of a smoothed clone placed below the original mesh. Like with Mark's process, the lower resolution clone will bleed through in the areas of smoothing that become raised
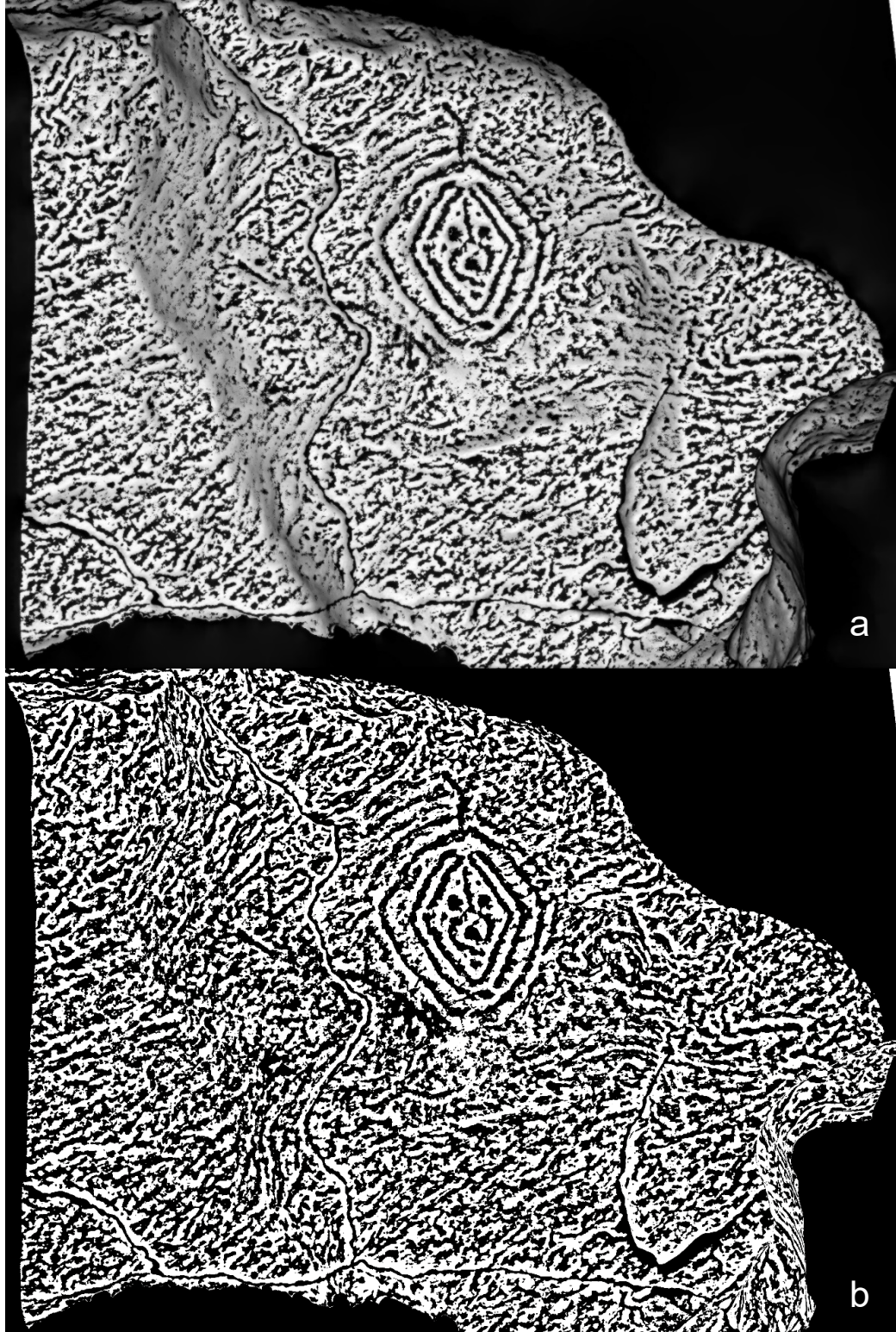
Figure 53: a) CHOH-26 "digital rubbing" following Mark's method; b) CHOH-26 "digital rubbing" with revised method.

a

b
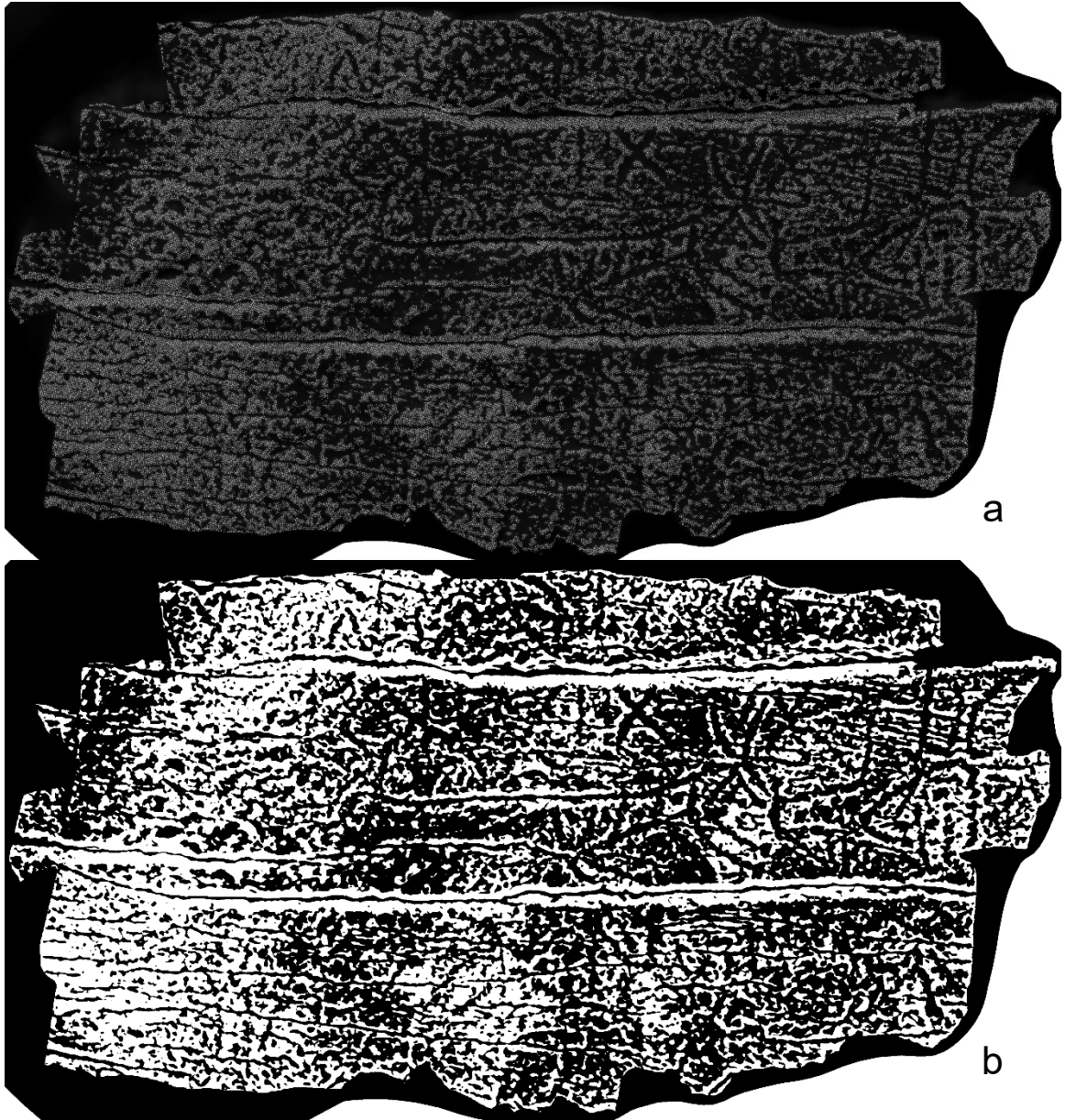
Figure 54 (above): a) Dighton Rock "digital rubbing" following Mark's method; b) Dighton Rock "digital rubbing" with revised method.

Figure 55 (right): Cutaway section drawing illustrating the premise of placing a smoothed mesh beneath the original
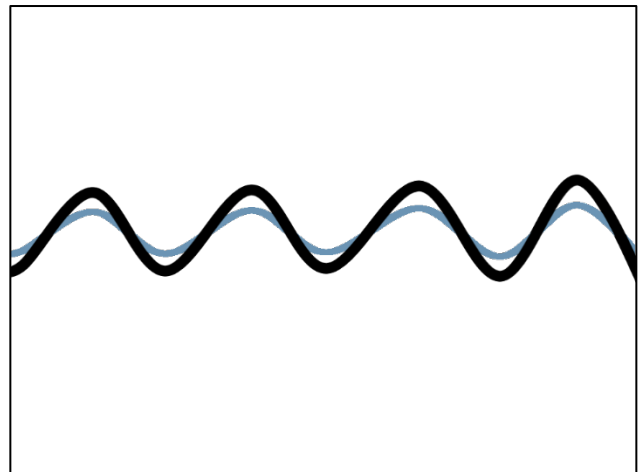
above the original mesh. **Figure 55** illustrates the concept with sine waves representing the original and smoothed meshes. The original mesh (in black) sits atop the smoothed mesh (in blue). From a top-down view, the less amplified curvature of the smoothed clone peeks through only at low points of the original mesh.

Applying Laplacian smoothing to a clone of CHOH-26 produces a viable if heavy-handed colorization of the site's petroglyphs. This method unfortunately includes significant noise from the natural irregularities in the rock's surface. This approach also requires that one set unique color values for each mesh in order to create a visual contrast, which is primarily a disadvantage where the original rock texture is attached to the scan via the RGB color channel. **Figures 56-59** show the application of this method.

The images also show that with a progressive increase in smoothing, more of the cloned mesh comes through and lines both natural and anthropogenic become more distinct, albeit with a commensurate loss of fine detail. **Figures 56-57** show the original mesh in black and the smoothed mesh in white, while **Figures 58-59** show the colors reversed. The cloned meshes in **Figures 57-58** have been equally smoothed; **Figure 56** shows the least smoothing and **Figure 59** evinces the greatest smoothing. This approach appears useful for quick, binary segmentations but is limited both in customizability of the visualization (compared to a scalar field) and in the obtainable clarity of visualization.

The third method I attempted simply takes the previous method a step further. We compute distance between the Master Cloud and a downsampled or smoothed clone to imprint the difference on a scalar field. The methods used here build upon my findings in experimenting with DeGayner's method. After additional trial and error, I homed in on a couple procedures for generating the simulacrum mesh which seemed to
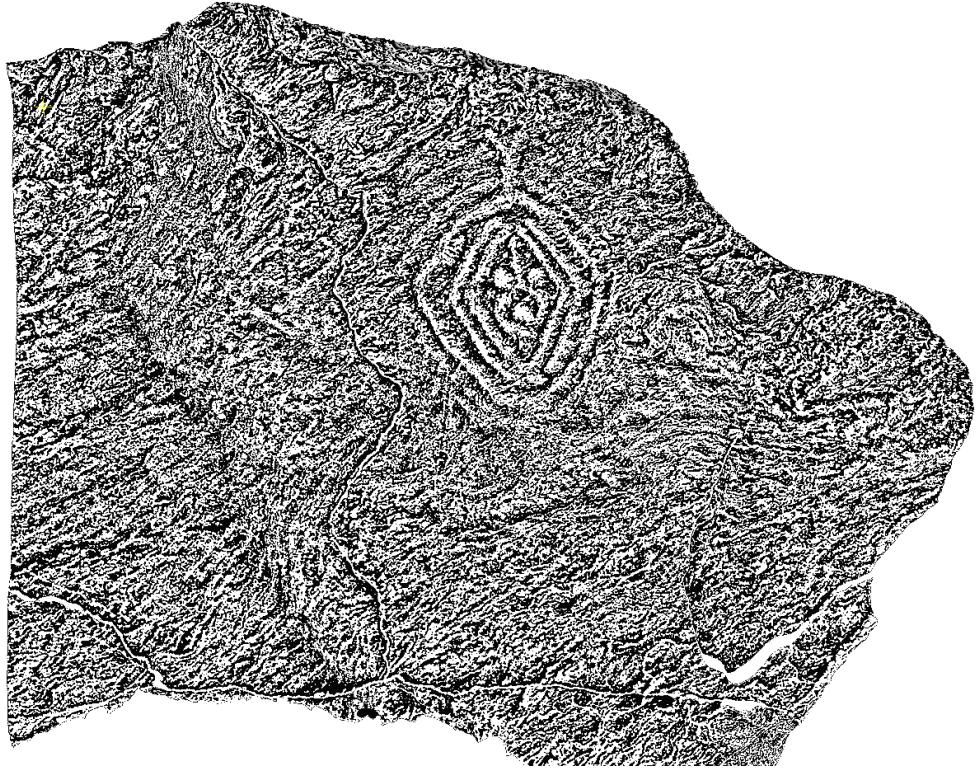
Figure 56: CHOH-26 smoothed once, color set to white, against backdrop of the original, color set to black.
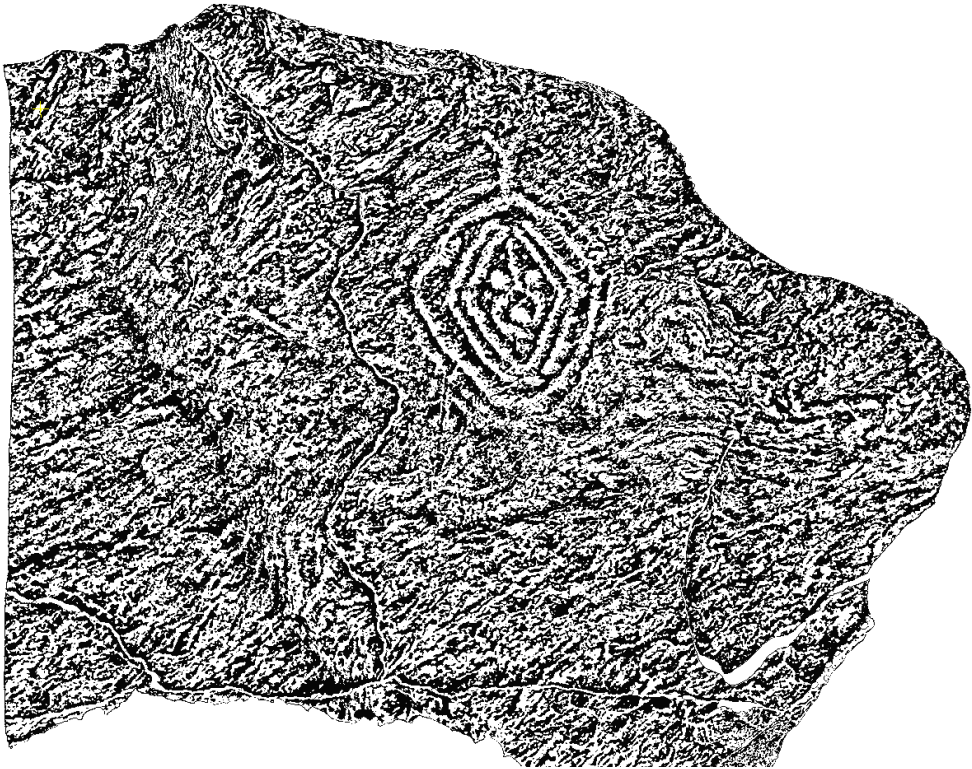
Figure 57: CHOH-26 smoothed three times, color set to white, against backdrop of the original, color set to black.
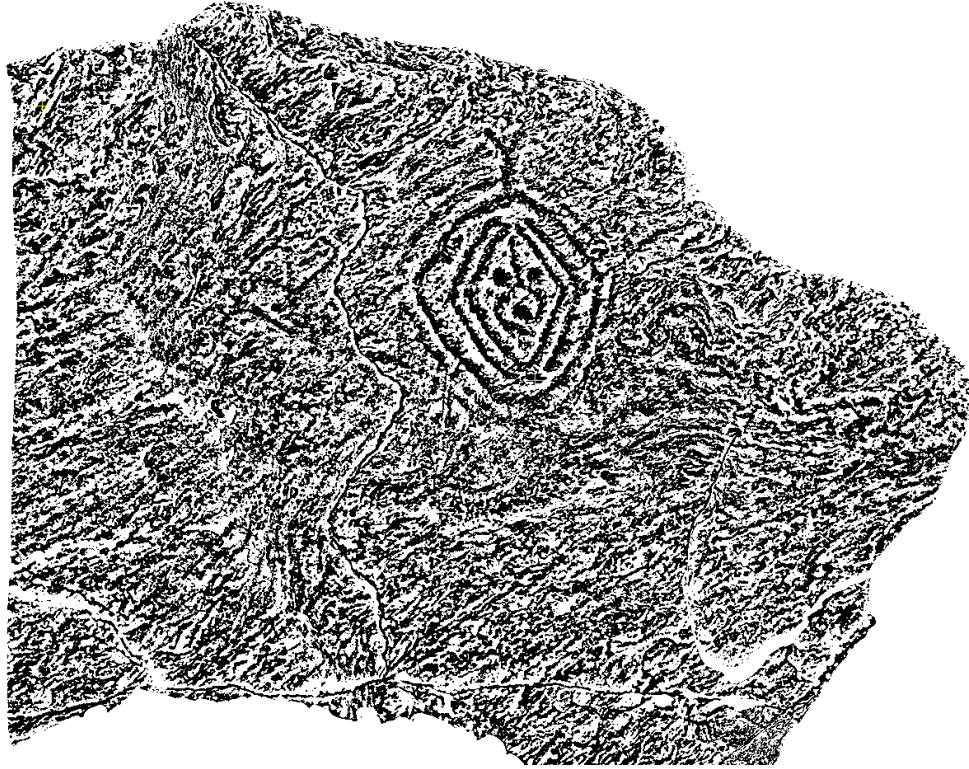
Figure 58: CHOH-26 smoothed three times, color set to black, against backdrop of the original, color set to white [i.e., Fig. 57 with color inverted].
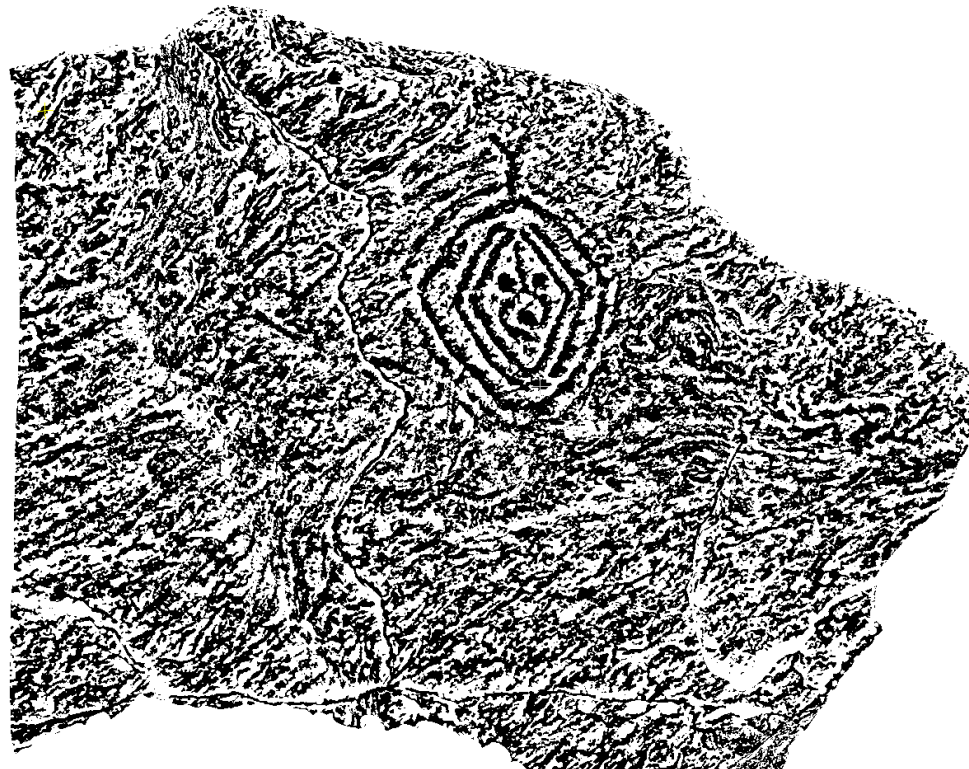
Figure 59: CHOH-26 smoothed six times, color set to black, against backdrop of the original, color set to white.

work best under certain conditions. The first route is characterized by subsampling the point cloud to create a new, downsampled mesh, while the second option is to clone and smooth the original mesh. With either approach there is still considerable room for variation.

Subsampling of the Master Cloud may be accomplished via space, octree, or randomly. That is, the user can set minimum space between points, octree subdivision level, or specify the number of points to randomly sample. The principle by which visualization is achieved is the same: distance measurement between the original scan and a simulacrum of the unaltered stone. Yet, rather than using Gaussian blurring or Laplacian smoothing alone to form the simulacrum, 'smoothing' is achieved by feeding fewer points to the mesh-creation process. This gives us a simulacrum that retains global curvature but lacks fine surface detail. The problem with this is that 'smoothing' by this method is anything but smooth, and each of the three sampling strategies produced equally poor results by themselves. I therefore found it necessary to apply Laplacian smoothing to the subsampled mesh before computing distance, otherwise the jaggedness of the recreated mesh leads to an arbitrarily mottled visualization. I found it expedient and effective to subsample between one and ten percent of the original mesh.

Our second option is to simply clone the mesh and use Laplacian smoothing exclusively to generate the simulacrum. While the input parameters for Laplacian smoothing can be freely adjusted, numerous trials with several scans from our dataset suggested that between twenty and forty iterations conducted at a smoothing factor of 0.2 worked well for visualizing glyph details (*Fig. 62*). In all trials to this point, the colorizations created by simply cloning and smoothing the original mesh evinced improved detail compared to colorizations derived from a subsampling approach. Moreover, the Delaunay-generated mesh tends to imperfectly recreate anything but very
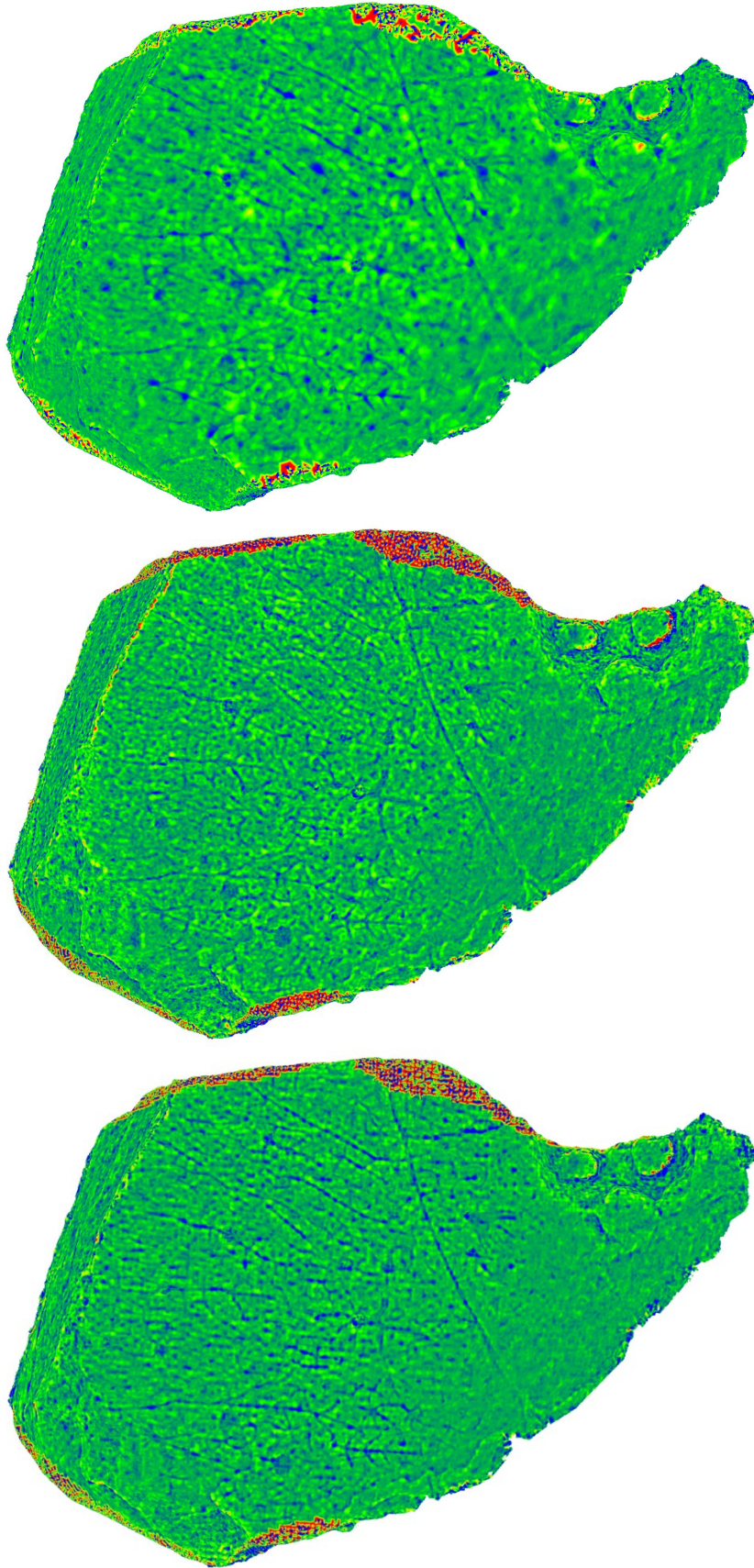
Figure 60: Colorizations of Judaculla Rock generated by distance computation to a reconstructed mesh. These meshes were generated by subsampling the master cloud via three methods. From left to right: octree (7), space (0.0589), randomly by specified points (23,088).
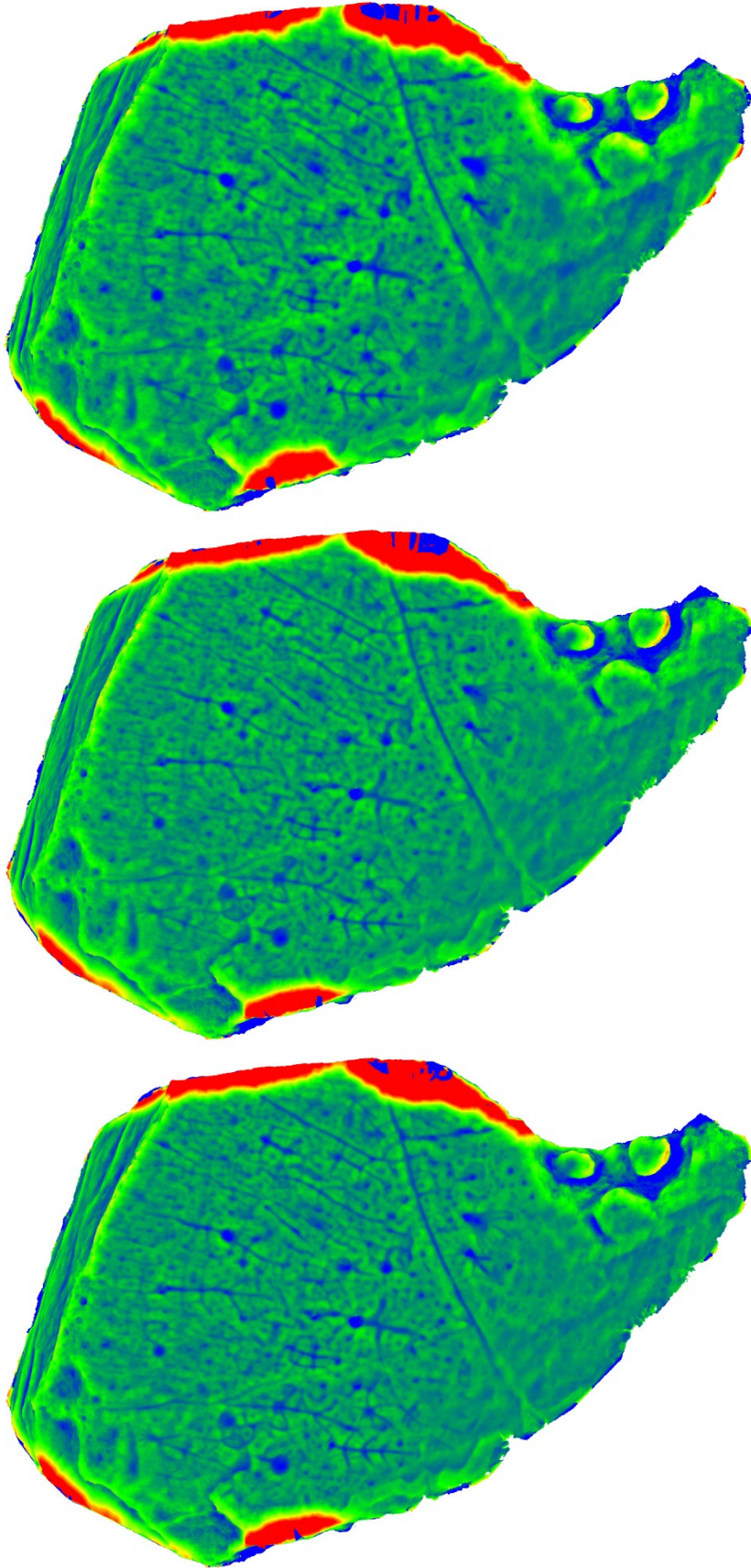
Figure 61: Colorizations of Judaculla Rock generated by distance computation to a reconstructed and smoothed mesh. These meshes were generated by subsampling the master cloud via three methods, then smoothing twenty iterations at a smoothing factor of 0.2. From left to right: octree (7), space (0.0589), randomly by specified points (23,088).
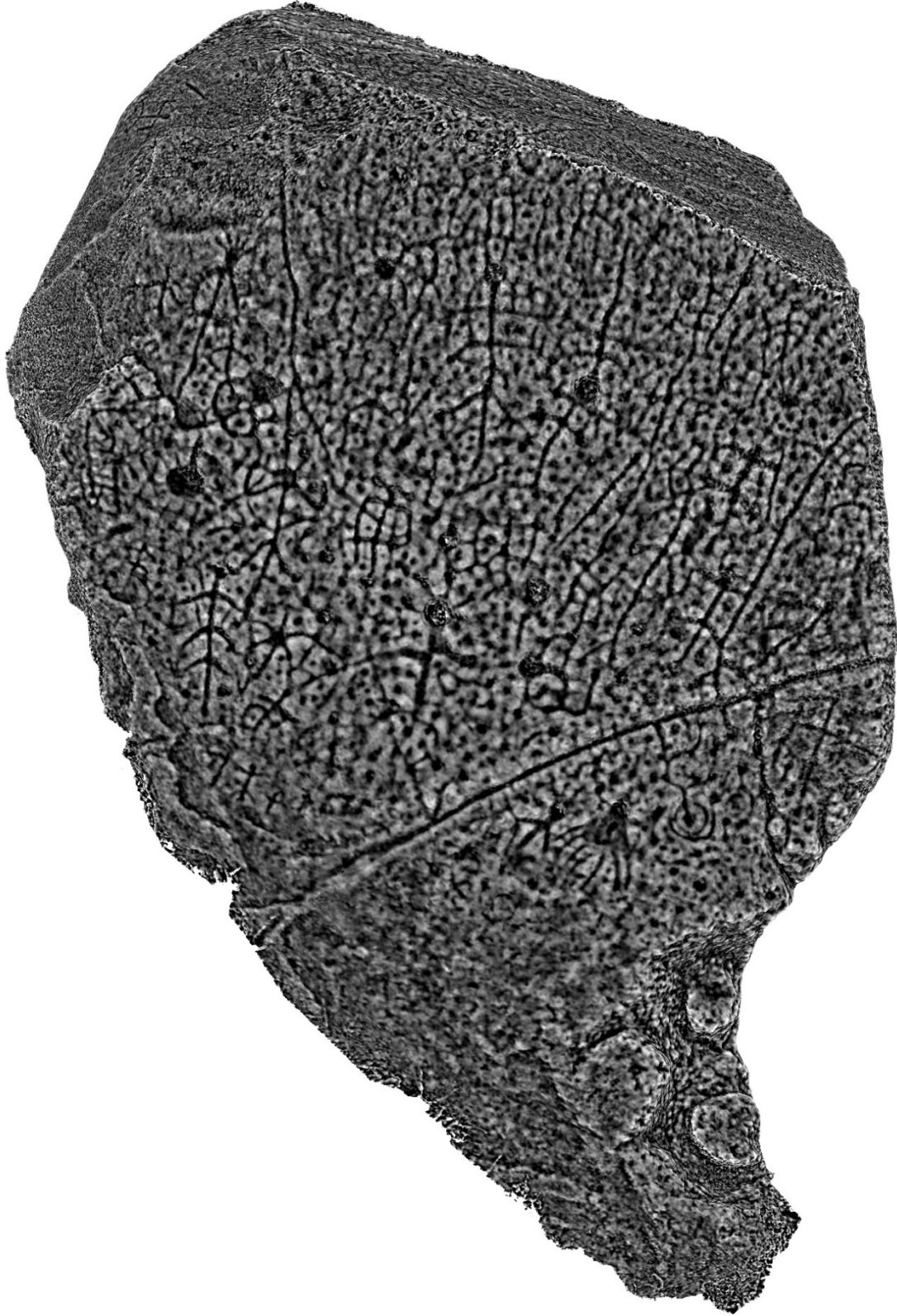
Figure 62: Colorization of Judaculla Rock generated by distance computation to a smoothed clone. The cloned mesh was smoothed 20 iterations at 0.2 smoothing factor.

flat scans. Similar to methods employing a fit plane, this results in completely inaccurate and mottled colorizations around curves and the sides of rocks.

The three most promising methods outlined thus far then are distance to a fit plane with scalar field arithmetic, distance to a subsampled reconstruction, and distance to a smoothed clone. Yet, in comparing the three, the latter approach initially appeared superior. The former two routes offered only a couple of minor advantages. The first is that they are faster operations; however, the time savings were minimal since none of the operations required more than around twenty minutes to complete. The second advantage may be more aptly described as a disadvantage viewed in a positive light. The diminished detail of the first two approaches results in bolder and less ambiguous lines – at the expense of missing the most faint or eroded carvings. However, this same effect may be achieved by applying Gaussian blurring to the highly detailed visualization derived from a smoothed clone. Thus, there is little argument for preference on this account. The failure of the first two methods, however, to truly depict surface details in all three dimensions offers a glaring disadvantage.

On the verge of accepting the primacy of using a smoothed clone for all colorizations, I conducted work on CHOH-3. This scan possessed a much greater number of points than any of the other scans heretofore experimented upon. The mesh for CHOH-3 was cloned and smoothed twenty iterations at a smoothing factor of 0.2 (**Fig. 63**). Surprisingly, I found the results incongruent with my results using the same process on other scans. The final visualization did not remotely enhance the visual contrast of known carvings on the stone, whereas a colorization using a one percent subsample of the point cloud returned an extremely effective visualization. From personal observation of the stone and documentary evidence, I knew that CHOH-3 is approximately the same size or smaller than other sites in our dataset. Yet, the collected point data for CHOH-3 outnumbers our next largest point cloud by a factor of nine. This

led me to hypothesize that point cloud density played a key role in the failure of what had been so far an ideal method. I had throughout this work increasingly suspected that the number of points collected relative to the real-world area covered by the scan posed an unavoidable problem as an uncontrolled variable needing to be addressed.

I therefore first resolved to attempt a task that had previously appeared fraught with uncertainty: determining the relationship between a real-world unit of measurement and the distances returned in 3D modelling software. To this end, I gathered what documentation existed that could indicate the size of the petroglyph stones and individual carvings. This information could then be cross-referenced with distance measurements taken in CloudCompare to deduce the unit of measurement used by the 3D model. The unit used in some scans could be said with greater certainty.

CHOH-3, CHOH-26, and the Pimmit Run boulder were well documented by Doering and Collins (2013), and I found these scans consistently used millimeters as their standard unit. Despite its long history, Dighton Rock lacked well documented measurements. I therefore relied on the NRHP nomination form (Hale 1971), rough descriptions and photographs of individuals next to the stone for scale. Fortuitously, the extremely small unit of measurement helped eliminate other possibilities and I determined with relative certainty that the scan used tenths of a millimeter. Judaculla Rock proved likewise difficult to find measurements for, but a detailed diagram with thirty-centimeter scale produced by Loubser, Ashcraft, and Wettstaed (2018:209) led me to conclude that the high-resolution scan reports distance in half meters.

With this information I was able to calculate the points per square meter of real-world surface area (i.e., point density) in each scan. The results are shown in **Table 3**. Though there is still some uncertainty to these conversions without further corroboration through fieldwork or additional documentation, they approximate the point densities sufficiently well.

Table 3. Surface Areas and Point Densities of Petroglyph Scans

Name	Site No.	Points	Surface Area	Calculated Point Density
CHOH-3	None	24,241,975	5.152 m^2	4,705,498.42 p/m^2
CHOH-26	18MO0134	2,586,346	3.566 m^2	725,232.53 p/m^2
Pimmit Run Petroglyph	44FX3079	1,433,999	2.064 m^2	694,625.61 p/m^2
Octoraro Creek Petroglyphs	18CE0398	502,307	15.539 m^2	32,325.65 p/m^2
Dighton Rock	BRK.902	221,739	1.521 m^2	145,820.48 p/m^2
Judaculla Rock	31JK0003	1,086,538	24.577 m^2	44,209.55 p/m^2
Reef Bay Petroglyphs	[Unknown]	972,129	11.629 m^2	83,593.80 p/m^2
Embden Petroglyphs	ME069.004	7,898,155	14.818 m^2	533,022.98 p/m^2

Table 4. 3D Scans of Additional Petroglyph Sites Employed in the Final Portion of This Study

Name	Site No.	Location	Source	Triangles	Vertices	Skin	Size	File	Equipment
Reef Bay Petroglyphs	[Unknown]	St. John, U.S. Virgin Islands	Mark 2022 [sketchfab.com]	1,935,104	972,129	1	88.6 mb	.ply[1]	[Not given]
Embden Petroglyphs	ME069.004	Somerset County, Maine	NEARA 2023 [sketchfab.com]	15,609,542	7,898,155	1	464.0 mb	.ply[2]	[Not given; likely iPhone 6 Plus or newer model]

[1] Converted from .fbx format
[2] Converted from .glb format

These calculations comprise the beginning steps in a final process I developed for colorizing petroglyph detail, offered in **Appendix B**. Possessing information about point density equipped me to adapt my previously outlined methods so that they could work with very detailed scans like CHOH-3. More importantly, control of this variable aided me in systematizing the colorization process so that it may flexibly work with the many different contexts in which it may be applied.

I selected the attributes of Loubser and Logan's (2017) Judaculla Rock scan as a baseline for devising this process since the smoothing-based colorization performed excellently at revealing small glyph details. This scan had a point density of 44,209.55 p/m^2, and the clone used in the colorization was smoothed twenty iterations at a smoothing factor of 0.2. This formed the basis for two formulas, each for a different method of achieving a colorization: Formula A would govern distance computations to a smoothed mesh clone, while Formula B would govern distance computations to a subsampled, reconstructed mesh. I chose to set 45,000 p/m^2 as a benchmark for smoothing a clone twenty iterations at 0.2 smoothing and assumed a direct linear relationship between the appropriate number of iterations and point density. Likewise, 45,000 p/m^2 was used in Formula B as an ideal point density to subsample a cloud down to for reconstruction.

With these formulas, both methods were able to effectively colorize the glyphs on CHOH-3 (*Figs. 64-65*). The application of these formulas also delivered positive results with other high-density scans by Doering and Collins (2013). Trials with different benchmarks moreover did not produce better visualizations, and the formulas were therefore not altered. After confirming the usefulness of this revised system on various scans in the dataset, I sought to test this method on a few new, unfamiliar scans.
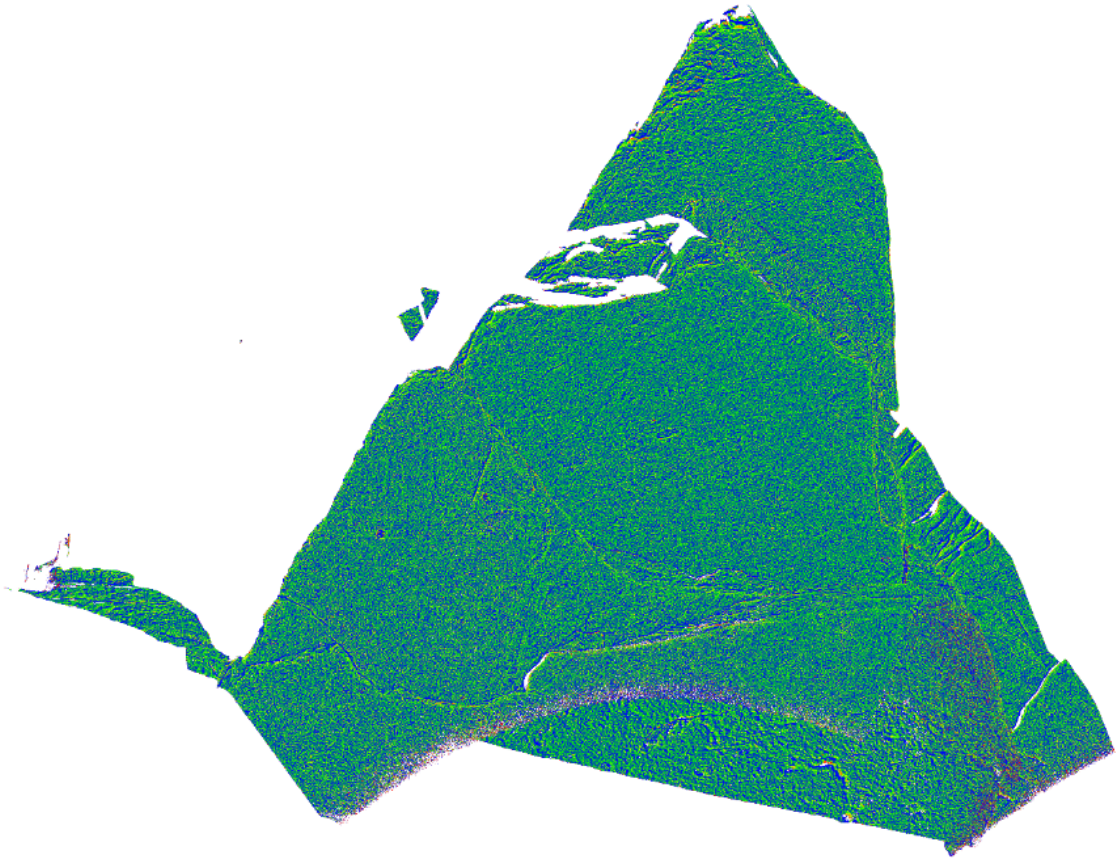
Figure 63: CHOH-3 smoothed 20 iterations at 0.2 smoothing factor.
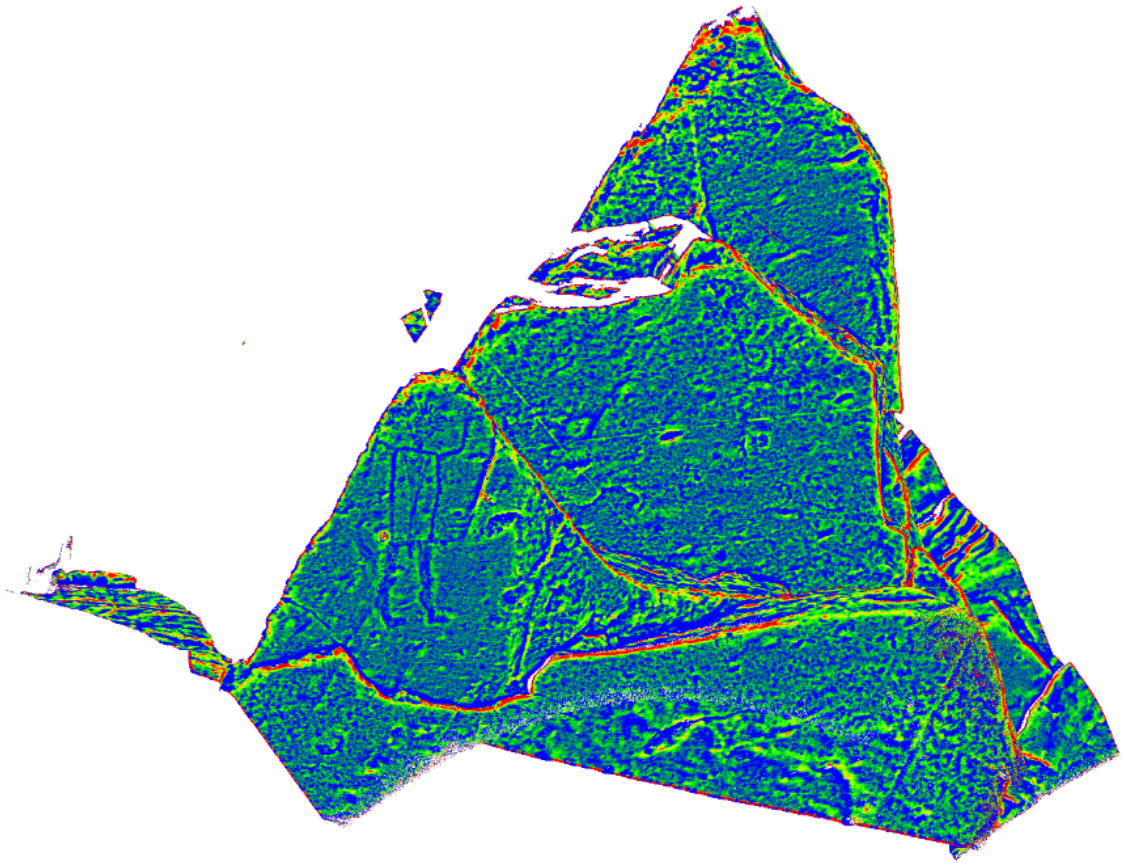
Figure 64: CHOH-3 smoothed 2000 iterations at 0.2 smoothing factor.
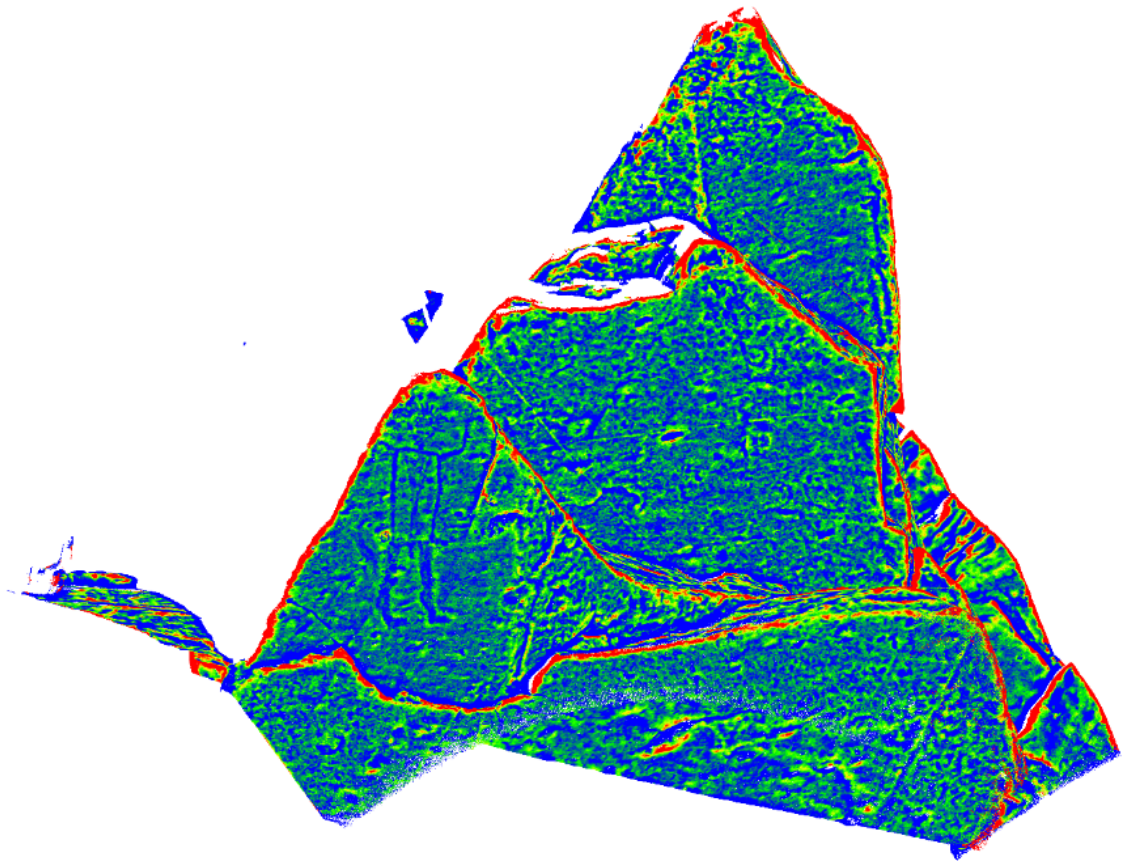
Figure 65: CHOH-3 subsampled to 45,000 points per square meter and smoothed 20 iterations at 0.2 smoothing factor.

I first downloaded a 3D model of a petroglyph stone found on the Kennebec River near Embden, Maine from the Sketchfab website. This scan was apparently recorded as well as uploaded by a member of the New England Antiquities Research Association. Like with the Dighton Rock scan, this data was therefore subjected to greater scrutiny. However, the scan appears to be the unaltered product of now commonplace consumer-grade scanning software, and the authenticity of the glyphs themselves is well-established. Having judged this 3D model to be unadulterated, I followed the process outlined in **Appendix B**. The scan came in .glb file format, which CloudCompare cannot read. I therefore used Aspose.3D, an application programming interface for the Python programming language, to run code that would convert the petroglyph scan into a .ply format. I was then able to open the file in CloudCompare.

I compared distance measurements on the scan to measurements on sketches made by E.W. Moore in 1894 and in a photo by Lenik (2002:57) to deduce the unit of measurement. After converting the surface area of the scan output by CloudCompare into square meters, I was able to calculate point density to use in Formula A. Determining that 237 iterations were needed at a smoothing factor of 0.2, I then generated a colorization by distance computation to a smoothed clone. Likewise, I used Formula B to determine the number of points to retain in a random subsample, and from here I followed the process for generating a colorization from a subsampled cloud. These colorizations are shown in *Figures 66-67*.

Crack-like fissures (*Fig. 68*) appear throughout the visualization created by smoothing the mesh; this is likely caused by scanning with an iPhone, as available applications typically stitch together smaller scanned areas to create a larger model. This was remedied in *Figure 67* by reconstructing the mesh from the original cloud as we would with a subsampled cloud. However, on some scans this will result in loss of visualization accuracy around the sides of a stone.
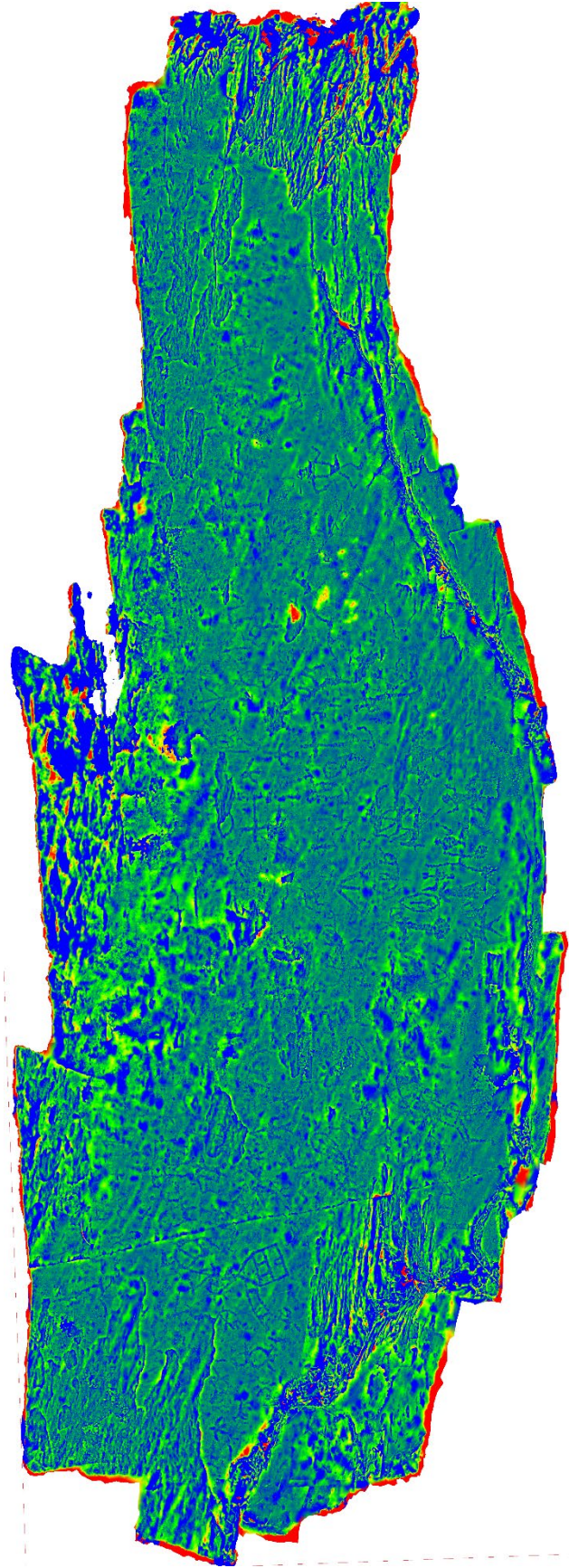
Figure 66: Embden Petroglyphs, subsampled (random 666,795 points), smoothed 20 iterations at 0.2 smoothing factor.
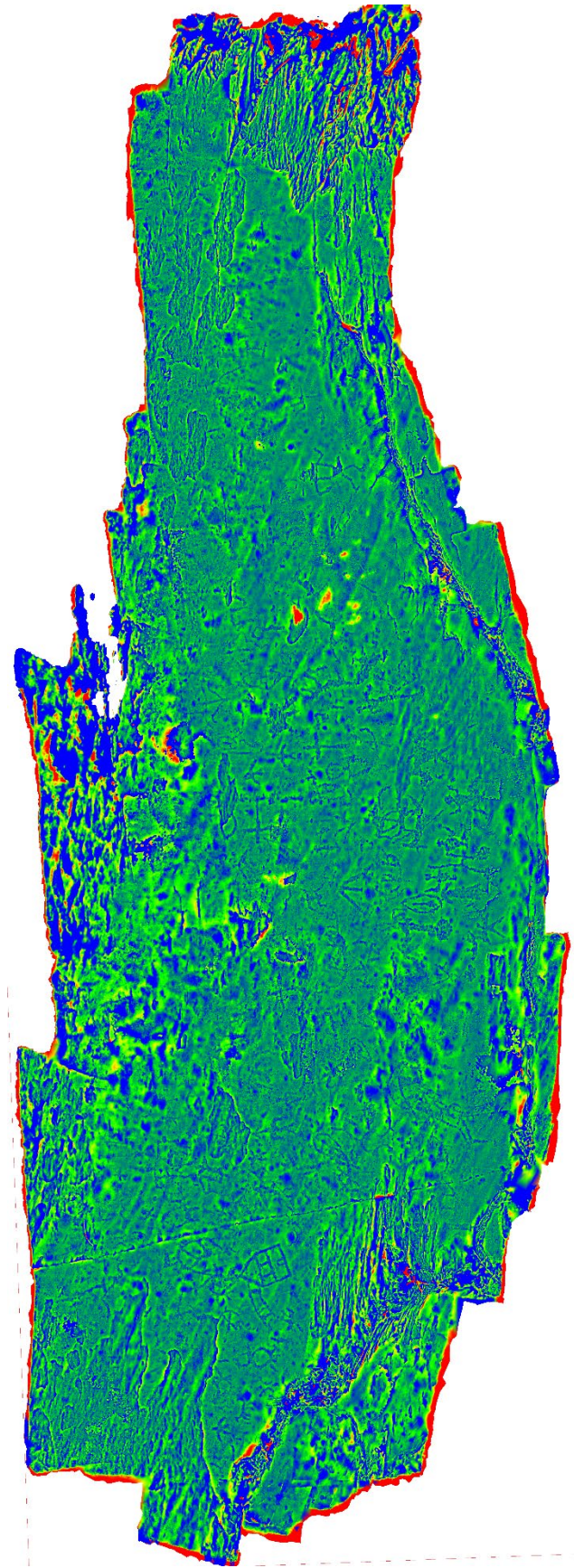
Figure 67: Embden Petroglyphs, reconstructed and smoothed 237 iterations at 0.2 smoothing factor.
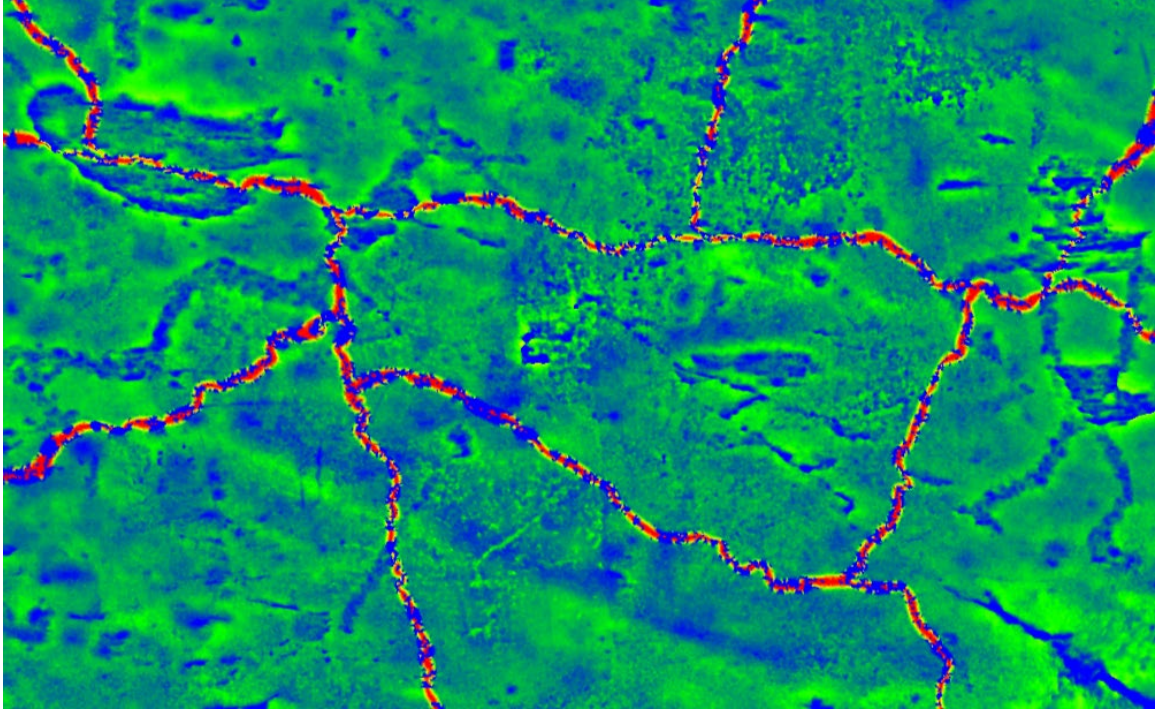
Figure 68 (above): Detail view of the fissure-like distortion in the scalar field generated via a smoothed clone. This is the result of the piecemeal recording method used by 3D recording software on equipment like smart phones.

a

b
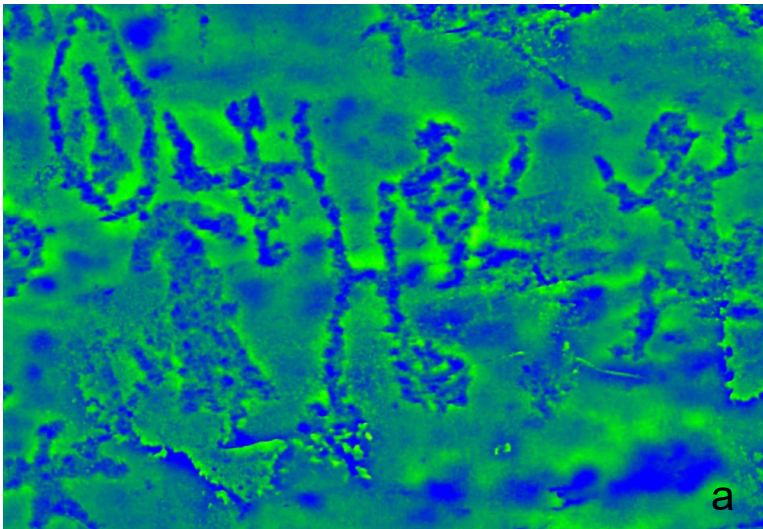
Figure 69 (left): a) Detail of several petroglyphs after colorization, next to (b) a sketch of them made by E.W. Moore in 1894.

The next scan covered petroglyphs from much further away: the island of St. John in the United States Virgin Islands. Besides the availability of the scan, these were chosen because the Reef Bay petroglyphs have been documented by researchers and posed an opportunity for comparison and corroboration of our colorization. Diagrams by Dubelaar (1991) allowed for easy conversion of surface area measurements. As with the Embden petroglyphs, I used the two revised methods, employed the appropriate formula for each, and generated two colorizations. The colorizations agree with the petroglyphs recognized in Dubelaar's diagrams and by the general public, corroborating their validity. However, they also reveal new petroglyphs which are so faint that they previously eluded notice. Note, for example, the hints of overlapping clusters of faces (*Fig. 74*) which are now too worn to be seen by the naked eye. Other unrecorded petroglyph details are plainly visible, such as a repetition of an existing eye motif and many cupules (*Fig. 75*).

Figure 70: Photograph by Scofield and Allmon (1956:220) of watercolor paint applied to petroglyphs at Reef Bay
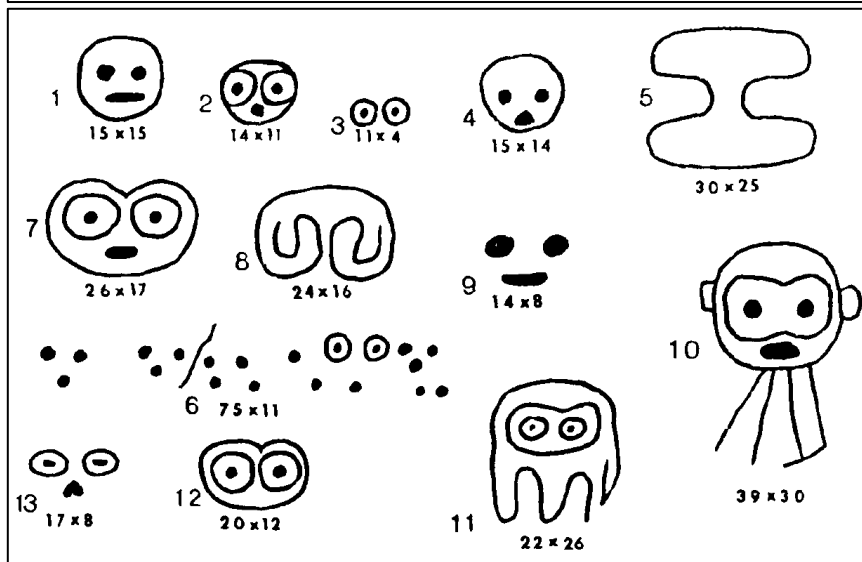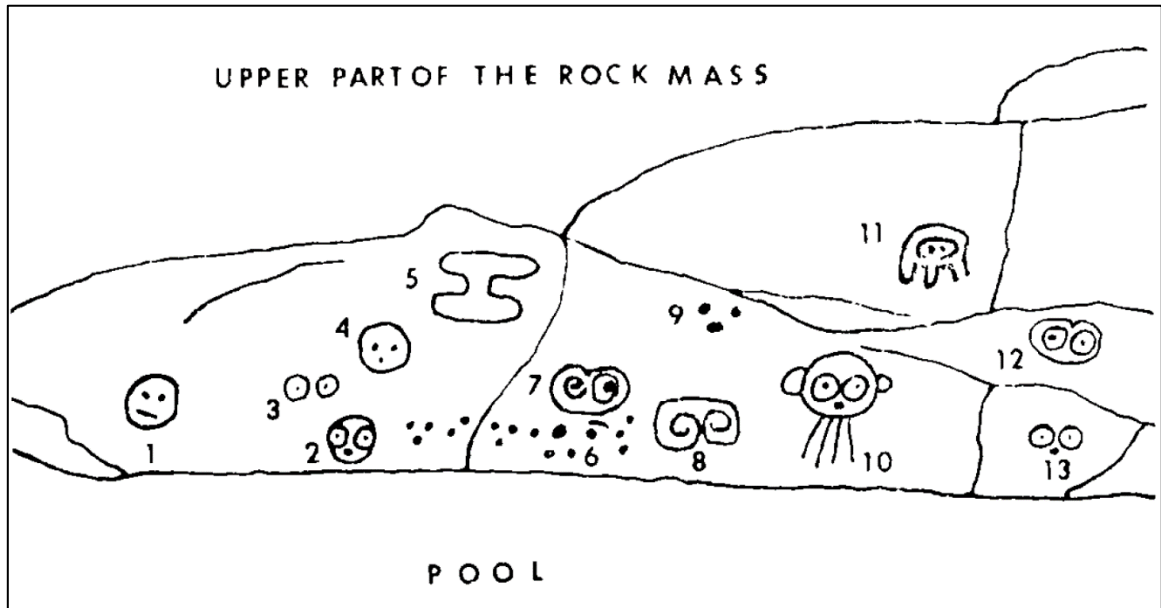
Figure 71:
Diagrams of
Reef Bay
petroglyphs by
Dubelaar
(1991:958).
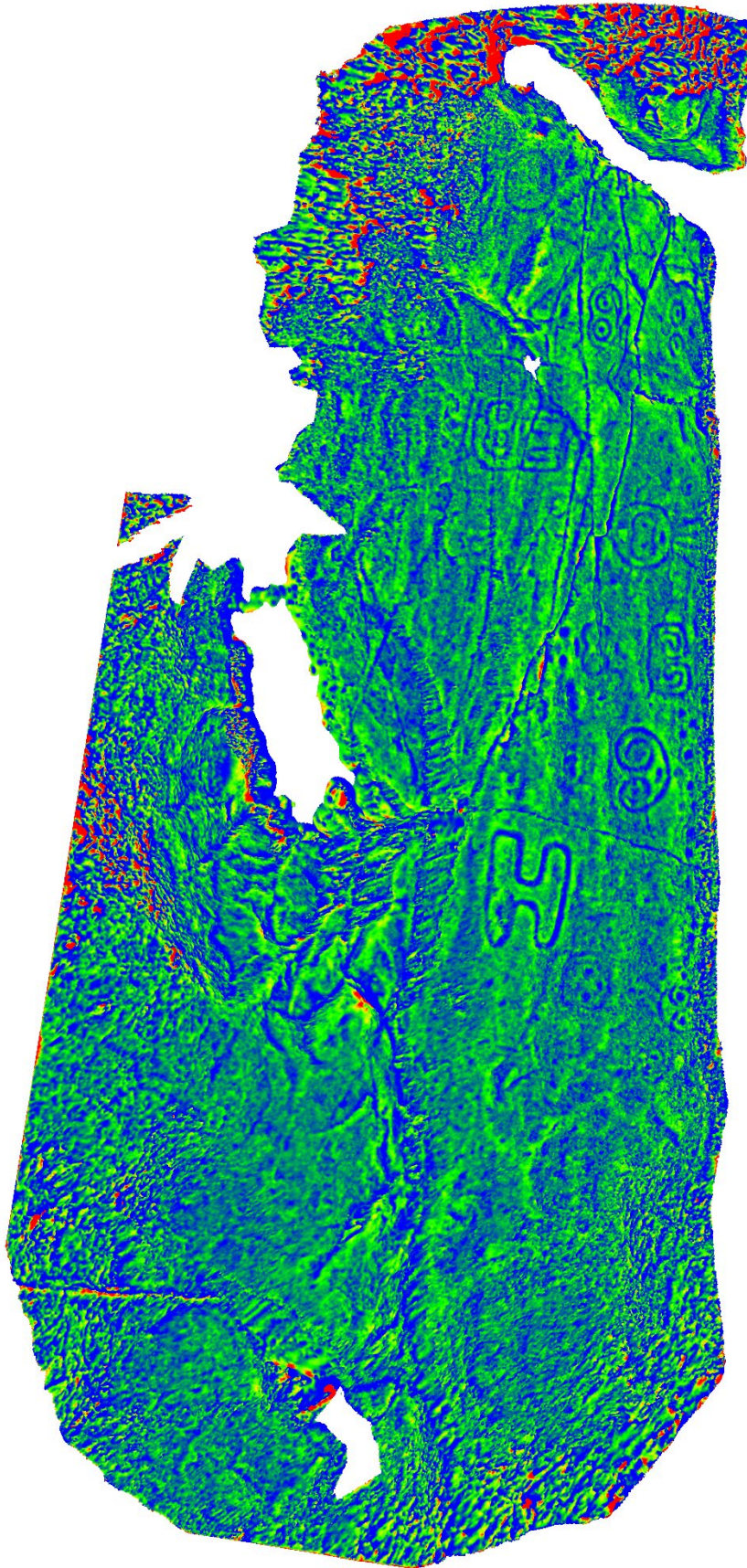
Figure 72: Reef Bay petroglyphs, subsample (random 523,313 points), smoothed 20 iterations at 0.2 smoothing factor.
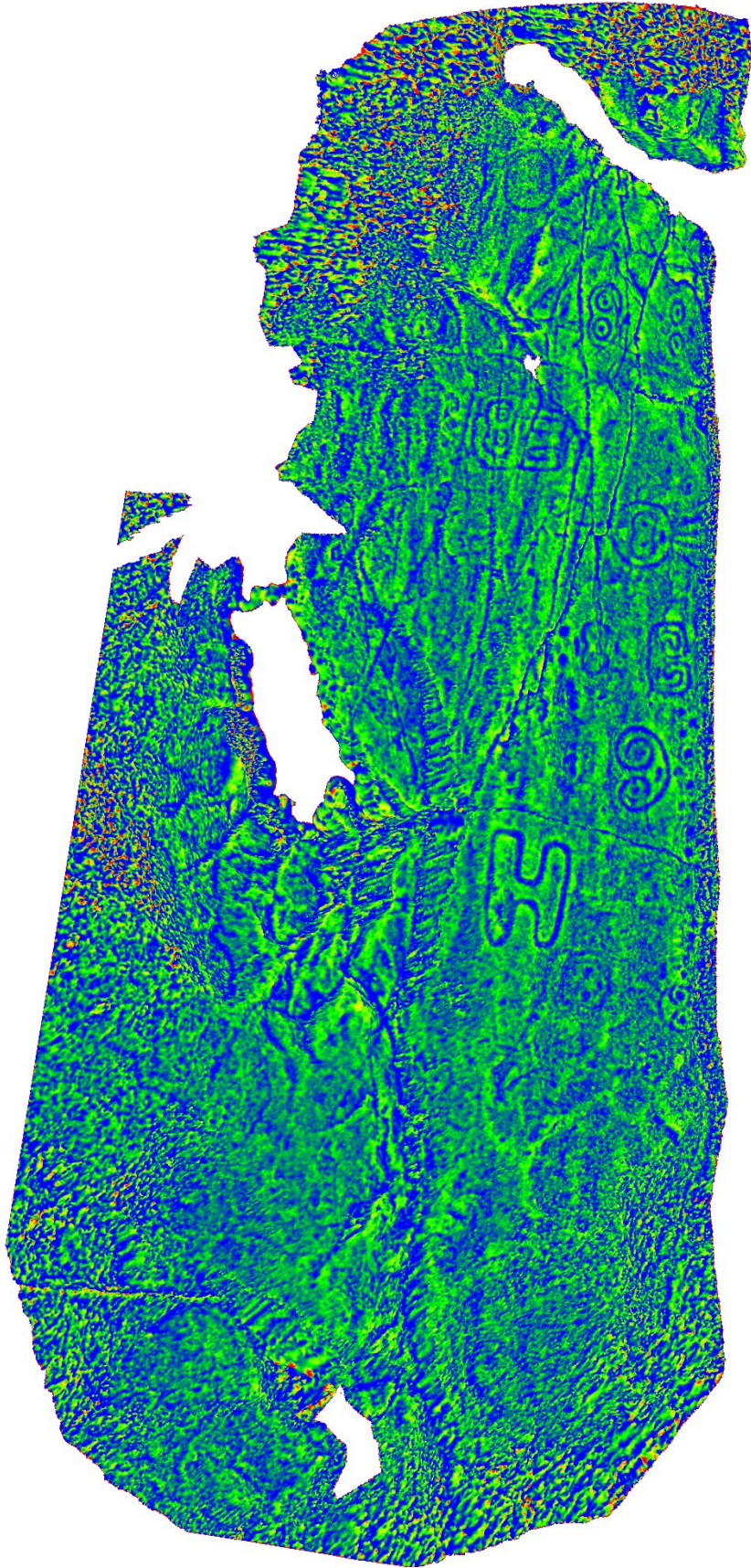
Figure 73: Reef Bay petroglyphs, smoothed 37 iterations at 0.2 smoothing factor.
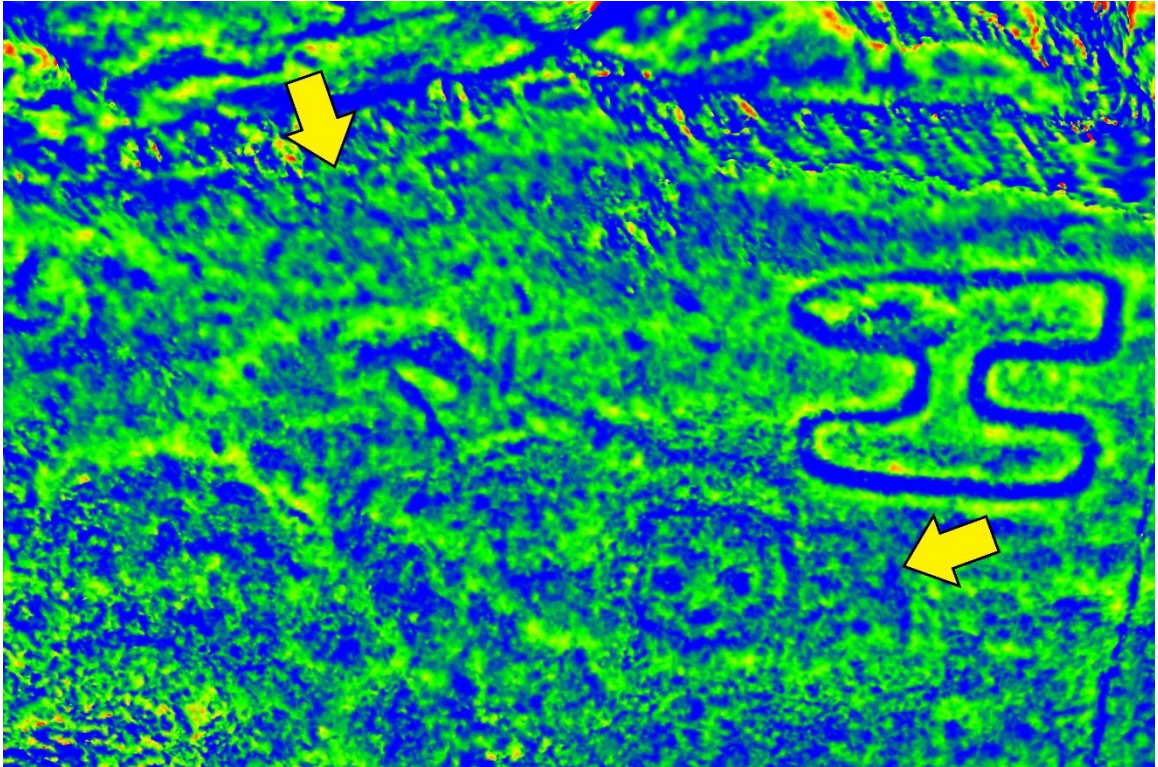
Figure 74: Detail of faint but perceptible glyphs with indicator arrows; these appear to be overlapping circles with cupules and are perhaps meant to depict faces.
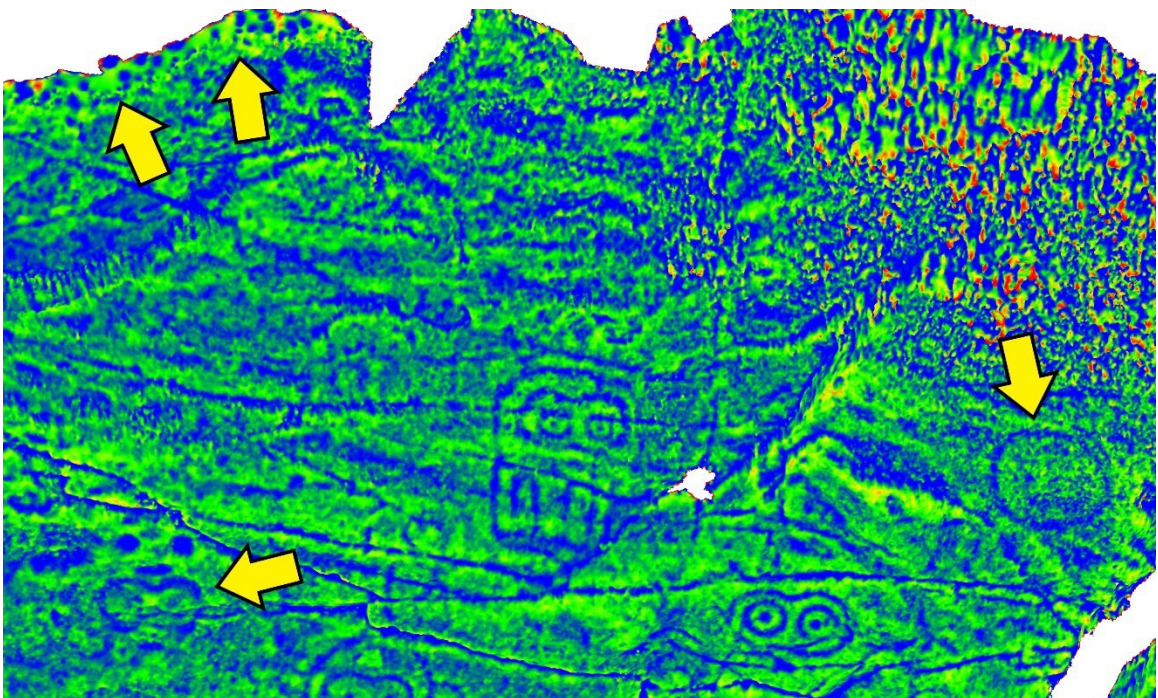
Figure 75: Detail of unrecorded glyphs with indicator arrows; these include groups of cupules, the repetition of an 'enclosed eye' motif, and an apparent face.

I lastly return to a scan in our original dataset and compare my colorizations of Dighton Rock to its depictions through time. ***Figures 77-78*** show Dighton Rock colorized according to my method. Perhaps the most significant conclusion that can be made from the analysis of Dighton Rock concerns how utterly suspect many pre-twentieth-century depictions of complex petroglyphs now appear. In ***Figure 76*** we see some of the earliest of the now innumerable interpretations of Dighton Rock. While there is generally some commonality between the drawings, they all seriously deviate from the reality of the carvings which they are meant to depict. This is not to mention the additional mistakes introduced by repeated, imperfect copying. Mallery, from whom these specific diagrams were sourced, does not accurately reproduce either of the earliest sources for John Danforth's sketch, which are copies made by Isaac Greenwood in 1730 (Delabarre 1917). Further still, the great discrepancy between Greenwood's two handmade copies leaves us to ponder the actual appearance of Danforth's original. This gives us cause to reevaluate sources whose authority was previously accepted.

Over the course of more than 340 years, perhaps only one of the many sketches and reproductions of Dighton Rock has discerned the second, stylistically similar zoomorph hidden in the palimpsest immediately to the right of its companion. Ironically, it was Edmund Delabarre who recognized the markings and depicted them in a sketch alongside his own fanciful inventions, such as the alleged inscription of Miguel Corte-Real (Delabarre 1919:416). Neither of the zoomorphs as he draws them are entirely accurately portrayed and the front half of the figure on the right is his conjecture; he assumes it to be a repetition of the 'deer' to the left. Nonetheless, the oversight by previous observers is all the more striking given the clarity with which the less disfigured zoomorph may be perceived, as evinced by numerous accurate representations of the animal on the left since at least Stephen Sewell's 1768 sketch of the stone. Thus, even with the exact pattern to be recognized plainly before them, sitting mere inches from its
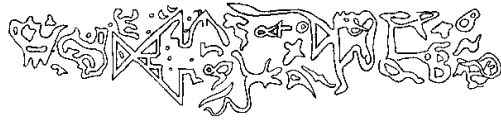
Danforth, 1680

Baylies and Goodwin, 1790

Cotton Mather, 1712
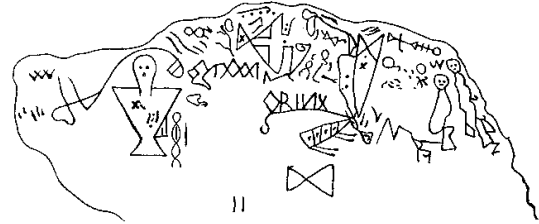
E. A. Kendall, 1807
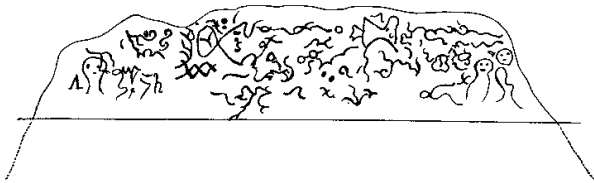
Isaac Greenwood, 1730

Job Gardner, 1812
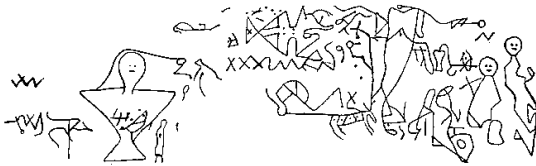
Stephen Sewell, 1768
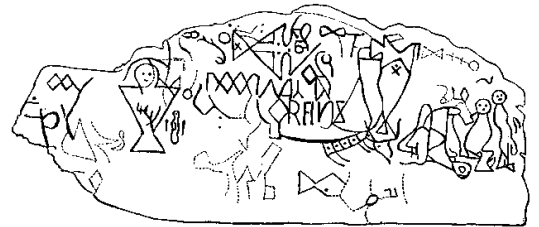
Rhode Island Historical Society, 1830
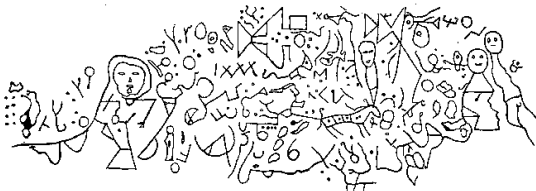
James Winthrop, 1788

Henry R. Schoolcraft, 1854

Figure 76: Compilation of depictions of Dighton Rock through time. Reproduced from Tufte 1990:72, after Mallery 1893:762-763.

93
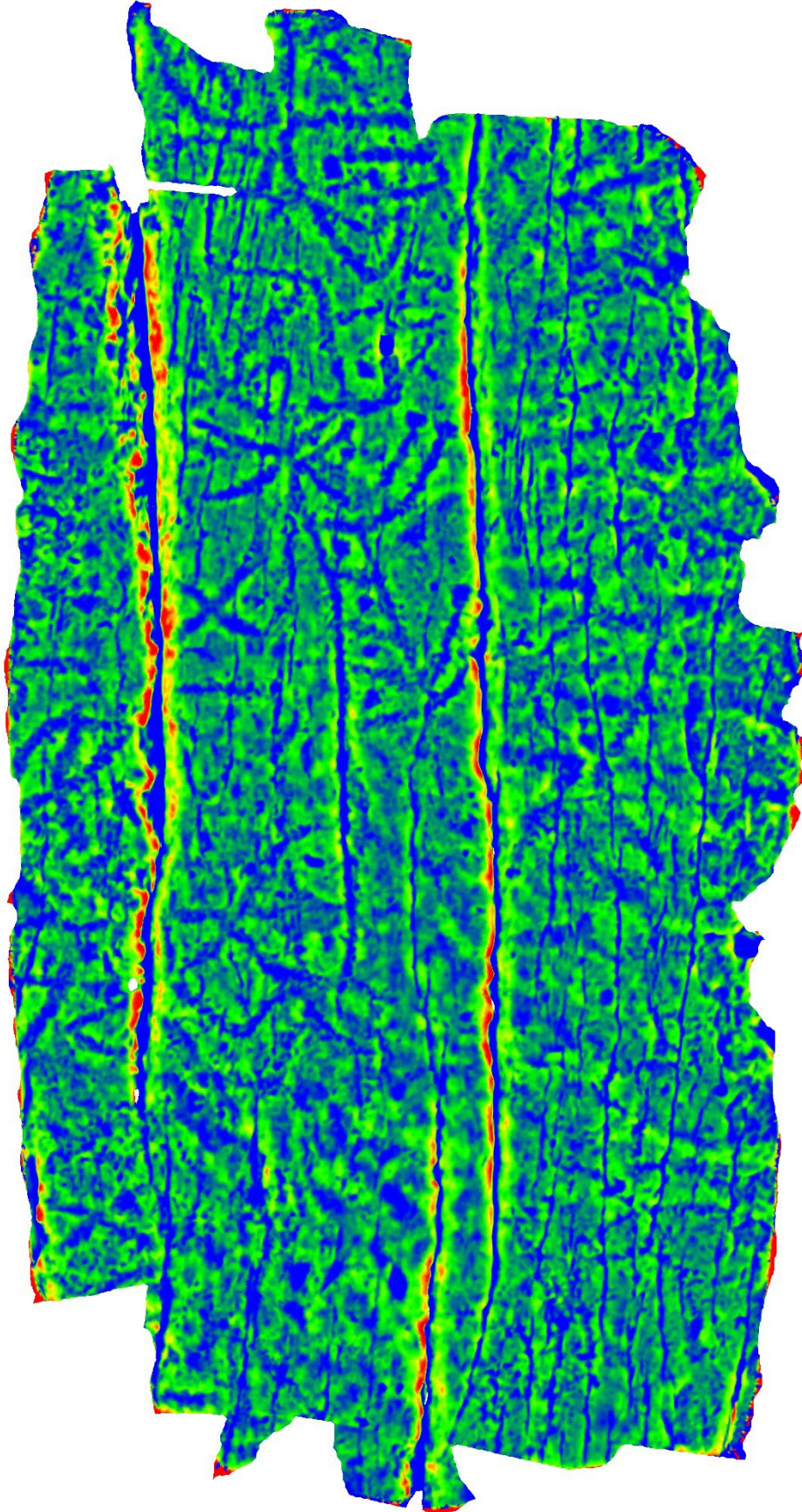
Figure 77: Dighton Rock petroglyphs, subsample (random 68,248 points), smoothed 20 iterations at 0.2 smoothing factor.
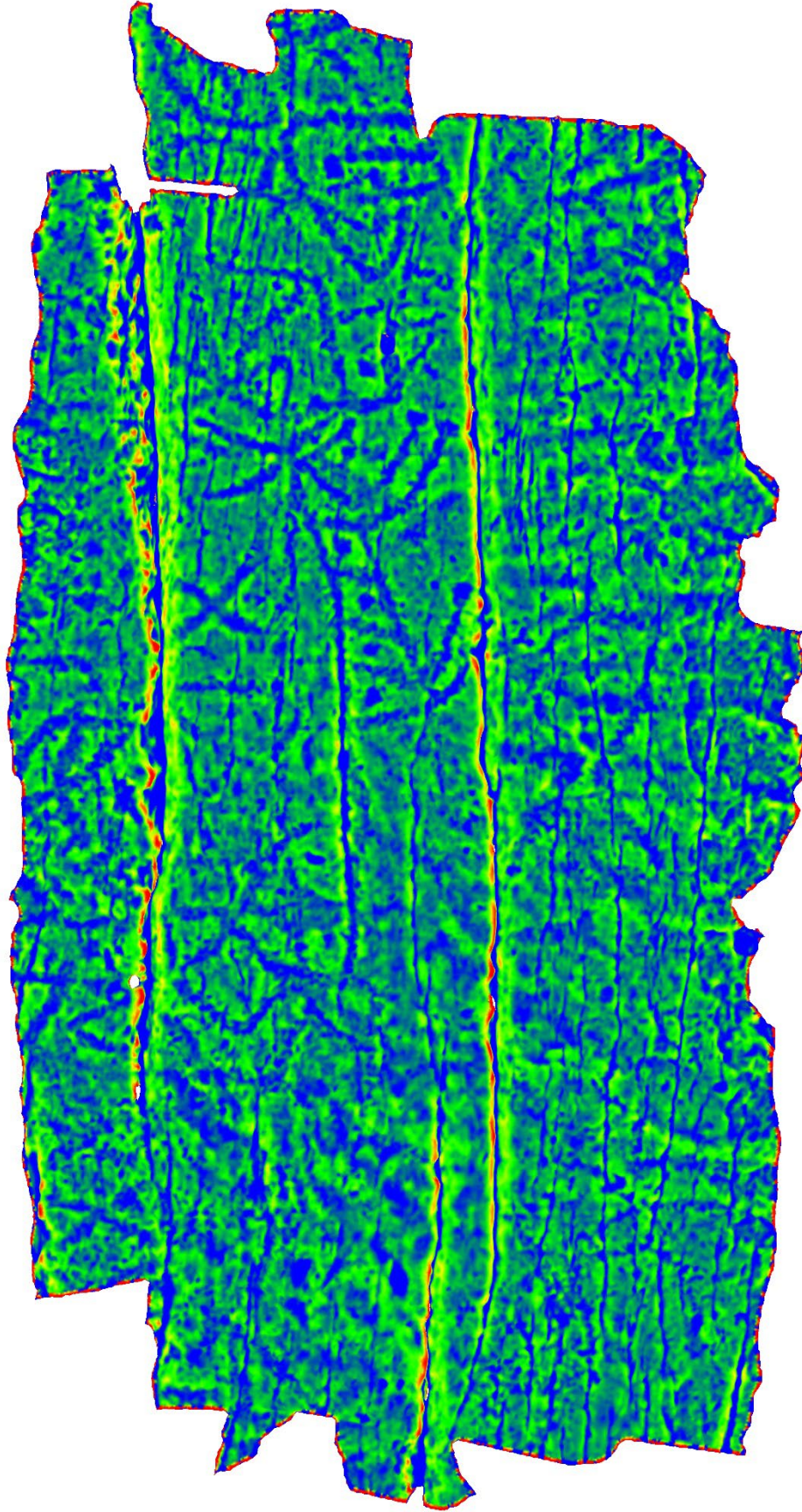
*Figure 78: Dighton Rock petroglyphs, smoothed 65 iterations at 0.2 smoothing factor.*

counterpart, countless researchers could not detect the motif. There is cause to consider that these figures may have been retouched as described by Hunter. Our colorization shows lines which may have comprised the zoomorph and which are clearly less distinct than others, perhaps indicating partial reengraving of an initial figure. The more significant contribution our colorizations have to make lies in what they can disprove. Delabarre (1928:172) goes so far as to assert that glyphs outlined in *Figure 79b* are "Indian glyphs *overlying and obscuring* the Cortereal [*sic*] inscription" [emphasis added].

Yet, *Figures 77-78* clearly demonstrate the contrived nature of Delabarre's alleged Portuguese inscription. Even setting aside the likelihood that someone has deepened the carvings to agree better with the "signature" of Miguel Corte-Real, we see in the visualization no basis for privileging a combination of lines that would make Latin script. To interpret the 'C' and 'O' advocated by Delabarre requires we ignore connected lines of equal thickness. Delabarre's 'R' likewise requires that we turn a blind eye to inconveniently connecting lines and connect ones that are more nebulous. The entire rest of the name is plainly concocted from a few indiscernible marks. The colorizations we've generated therefore serve to reaffirm the haphazard, confirmatory manner in which Delabarre decided on which lines to incorporate into an image. We gain additional evidence against his Portuguese hypothesis, which pseudoscientists continue to employ in colonial projects of Indigenous erasure.

I conclude this section by directing the reader to **Appendix C**, where I include photographs of the rest of the main dataset colorized according to the finalized methods just demonstrated. These include views of the sides of scans, where applicable. It should be kept in mind that though there are generally two images for each scan (representing one from each route to colorization), the scalar fields generated by this process allow for countless combinations of display parameters. Presenting the range of

customization options with a scalar field would be better achieved by a video, but

imagery is naturally more favorable to this medium.
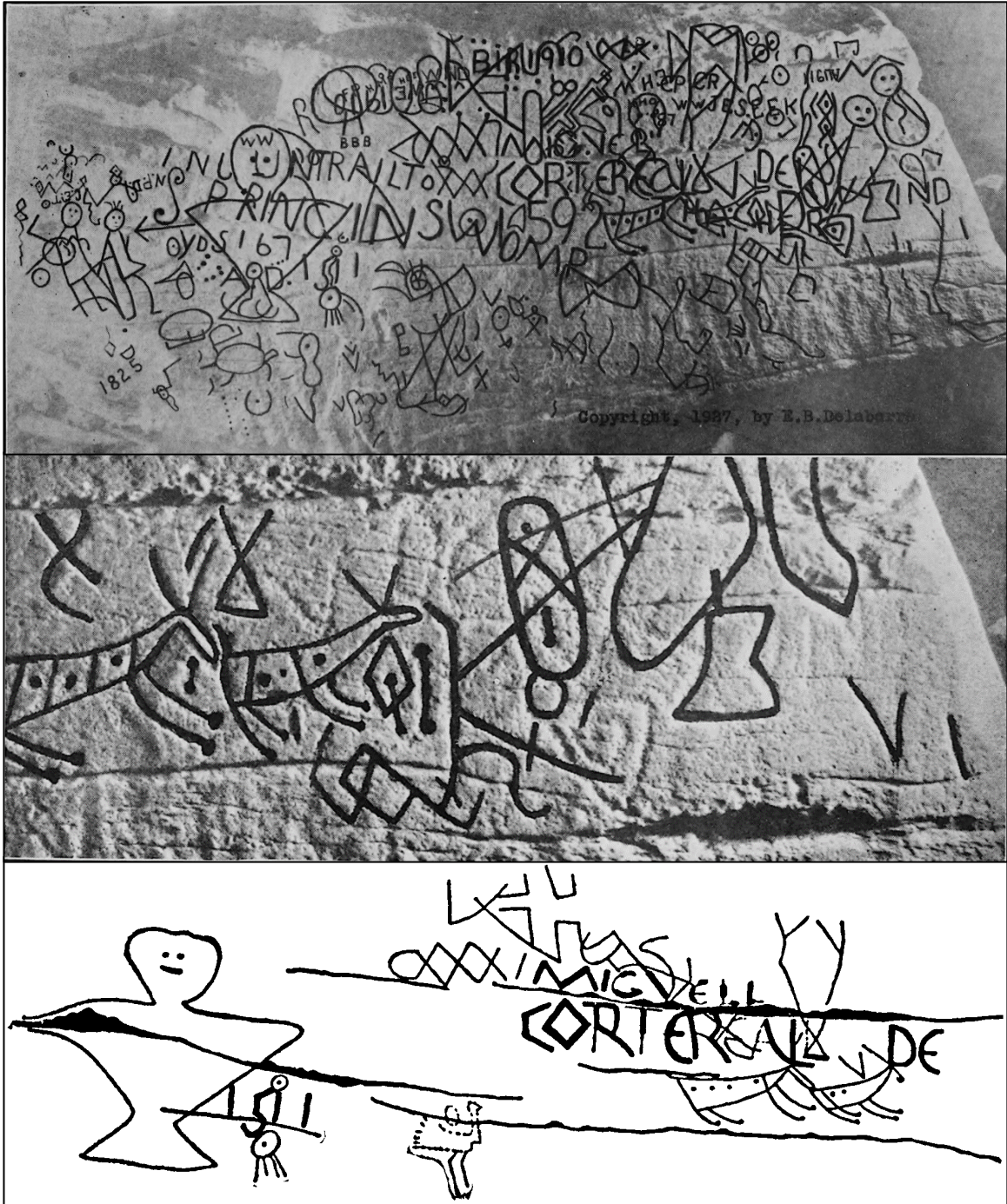
Figure 79: Delabarre's interpretations of Dighton Rock with demonstrably fictitious glyphs; from top to bottom: a)1928:186, fig.35; b)1928:172, fig.28c; c)1919:416, fig.7
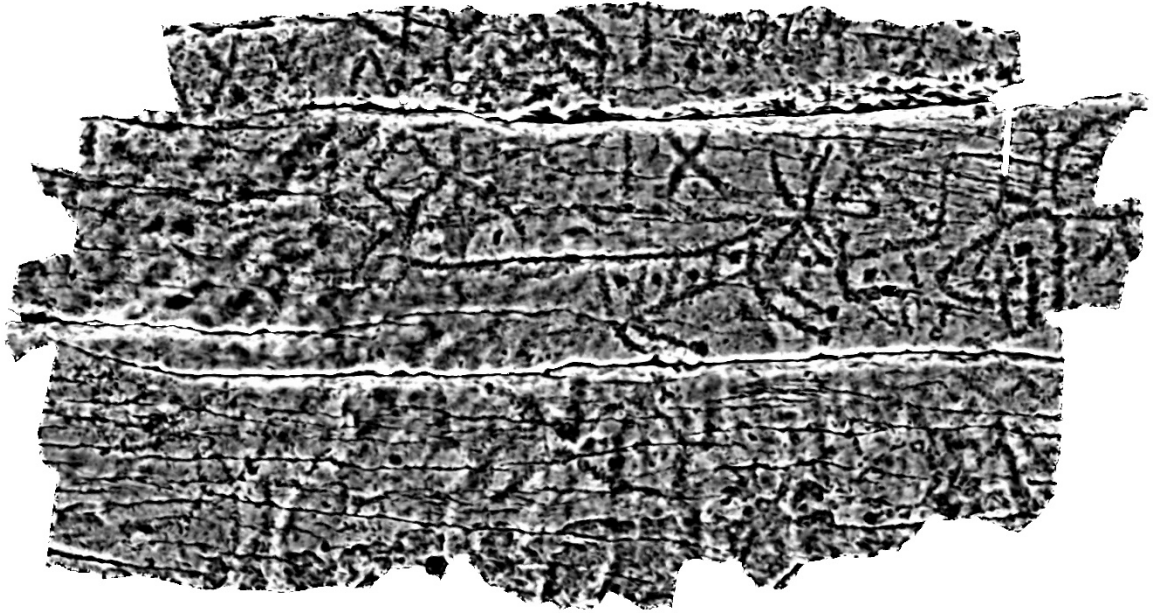
Figure 80: Dighton Rock colorization in Fig. 78 set to a gray color scale and display parameters adjusted.
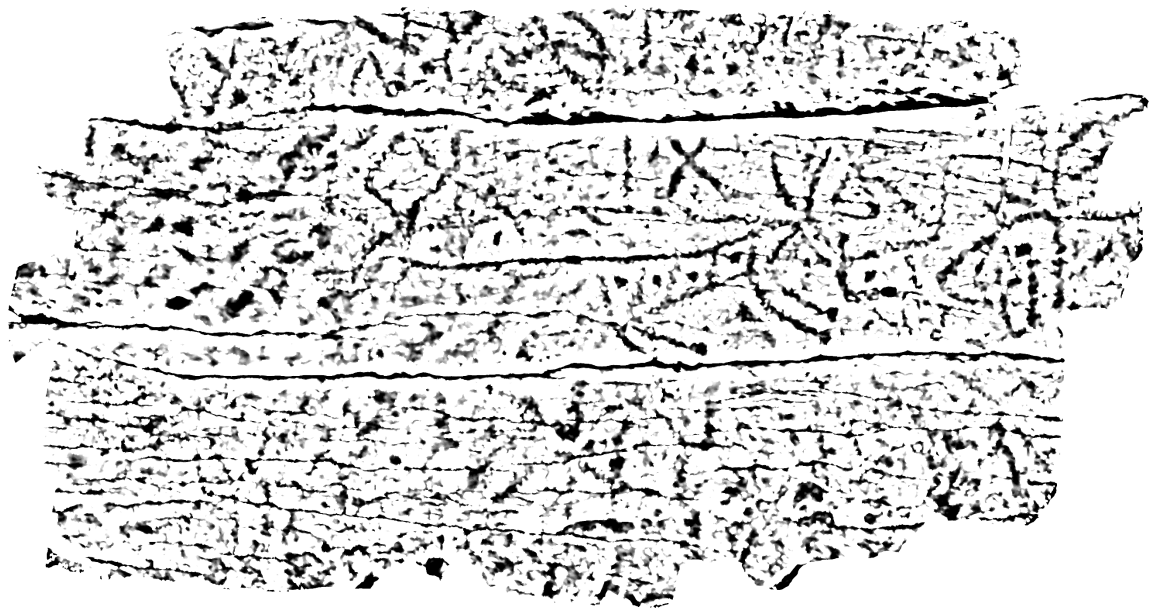
Figure 81: Colorization in Fig. 80 filtered by value to isolate the strongest features of the engravings.
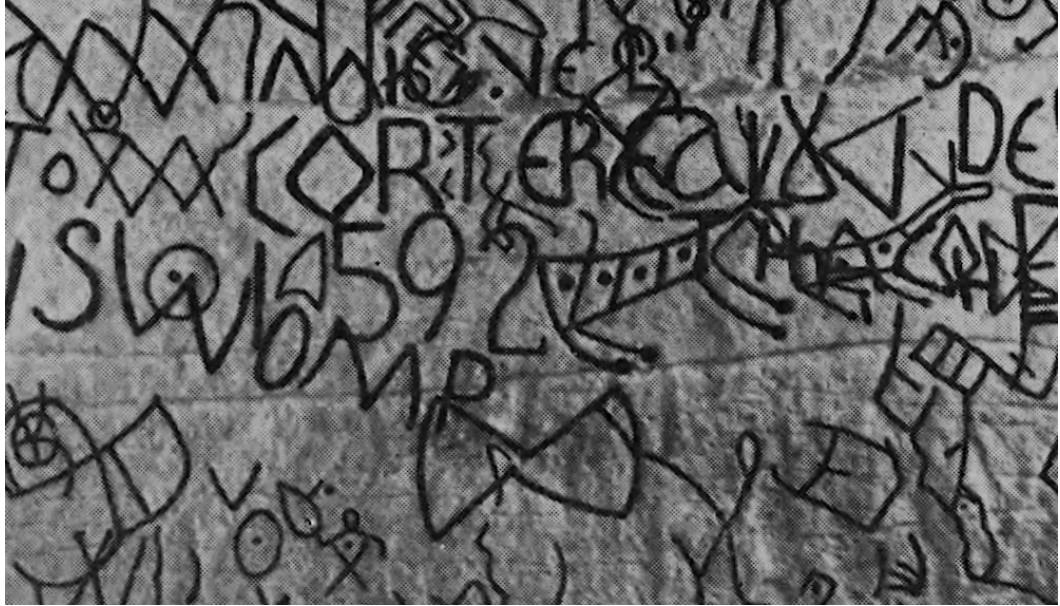
Figure 82: Crop of Fig. 79d, reduced to the area of our scan.

Chapter 3: Summary and Discussion

This last chapter reiterates the research problem, revisits the path that led to my finalized process, and summarizes the key lessons learned. A greater portion of this chapter is dedicated to situating these results within petroglyph research writ large and discusses the implications of my findings. As I stated in Chapter 1, this research has sought to fill a pressing need in the archaeology of images on stone by developing an objective methodology for improving the visual contrast of petroglyphs in 3D scans. This work was designed as a series of iterative trials applying a quasi-experimental pretest-posttest research technique. Pre- and post-intervention observations were used to ascertain whether different manipulations to a 3D model were effective in improving petroglyph visibility. Existing tools for petroglyph visualization were also evaluated for their efficacy and usefulness. Together these lessons informed the creation of novel procedures for petroglyph colorization which were applied to two unfamiliar scans as well as the original dataset. The results were again scrutinized in post-intervention observations.

This study began with an exploration of some 'out-of-the-box' visualization options with software such as MeshLab. These were deemed useful but ultimately limited in their capabilities. I next evaluated and attempted to improve upon a method used by DeGayner, Rodriguez, and Moss, but in testing discovered the limitations and even danger of manual point selection in the formation of a simulacrum. This finding necessitated a shift in my approach. I evaluated Horn et al.'s Topography Visualisation Toolbox and, while finding it did not fulfill the needs identified by this research, found in it a theoretical foundation for our methodology. From this point of departure, I developed three routes to colorization but found the uncontrolled variable of point density an unavoidable barrier to progress. However, it also proved to be the linchpin in an alternate method which could achieve our goals. I revised my process to work with point density

as a key factor and developed guidelines to this end. I finally demonstrated the utility of this revised process on our original and a secondary dataset. The final products confirm that the process performed as expected and substantiate its capacity for visualizing the small details of rock markings.

Ultimately I developed three functioning methods, two of which I judged highly effective for making rock markings visible. The less effective but generally satisfactory method employed a distance computation against a fit plane, Gaussian filtering of the scalar field, and then scalar field arithmetic (Method 1). The two highly effective methods employed either a subsampled and smoothed reconstruction of the original mesh (Method 2) or a smoothed clone of it (Method 3) in conjunction with information about point density. There are some advantages, disadvantages, and constraints to consider, both as a whole and between the several methods.

Method 1 and Method 2 can be completed much faster than Method 3 on larger scans. Method 1 is by far the quickest operation. Method 2 outshines Method 3 in speed to completion, particularly when a very dense point cloud is being handled. The large number of smoothing iterations in Method 3 – 2000 with some of our denser point clouds – required anywhere from ten to fifteen minutes; the distance computation between the original cloud and the still very detailed clone required at times another thirty. Processing speeds for these operations will likely vary significantly depending on the hardware of the user, but it is clear that Method 2 demanded fewer resources. On the densest point clouds, Method 2 took around one third of the time required by Method 3. Smoothing twenty iterations is a quick procedure and the distance computation to the lower resolution, reconstructed mesh proves a simpler calculation, also shortening the process. Method 1 or Method 2 may therefore be preferable for quick preliminary colorizations. Method 1 may be particularly useful in this regard because it is the only method of the three which does not require knowledge of surface area or point density to

complete. Returning to the matter of expended time, however, it is worth noting that with point densities under 1,000,000 p/m^2 all methods required less than a few minutes to complete.

Of course, rapidity on those denser scans comes at a cost. The significant disadvantage of Method 1 and Method 2 is their failure to accurately visualize the sides of rocks. Method 1 is more deficient in this regard: it cannot reveal any details perpendicular to the fit plane, and accuracy is diminished the further the mesh strays from parallel. Method 2 can in fact show glyph details around edges and sides, but this method proves extremely sensitive to slight imperfections in the recreation of the mesh and these imperfections are more likely to occur around turns and edges. This causes large distances to appear in the distance computation which then obfuscate glyph details. This is why a direct clone of the mesh functions so well, as the differences are solely the result of our smoothing and there are no confounding variables like imperfect mesh reconstruction. With the Embden petroglyphs, I found unforeseen benefits in reconstructing the mesh as well. Reconstructing the mesh rather than simply cloning it fills the gaps resulting from an MMS stitching together smaller scan areas. It was in fact necessary to adapt Method 3 in this way to obtain a suitable colorization.

I also found in the course of the research that, below a certain point density, 3D scans unfortunately do not appear archaeologically useful. Though perhaps self-evident, it is worth reiterating that the number of points collected for a given area matters as much as the accuracy of each point collected. No process can achieve colorization of glyphs on a surface where data about the surface is missing. Below 45,000 p/m^2, I observed a steep decline in capacity for visualization commensurate with the loss in data quality. The lower resolution scan of Judaculla Rock, for example, was excluded from further testing when it became clear that the point density was insufficient to show petroglyph details. Thus, while scans slightly below the point density threshold I have set

might still be capable of generating decent colorizations, no guarantees can be made that the methodology will function as intended. With scans at or above 45,000 p/m^2, my methods are sufficiently sensitive to make full use of the scan resolution, revealing petroglyphs that are otherwise imperceptible to the naked eye, both in field conditions and even by other visualization methods.

We should also contemplate the quality of data brought to bear on this topic, for only a few scans were survey-grade and professionally recorded. I created this methodology intent on making it adaptable to a range of scans yet was still surprised by how well it performed with 3D models created and made available by the general public. These scans were not intended for this kind of work, and the successful colorizations derived from them show what can be done with minimal equipment. The scan of Judaculla Rock from which which we generated exceptional colorizations was recorded with an iPhone 6 Plus, while newer models of smart phones are continuously adding to the technological capabilities of these ubiquitous devices. Our success with avocational data speaks also to the possibilities with professional recording using modern TLS, for even the professionally recorded scans in this study were made with the equipment available a decade ago.

The question of equipment capability also has relevance as it relates to the manner in which petroglyphs were made – or at least how we find them today. In some instances, the marks composing petroglyphs are so slight that they even fall below the sub-millimeter measurement accuracy of survey-grade TLS equipment. This is more common in particularly eroded glyphs or with markings made by abrasion, where a strong color contrast between weathering rind or rock varnish and underlying rock allowed for an image to be made with little removal of material. Under these conditions, this methodology will likely fail to create a discernible visual contrast, and it may be better to apply the kinds of image enhancement techniques used for improving the

visibility of pictographs. Indeed, any of the scans colorized in this study might also contain pictographs or petroglyphs made by contrasting the color of the weathering rind. This is one reason that it is extremely useful to have an image of the stone attached to the scan as a texture. Terrestrial laser scanning, mobile mapping systems, and photogrammetry can nonetheless be useful at such sites due to the possible co-occurrence of more deeply incised petroglyphs.

The very nature of the colorization process introduces an unavoidable limitation which affects not only my methodology but tools like TVT as well, which operates on a similar premise. The manipulations to the model which allow colorization cannot differentiate between carvings and small natural features of a similar depth. This is the source of significant noise in our visualizations, as the microtopography of the stone is as prevalent as the evidence of human agency. In isolating and making visible images on stone within a 3D model, there are essentially two steps which must be completed:

A) Eliminate global curvature from the colorization.
B) Eliminate the remaining natural features from the colorization.

Unfortunately, B involves a judgment call which is beyond the capabilities of our process; such judgments are consigned to the realm of expert manual segmentation. This is perhaps a blessing as well since natural features are sometimes incorporated into the creation of imagery. At CHOH-3, for example, the human figure's eyes are in fact quartz inclusions intentionally integrated into the glyph. Ultimately, we must accept that A is more realistic than B. In fact, A has been achieved here with my finalized process. In the absence of unassailable empirical evidence for human action on an area of stone, B is an act of interpretation and should thus always be presented coincident with A.

I regard the uniform manipulation of the point cloud or mesh as a particular strength of my colorization methods since we thereby minimize alterations based upon biased preconceptions and concomitant distortions to the finished product. The

difference may be seen in the juxtaposition between images in **Appendix C** and some of my failed revisions to DeGayner's method. We thereby improve the overall objectivity of the process. Yet, while one of the primary goals of this research has been to explore methods for the objective visual enhancement and isolation of rock markings, it may be necessary to accept that this task will always be, to some extent, an act of interpretation. In the sense that it strives toward unassailable objectivity, this work may even be doomed from the start. The technology at our disposal does not allow us to state definitively in all cases, based upon empirical evidence, that a given area of rock has or has not been altered by human labor. Thus, the work of enhancing glyph visibility begins subjectively with the researcher's recognition of a pattern indicating human action and ends subjectively when the researcher feels that their methods are no longer revealing additional markings (i.e., the researcher recognizes no additional patterns beyond what they deem natural, coincidental, or arbitrary). Even where technology can allow us to definitively identify human-made alterations to the rock, the scans on which this process relies have been made in the last decade at the earliest. They depict the rocks not as they were, but as they are: palimpsest canvases with several hundred years of colonial occupation and natural erosion adding to what may have already been a crowded ledger, the record of thousands of years spent in communion with Indigenous communities.

Even if one erases from the model those obvious examples of recent defacement, the ancient markings are altered by those who have come before to poke and prod these Native places, grinding with chalk and charcoal, tracing with fingers and walking sticks as they try to discern meaning in signs which were never intended for them. Hunter (2017:200) argues that the markings at Dighton Rock are "so interfered with and mutilated" that they are now "likely beyond the point of affording any useful lesson on antiquity or ethnography." As Hunter further notes, Dighton Rock has seen

constant abuse: it has been carved with graffiti; said graffiti has been chiseled away; the markings have been "chalked, painted, scrubbed, and more than likely clarified or improved with steel tools by people who wanted to see an inscription that was anything other than Indigenous" (200). While this author disagrees as to whether Dighton Rock has any lessons left to offer about the Indigenous past, it might first help us learn a different lesson by dispelling the 'Pompeii Premise' (*sensu* Schiffer 1985) permeating rock marking research. Even as we bring to light faint details ravaged by time, we must be mindful of the processes and temporal scale we contend with.

It seems that one of the greatest challenges to the objective recording and presentation of rock-borne imagery is the contradiction between what archaeologists desire and what is empirically possible. Archaeologists – this one included – seek legible, unambiguous diagrams of petroglyphs as they appeared on the day of their creation. Some are even more unrealistic in hoping to reconstruct glyphs exactly as their creators *intended* them. It is often overlooked that some markings may have *always* been indistinct, nebulously blending into the natural striations of the rock, and this may well have been the intention the creator. What these archaeologists wish to produce is at odds with the reality of many petroglyph sites as we find them today, which bear no shortage of hopelessly ambiguous lines. I conclude therefore that presenting these sites in their uncertainty, with their collateral 'noise,' is an important step in developing an objective research methodology for this area of study. While simplified line drawings, digital removal of graffiti, and other methods of enhancing and distilling the content of images on stone certainly remain useful, we must recognize them for what they are: acts of interpretation with underlying assumptions and judgements about things which are less than certain. Three-dimensional imaging enables us to see details invisible to the naked eye and represent these details in a myriad of ways; yet, despite this

technological advancement, the conclusions we draw and patterns we deduce are ultimately not so different from the simple, fallible chalking of generations before us.

While these visualizations did not ultimately produce the clean outlines which we may have hoped for, they will in their cautious presentation hopefully stand the test of time better than some of the depictions of other petroglyphs I have reviewed. Many of the confidently bold, clear diagrams we now rely on for destroyed petroglyph sites were not so clear as the authors would have us believe, as evinced by the myriad of ways that different observers chalked the same locations. This work has nonetheless succeeded in discovering previously unknown rock markings which I believe will be accepted by the archaeological community as legitimate. Markings revealed here in the colorizations of CHOH-26 eluded our notice during fieldwork, when I accompanied several experienced archaeologists on a trip to observe the rock. This serves as a testament to the difficulty archaeologists face in seeing and recognizing rock markings in real field conditions, as well as the value of analyzing three-dimensional scans in the lab as a method of field verification and to inform future survey.

With the growing availability of scanning equipment and the improving accuracy of consumer-grade hardware, such as LiDAR capabilities on some mobile phones, large-area scans of suspected petroglyph sites followed by lab analysis may serve as a preliminary to more intensive, focused fieldwork. In this way the procedures I have outlined may provide a solution to the problem of targeting specific areas for attention. These same methods have potential application in other arenas such as historical archaeology, where they may prove useful in making legible eroded gravestones, tablets, and so forth. Perhaps most importantly, these procedures will hopefully prove useful to the archaeological community not only for baseline documentation and interpretation, but also in preserving these sites for descendant communities and

dispelling the pseudohistories that would deprive these communities of their cultural patrimonies.

Though all too often overlooked when academics focus on empirical methodologies, the ethical implications for this work should not be ignored either. Petroglyph sites are meaningful to people in the present. This fact gives this research the power to be impactful, yet it also raises the stakes and risks doing real harm when culturally insensitive missteps occur. Robinson et al. (2021:419) have wisely called for "partnerships rather than appropriations" when engaging with rock-borne imagery. Collins, Doering, and Gonzalez (2019) offer a more exhaustive discussion of the ethical quandaries and potential pitfalls of this area of research. They note the balancing act placing open science (and concomitantly open access) at one end and the significant potential for misuse of information on the other. What begins with good intentions may result in "disreputable use of information, promoting looting, inappropriate replication of objects, or usage of site data for gaming or other online content" (2019:1). What is appropriate to replicate and publish may not be as clear as some would assume. For example, Indigenous ontologies do not necessarily subscribe to a stark boundary between the animate and inanimate, and many communities have expressed the belief that rock markings are living manifestations of ancestors. This suggests that discussions regarding the 3D scanning of rock-borne imagery should be closely intertwined with ethical debates about 3D modelling human remains (Spake, Nicholas, and Cardoso 2020). Collins, Doering and Gonzalez suggest that clear authorized use and limitation statements can help prevent damaging mistakes. They also suggest projects for beneficially partnering with communities, including digital repatriation or "capacity building and sharing with recognized and consenting tribal entities" (24). Any such project should include a discussion of data sovereignty, which is an issue ultimately central to any question of repatriation.

In addition to the disreputable use of information, we must also beware the use of disreputable information. There are empirical concerns as well as ethical ones in the overlap of this research with freely or publicly available data. Compared to traditional archaeological materials, provenience is just as important yet not generally equally emphasized when handling digital data. It is taken perhaps for granted that the information is valid. Yet, we may over time even see the dawn of fraudulent and manipulated 3D models offered as 'raw data' by pseudoscientists and pranksters. More innocent but equally hazardous to research are unknown errors underlying data generated in good faith. Basic peer review becomes impossible without knowing the exact methods applied by the originators of the information, increasing the likelihood that mistakes will go unrecognized. This problem can be exacerbated by the democratization of technologies enabling advanced recording techniques, seen in the growing availability of devices with 'plug-and-play,' out-of-the-box functionality requiring minimal skill or specialized knowledge from the end user. The automation of critical processes ensures these tools generally work as intended even though their inner workings may remain opaque to their operators, often giving the mistaken impression that devices are 'user-proof.' At the same time, rejection of all but professionally recorded scans would forsake a resource petroglyph scholarship desperately relies upon: the many enthusiastic volunteers whose efforts aid professional archaeologists. I do not presume to have answers to these vexations, but I maintain that they are too important to the future of this field to leave unsaid.

As I have thoroughly discussed in a previous chapter, this work builds upon and owes a great debt to previous research, especially the contributions of DeGayner, Rodriguez, and Moss, and Horn, Pitman, and Potter. At the same time, it carries this research into new territory by satisfying the practical needs of petroglyph scholarship which I have previously enumerated. In addition to the invention of a functional

109

methodology for petroglyph colorization, the lessons garnered by this work lead me to

formulate a list of recommendations for archaeologists engaged in similar projects.

Some of these recommendations pertain to the creation of data since the possibilities for

colorization are fundamentally constrained by the characteristics of the recording. I

recommend that a known scale of measurement be included in 3D scans, out of the way

of the surface being recorded, in addition to clearly communicating details like the unit of

measurement used by the file. This vastly simplifies the work of determining real-world

surface area and calculating point density. I also recommend that sites be recorded at a

minimum of 45,000 p/m^2 in order to ensure the usefulness of the scan for colorization

and simply for archaeological documentation. While not necessary for the colorization

techniques developed in this study, capturing imagery for use as a texture to the scan

can also prove invaluable both for discerning natural features in the rock and for

detecting imagery made through color contrast. I lastly recommend that the processes I

have developed be integrated into workflows for handling 3D petroglyph data and for

surveying spaces suspected of containing petroglyphs. Detecting unknown rock

markings and even relocating known sites are among the most challenging tasks facing

archaeologists. This can present a significant problem to cultural resource managers

who have a duty to identify, monitor, and protect rock marking sites on the lands they

steward. Implementation of these methods can help to alleviate this problem.

While I believe the presented techniques offer a viable route to visualizing

markings in many different contexts and circumstances, further research would benefit

this project greatly. Refining guidance on point cloud density seems a logical next step

for the immediate future. The 45,000 p/m^2 baseline developed here may not be ideal in

all cases. It is possible that different point densities are more conducive to creating

visual contrast given certain petroglyph characteristics or geological conditions. As just

one example, a site with very large, sprawling, shallow petroglyphs could perhaps be

visualized better by some adjusted formula. Despite the success of the methods outlined here, I also suggest that future research should continue to explore other strategies for achieving colorizations and compare them to my own. Many novel approaches remain to be thoroughly tested. There are a few potentially promising techniques which I toyed with but excluded from this report, like exaggerating point clouds via transformation to an axis, akin to vertical exaggeration applied to a topographic map. The use of TPI and how it compares to – or may enhance – the work in this study is also deserving of thorough interrogation. The implications of these methods for other archaeological scholarship also deserve attention in the future. While these techniques should work well with any kind of embossing or marking, their limitations outside of a petroglyphic context are untested. I suspect that they may work well on eroded gravestones, faint decoration or surface treatment of potsherds, and so forth. I would lastly recommend that further research should use stakeholder-approved datasets only for developing methodology, so that we do not perpetuate the presentation of open data without contextual understanding. We should also meaningfully collaborate from the planning stage with any potentially affected parties.

  Rock marking research is finally receiving its limelight in American archaeology, and with good reason. It is not only poised to redefine our understandings of ancient societies, but also to reconnect descendant communities with ancestral places and testify to the continuities and temporal depth of Native occupation. Those who describe rock markings as windows to the past are perhaps a little optimistic; if they are windows, they are decidedly opaque. The meanings of petroglyphs and pictographs are rarely so legible as we would like, and things needing redress in our interpretations of rock-borne imagery can and will fill volumes. First, however, it would be nice if we could all agree as to what we are looking at. It is my hope that this study will help contribute to that mission and perhaps even inspire further research. Indebted as this work is to the researchers

111

before me, it seems appropriate to end with a call to action in their own words – words

which still ring true nearly nine decades later:

> "Owing largely to methodological difficulties in the study of petroglyphs, archeologists have unduly neglected them….but when competent archeologists can be enticed to set aside their spades long enough to ponder petroglyphs, we may expect a much better understanding of this interesting subject." (Steward 1937:406)

APPENDIX A: GLOSSARY OF TERMS AND ACRONYMS

Acronyms

CHOH	Chesapeake & Ohio Canal National Historical Park
GWMP	George Washington Memorial Parkway
NRHP	National Register of Historic Places
NPS	National Park Service
LiDAR	Light Detection and Ranging
GIS	Geographic Information System
DEM	Digital Elevation Model
TLS	Terrestrial Laser Scanning
TPI	Topographic Position Index
MMS	Mobile Mapping System

Glossary of Terms

Note: Many of the following terms are used in literature and common vernacular with a wide variety of meanings and spellings. Throughout this work, however, they are applied in strict accordance with the denotations enumerated here.

Anthropomorph: Imagery representing or based upon the human form. This is generally used to refer to depictions of a whole body rather than more specific anthropomorphic imagery, such as depictions of the human hand. This term may be used to describe human-like representations of mythical figures and does not necessarily denote interpretation of a human being.

Cupule: A circular, cup-like depression ground into the surface of a stone.

Distance computation: A calculation of Euclidean distance between all of the points on two clouds or meshes. This computation is conducted as a single operation using a tool within the CloudCompare software. It outputs a scalar field attached to one of the input clouds. The scalar field contains the computed distance values and manifests them by color.

Downsampling: Subsampling the data in a point cloud or mesh for the purpose of reconstructing it at a lower resolution (i.e., with the loss of some fine detail).

Frottage: Image transfer of texture achieved by rubbing a marking material (e.g., graphite) against paper which is pressed to the surface being recorded. This is also referred to as 'rubbing.' Frottage is a longstanding technique for recording rock markings and has been applied to recording other cultural resources, such as gravestones.

Light Detection and Ranging (LiDAR): A remote sensing method which uses light for electronic distance measurement. Though technically covering any use of light for this purpose, the term is most commonly applied to the use of near infrared lasers in a pulsed Time-of-Flight system. LiDAR can generate dense, highly accurate point clouds and is found in aerial applications, terrestrial laser scanners, and portable handheld devices.

Master Cloud: The original, unmanipulated point cloud generated by scanning a real-world object and which forms the basis for the colorization process. The Master Cloud may nonetheless be *preprocessed* through the removal of recording errors, like plants and debris included in the scan.

Mesh: An entity which uses conjoined polygons to represent the 3D surface of an object. A mesh is a polygonal representation of a point cloud, which forms the vertices of the mesh. The meshes used in this work are constructed from triangles, but other polygon models also exist.

Mobile Mapping System (MMS): A portable, handheld system for capturing spatial environments. Mobile Mapping Systems may use laser line, photogrammetry, structured light, LiDAR, or other manners of data collection.

Motif: A singular design or marking, typically one discernible by a pattern of repeated use.

Petroglyph: Imagery made in rock by carving (such as by pecking, etching, and incising) or abrading (such as by scratching or grinding). While in some instances petroglyphs are formed by simply removing the darker surface layer of the rock to reveal a contrasting color beneath, in other cases images are made visible primarily by the depth of their relief. Petroglyphs are thus distinguished from other types of rock markings by the removal of material to make an image.

Pictograph: Imagery made on a rock or rock-like surface by the addition of a foreign material such as paint or charcoal.

Photogrammetry: Photogrammetry takes many forms, having been applied for many different purposes. In this work, I refer to the triangulation-based system of three-dimensional data capture involving Structure-from-Motion and Multi-View Stereo for the purpose of image-based modelling. In simplest terms, a series of images of an object taken at different angles are input into specialized software. This software extracts key parameters of the capture device like position and focal length, and with this information uses trigonometry to calculate distances. The software then automatically generates a point cloud (and sometimes mesh) of the object from this information.

Point cloud: A collection of points precisely defined in space according to a coordinate system. In this work, point clouds encompass the three-dimensional data about the surface of real-world objects.

Rock markings: Also called "images on stone," this is a collective term referring to several types of human expression through the medium of stone. I apply the phrase 'images on stone/rock' or 'rock markings' to refer generally to petroglyphs and pictographs, as well as 'mudglyphs' despite the technically different medium of the latter.

Whereas other authors frequently refer to 'rock art' with the same meaning, I eschew the inaccurate and reductive characterization of rock markings as 'art.' This is a term borne of Western traditions and incompatible with the worldviews of the markings' Indigenous creators. Moreover, it has been firmly rejected by many descendant communities for its trivial treatment of significant cultural sites. Unless specifically qualified (e.g., "portable/mobiliary images on stone"), this phrase is used to refer to nonportable site types.

Rock varnish: A thin surface coating that develops on rockfaces through the adhesion and conglomeration of miniscule particles deposited by wind, water, and erosion of the stone itself. Rock varnishes are variously composed; their particulates often include silicates and iron oxides, and they may capture organic materials.

Rock-borne imagery: An umbrella term under which all forms of rock marking and stone configuration are subsumed.

Scalar field: "A function of spatial coordinates giving a single, scalar value at every point," (Attenborough 2003:456). The gradients in magnitude across a scalar field are visually manifested by a color ramp. In this work, the scalar fields generated represent distance values between an original point cloud and a simulacrum.

Simulacrum: A 3D model which is measured against the Master Cloud in the colorization process. This model essentially simulates the unaltered surface of a stone by removing fine detail.

Structured-light scanning: A triangulation-based system of three-dimensional data capture wherein linear light patterns are projected onto a surface, captured with a camera or other recording device, and analyzed with specialized software to calculate distances between the surface and the scanner. The interaction of the known light patterns with the surface topography of the object makes these calculations possible.

Style: A specific or specialized way of making imagery that may correspond to specific cultural, spatial, and temporal settings. In other words, this is essentially a consistent grammar of visual expression within a community of practice which some archaeologists argue has diagnostic and chronological value.

Superposition: The relative positioning of rock markings that occupy the same space. As in the law of superposition, the placement of markings over each other can hypothetically allow relative dating. This is somewhat of a misnomer, however, as the creation of petroglyphs does not necessarily create a clear depositional sequence. In other literature, this is more appropriately called superimposition (i.e., one carving is superimposed over another).

Terrestrial Laser Scanning (TLS): A method of scanning in which a stationary, grounded device uses laser light to capture three-dimensional data about an object. Terrestrial laser scanners generally operate on the Time-of-Flight principle, though some Phase-Shift and laser triangulation systems are used. This method of scanning produces a point cloud and may include photorealistic image capture and/or georeferencing depending on the model of scanner used.

Time-of-Flight (ToF): A system of measurement in which the time taken to reach an object is used to determine distance. LiDAR systems commonly employ a ToF principle, measuring the time for laser light to be reflected off a surface and using the known speed of light to then calculate distance.

Triangle: A polygon consisting of three line segments connecting three vertices which is used in reconstructing the surface of a point cloud. A triangle is a type of polygonal facet or 'face,' which is the basic building block of a mesh.

Vertex/Vertices: The points at which the edges of a polygonal facet meet on a 3D model. The vertices of a mesh are the same as its point cloud; the term vertex simply indicates that a point is functioning as part of a relationship between two or more lines.

Weathering rind: The exterior surface of a rockface which has been directly exposed and subjected to geophysical processes that mechanically and chemically alter the stone. For example, the preferential leaching and dissolution of minerals can contribute to changes in the rock. These processes create a distinguishable 'rind' which is perceptibly different from the fresh stone beneath it. As weathering rinds are primarily created by erosional rather than depositional forces, they cannot be considered coatings like rock varnishes. A weathering rind may be covered by rock varnish.

Zoomorph: Imagery apparently representing or based upon an animal. This includes representations of insects, birds, and quadrupeds. While 'anthropomorph' is preferred for representations unequivocally derived from the human form, 'zoomorph' may be used to describe more ambiguous or abstract representations.

APPENDIX B: INSTRUCTIONS FOR THE APPLICATION OF A NOVEL METHODOLOGY

B1. Methods of Colorization

Method 1. Distance to a flat plane with Gaussian blurring and scalar field arithmetic:

5) Fit a plane to the mesh or cloud.
   a. With the Master Cloud or mesh selected, *Tools>Fit>Plane*
6) Compute distance between the plane and Master Cloud.
   a. With both the plane and point cloud selected, *Tools>Distances>Cloud/Primitive Dist*
7) Apply a Gaussian filter to the created scalar field; the default sigma value offered by CloudCompare generally works well.
   a. With the Master Cloud or mesh selected, *Edit>Scalar Fields>Gaussian Filter>(selected sigma value)*
8) Subtract the blurred scalar field from the original scalar field.
   a. *Edit>Scalar Fields>Arithmetic>(SF1 minus SF2)*
9) Rename the resulting scalar field as desired.
   a. With the Master Cloud selected and appropriate scalar field visible, *Edit>Scalar Fields>Rename*

Method 2. Distance to a subsampled and smoothed mesh:

1) Follow the steps outlined in B2; complete Formula B.
2) Select and random subsample the Master Cloud with the number of points to subsample determined by Formula B.
   - With the Master Cloud selected, *Edit>Subsample>method: random, remaining points: (value from Formula B)*
3) Select and remesh the subsampled cloud using Delaunay 2.5D (best fitting plane).
   - With subsampled cloud selected, *Edit>Mesh>Delaunay 2.5D (best fitting plane)*
4) Apply Laplacian smoothing to the subsampled mesh, 20 iterations at a smoothing factor of 0.2.
   - With subsampled mesh selected, *Edit>Mesh>Smooth (Laplacian)>20 iterations, 0.2 smoothing factor*
5) Compute distance between the subsampled mesh and Master Cloud.
   - With both the subsampled mesh and Master Cloud selected, *Tools>Distances>Cloud/Mesh Dist*
6) Rename the resulting scalar field as desired.
   - With the Master Cloud selected and appropriate scalar field visible, *Edit>Scalar Fields>Rename*

Method 3. Distance to a smoothed clone of the original mesh:

7) Follow the steps outlined in B2; complete Formula A.
8) Select and clone the original mesh.
   - With the original mesh selected, *Edit>Clone*
9) Apply Laplacian smoothing to the cloned mesh with the number of smoothing iterations determined by Formula A.
   - With cloned mesh selected, *Edit>Mesh>Smooth (Laplacian)>(input parameters)*

10) Compute distance between the cloned mesh and Master Cloud.
- With both the cloned mesh and Master Cloud selected, *Tools>Distances>Cloud/Mesh Dist*

11) Rename the resulting scalar field as desired.
- With the Master Cloud selected and appropriate scalar field visible, *Edit>Scalar Fields>Rename*

B2. Process of Surface Area and Point Density Calculation

1. [As needed] Clean mesh of erroneous points (e.g., leaves and branches, scanning errors, etc.)
2. Calculate the scan's surface area.
   a. Determine unit of measurement. It can be helpful to select the mesh and use the point picking tool to measure between two points of known real-world distance.
   b. With mesh selected, *Edit>Mesh>Measure Surface.*
   c. Use the determined unit of measurement to convert the computed surface area (given in squared units) to square meters (m^2).
3. Calculate point density.
   a. Select the point cloud and note the number of points.
   b. Divide the number of points by the surface area to arrive at points per square meter (p/m^2).
4. Apply Formula A or Formula B in creating a visualization with a smoothed clone or subsampled point cloud, respectively.

B3. Formulas for Use in Colorization Process

Where p is the number of points in the cleaned point cloud and m^2 is the surface area of the cleaned mesh in square meters,

Formula A: $(p/m^2 \div 45{,}000) \times 20 = smoothing\ iterations$
Formula B: $45{,}000 \times m^2 = points\ to\ random\ subsample$

If the product of Formula B is nearly equal to or greater than the point density (p/m^2) of the scan, forego a subsampling approach and use Formula A instead. If Formula A returns a value below twenty, the colorization may perform poorly; smooth at least ten iterations regardless of value.
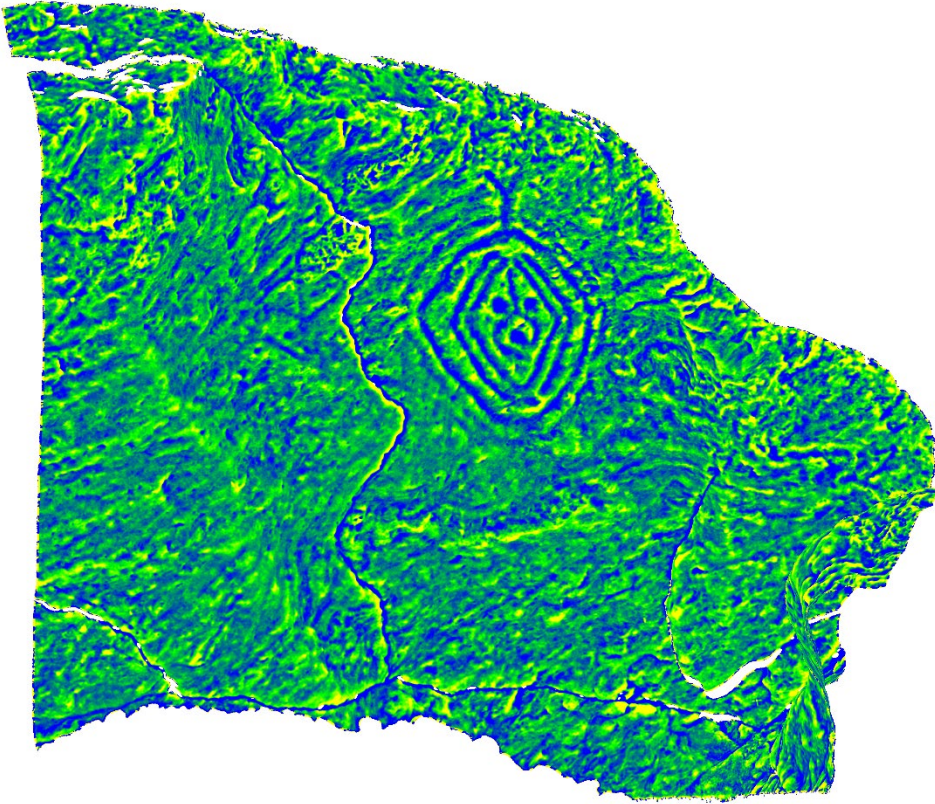
Figure C1: CHOH-26, colorization using Formula A. Simulacrum smoothed 322 iterations at 0.2 smoothing factor.
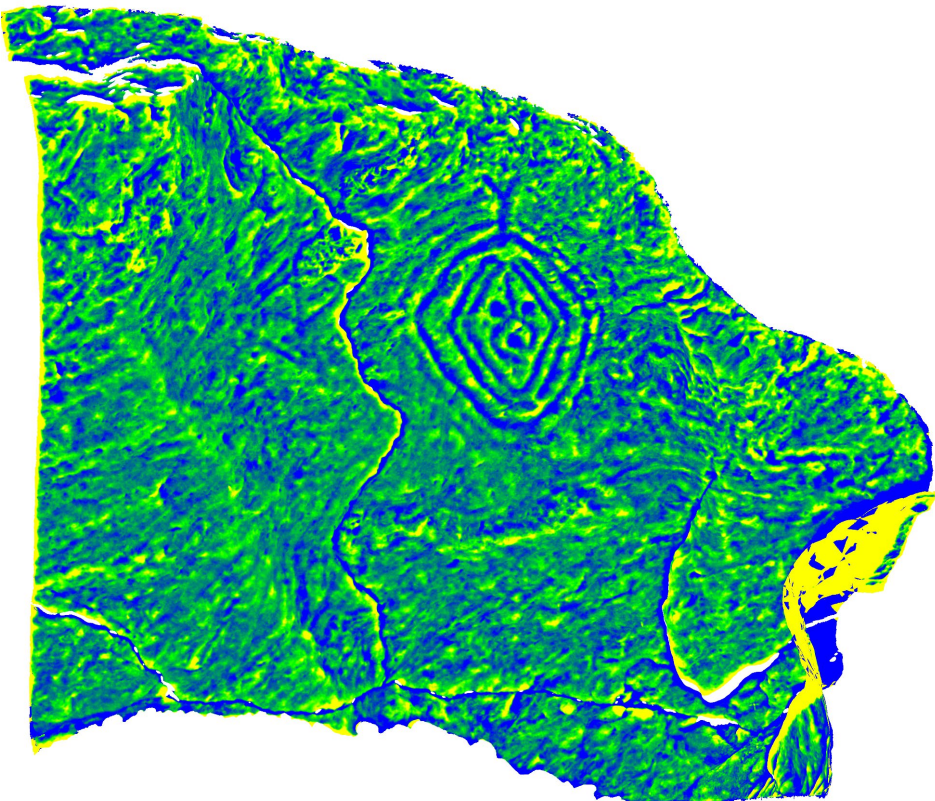
Figure C2: CHOH-26, colorization using Formula B. Simulacrum random subsampled 160,480 points, then smoothed 20 iterations at 0.2 smoothing factor.
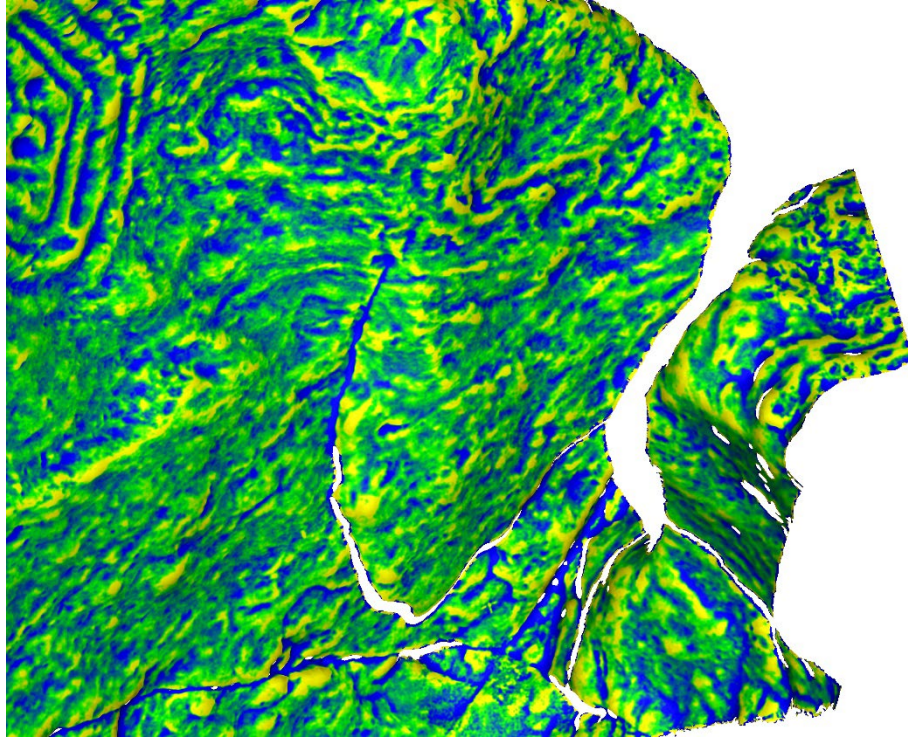
Figure C3: CHOH-26, crevice detail. Colorization using Formula A.
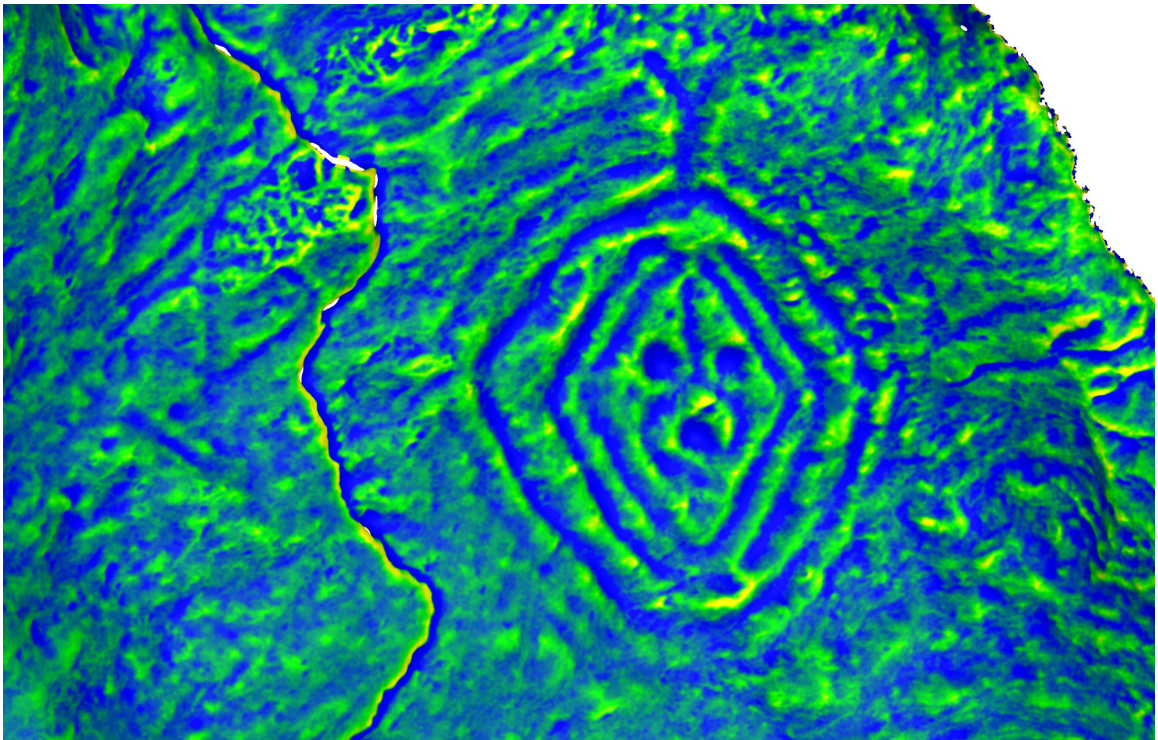
Figure C4: CHOH-26, detail view. Colorization using Formula A.
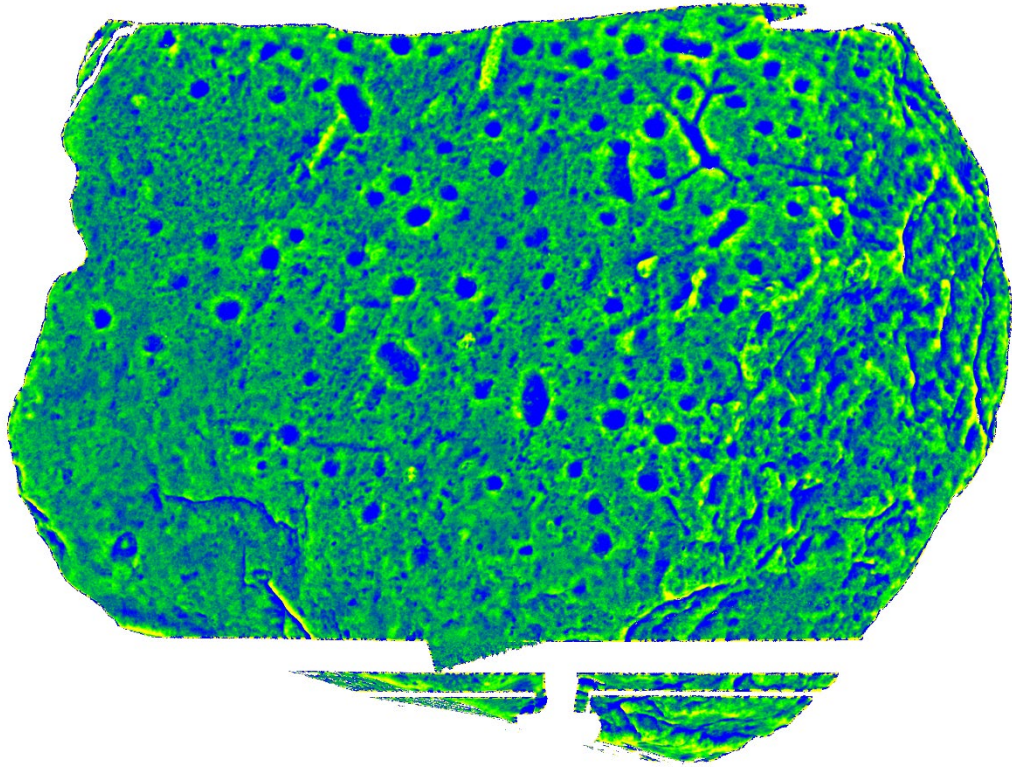
Figure C5: Pimmit Run Petroglyph, colorization using Formula A. Simulacrum smoothed 309 iterations at 0.2 smoothing factor.
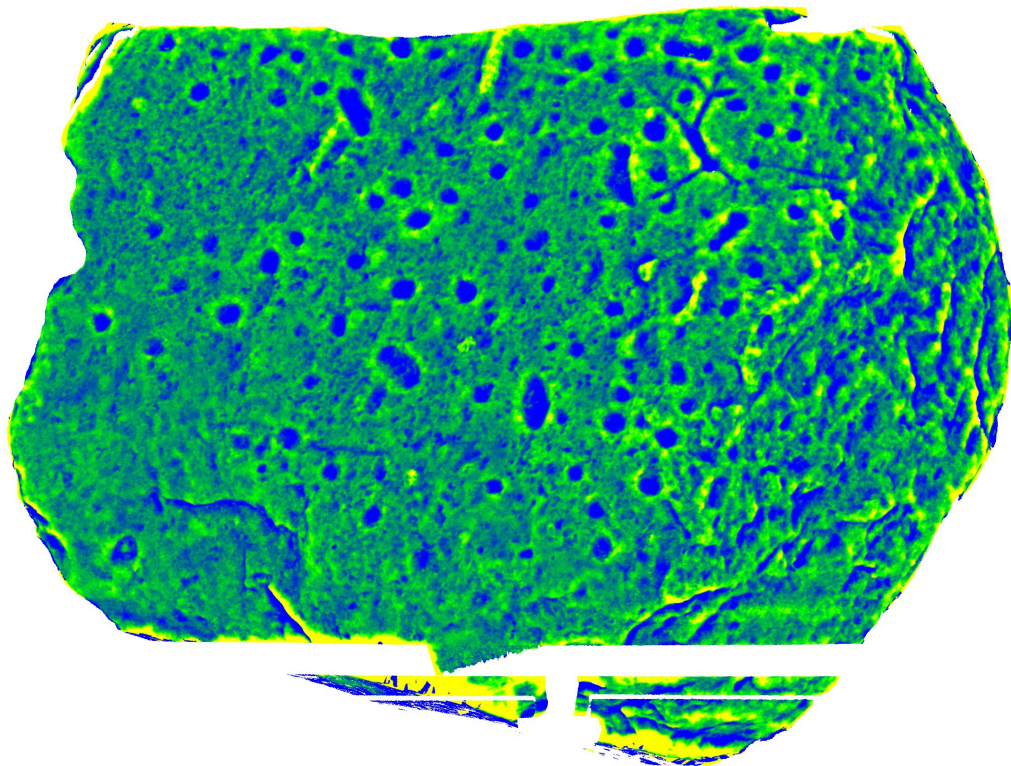
Figure C6: Pimmit Run Petroglyph, colorization using Formula B. Simulacrum random subsampled 92,899 points, then smoothed 20 iterations at 0.2 smoothing factor.

Side B

Side A
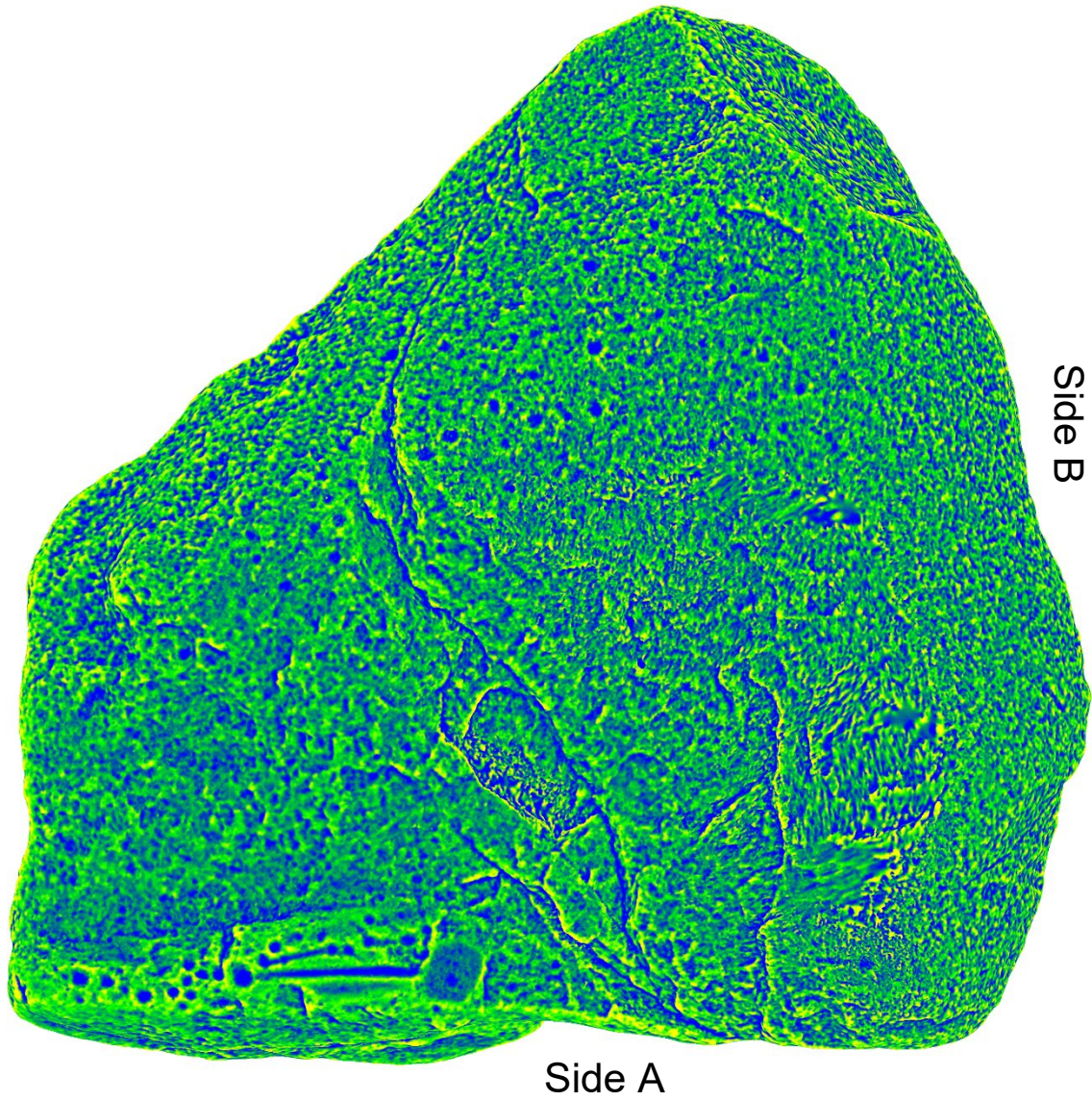
Figure C7: Octoraro Creek Petroglyphs, colorization using Formula A. Simulacrum smoothed 14 iterations at 0.2 smoothing factor. [Due to low point density (under 45,000 p/m^2), only a colorization according to Formula A was performed.]

Figure C8: Octoraro Creek Petroglyphs, Side A. Colorization using Formula A.

Figure C9: Octoraro Creek Petroglyphs, Side B. Colorization using Formula A.
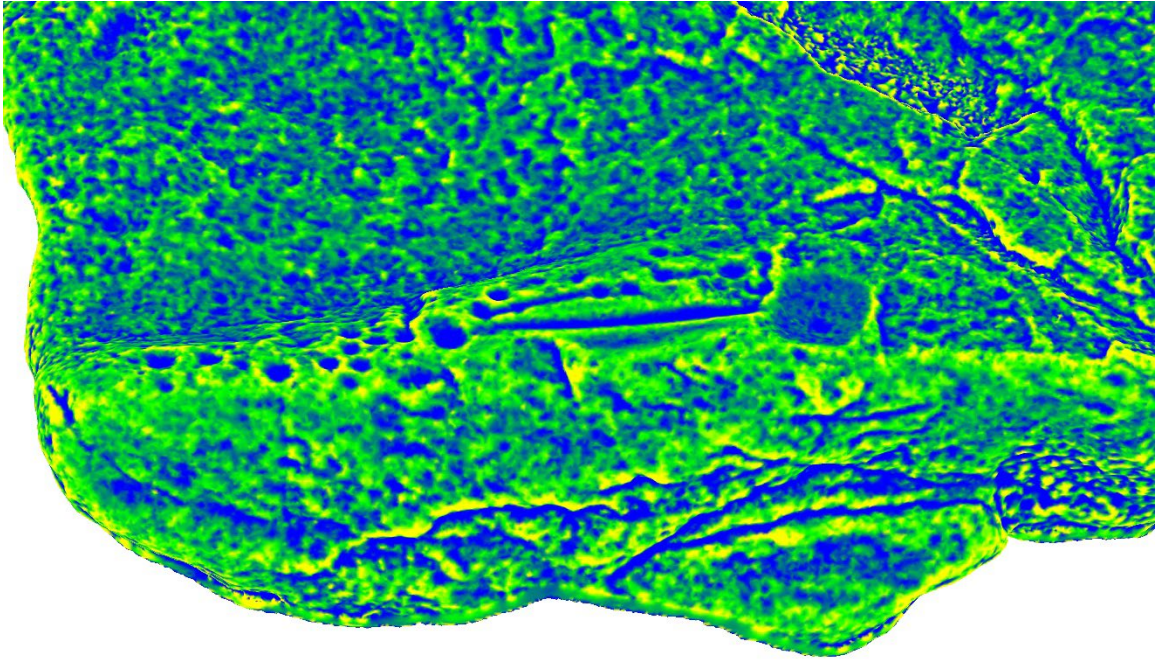
Figure C10: Octoraro Creek Petroglyphs, Side A, detail view. Colorization using Formula A.

Figure C11: Judaculla Rock, colorization using Formula A. Simulacrum smoothed 20 iterations at 0.2 smoothing factor. [Due to point density being ~45,000 p/m^2, only a colorization according to Formula A was performed.]
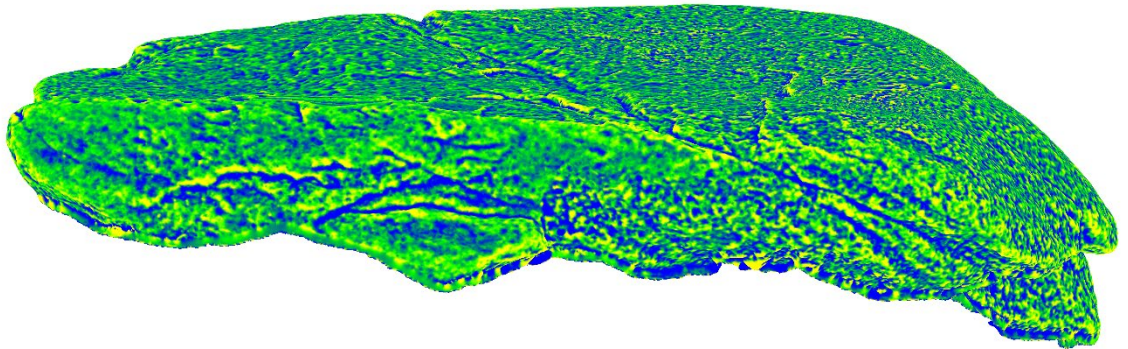
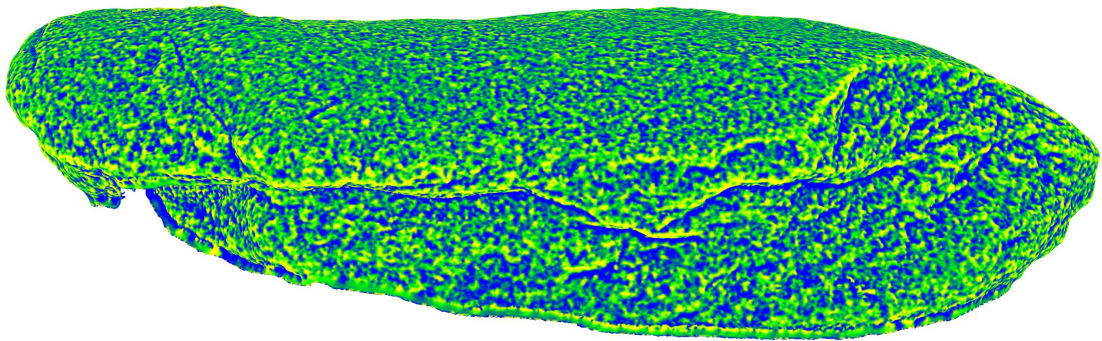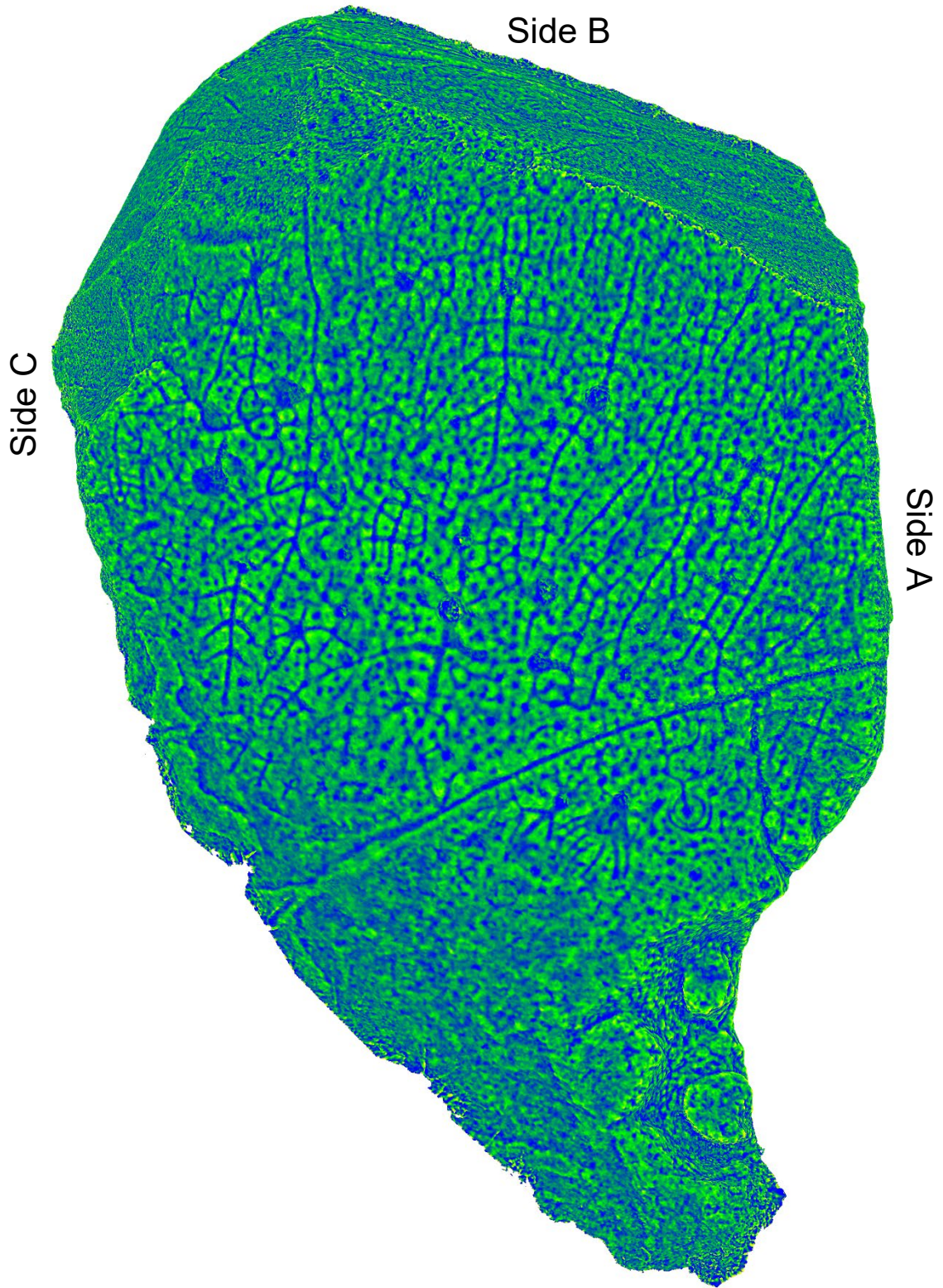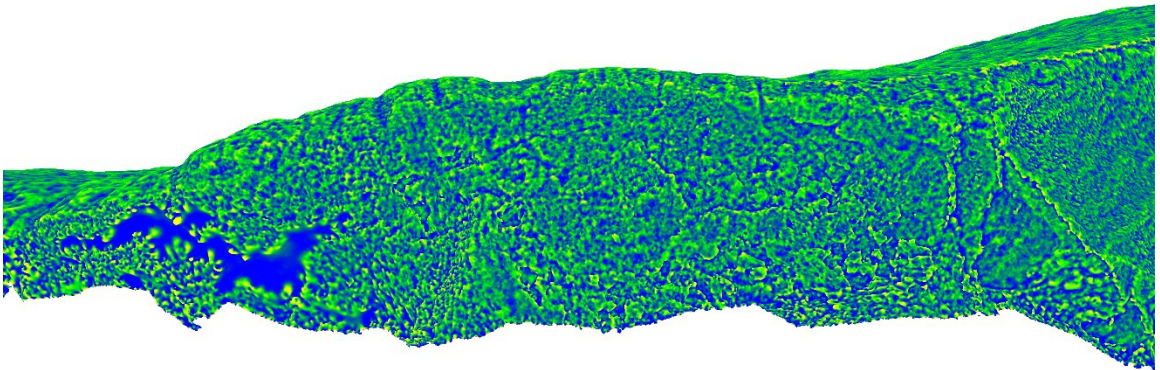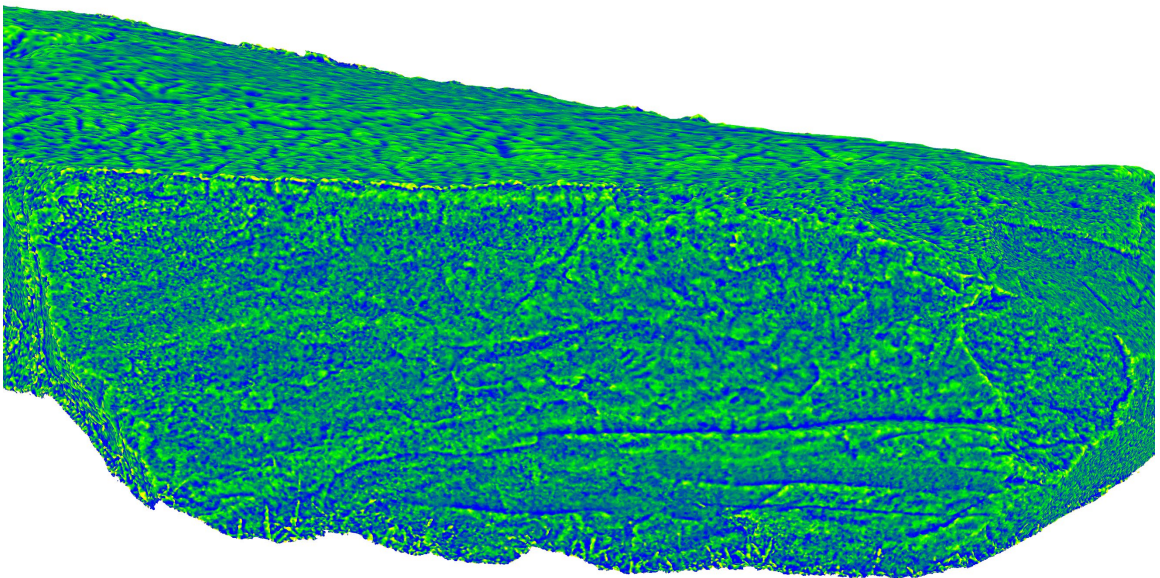*Figure C12: Judaculla Rock, Side A. Colorization using Formula A.*

Figure C13: Judaculla Rock, Side B. Colorization using Formula A.
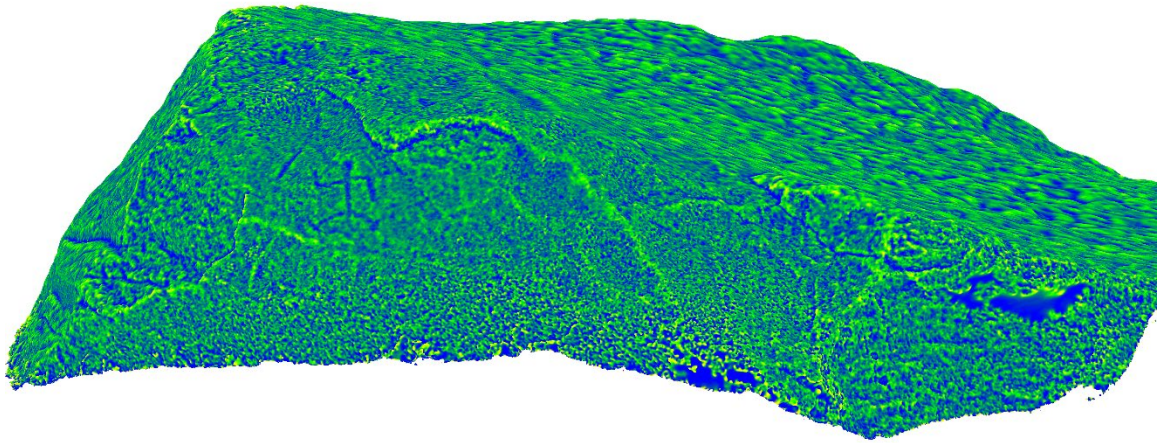
Figure C14: Judaculla Rock, Side C. Colorization using Formula A.

BIBLIOGRAPHY

Agnew, Neville, Janette Deacon, Nicholas Hall, Terry Little, Sharon Sullivan, and Paul S.C. Taçon, eds. 2015. *Rock Art: A Cultural Treasure at Risk*. Los Angeles, CA: The Getty Conservation Institute.

Andrews, Thomas D., and Jack W. Brink. 2022. "Using retroReveal as a Complement to DStretch for Enhancing Red Ochre Pictographs." *Canadian Journal of Archaeology* 46(1): 1-15.

Anonymous. 1929. "The Prehistoric Petroglyphs of the Susquehanna." *Maryland Academy of Sciences Bulletin* 8(4): 7-10.

Aspose Pty Ltd. 2023. *Aspose.3D for Python via .NET*. Application Programming Interface. Version 23.9.1, released October 5, 2023.

Associated Press. 2021. "A Cave with Ancient Drawings Has Been Sold, But Not to the Tribe That Hoped to Buy It." *National Public Radio*, September 14, 2021. https://www.npr.org/2021/09/14/1037081978.

Attenborough, Mary. 2003. *Mathematics for Electrical Engineering and Computing*. Oxford: Newnes.

Bai, Chuanping, Yangyang Liu, Pengbo Zhou, Xiaofeng Wang, and Mingquan Zhou. 2023. "BEGL: Boundary Enhancement with Gaussian Loss for Rock-Art Image Segmentation." *Heritage Science* 11, art. 17. https://doi.org/10.1186/s40494-022-00857-5.

Bain, James G. 1971. *Techniques and Procedures for Rock Art Recording*. Archaeological Society of New Mexico, Supplement Vol. 1. Albuquerque, NM.

Beaudoin, Greg, and Tabitha Eagle. 2009. *C&O Canal NHP Rock Art Survey*. Report prepared for the National Park Service.

Beverley, Robert. 1705. *The History and Present State of Virginia, In Four Parts*. Book 3, *The Native Indians, their Religion, Laws, and Customs, in War and Peace*. London: Printed for R. Parker, at the Unicorn, under the Piazza's of the Royal-Exchange.

Bock, Frank G., and Alice J. Bock. 1991. "Rock Art Recording: The Need for Thorough Research in Order to Provide Sufficient Retrieval Data." *Proceedings of the Society for California Archaeology* 3:175-193.

Brady, Liam M. 2016. "Contemporary Indigenous Relationships to Archaeological Features: Agency, Affect, and the Social Significance of Rock Art." *Heritage and Society* 9(1): 3-24. https://doi.org/10.1080/2159032X.2016.1246153.

Brink, Jack W. 2007. "Rock Art Conservation Research at Writing-On-Stone Provincial Park, Alberta." *Revista de Arqueología Americana*, no. 25, 55-99. https://www.jstor.org/stable/27768516.

Brooks, Dennis. 2017. "18CE398 Rock Engraving - Octoraro River, MD USA." *Sketchfab*. 3D Model. Published online October 27, 2017. https://sketchfab.com/3d-models/18ce398-rock-engraving-octoraro-river-md-usa-77ad94443a8d4daeba0d3c9faa28accc.

Charles, Tessa K., Alejandro Castilla, and Ryan M. Bodenstein. 2022. "Need for Portable Accelerators in Cultural Heritage." *Proceedings of the 13th International Particle Accelerator Conference (IPAC2022), June 12-17, 2022, Bangkok, Thailand*, 808-810. Geneva, Switzerland: JACoW Publishing. https://doi.org/10.18429/JACoW-IPAC2022-TUOZGD1.

Clewlow, C. William, Jr., and Mary Ellen Wheeling. 1978. *Rock Art: An Introductory Recording Manual for California and the Great Basin*. Los Angeles, CA: University of California, Los Angeles Institute of Archaeology.

Clogg, Phil, Margarita Díaz-Andreu, and Brian Larkman. 2000. "Digital Image Processing and the Recording of Rock Art." *Journal of Archaeological Science* 27(9): 837-843. https://doi.org/10.1006/jasc.1999.0522.

Collins, Lori D., Travis Doering, and Jorge Gonzalez. 2019. "The Use and Potential Misuse of 3D and Spatial Heritage Data in Our Nation's Parks." *Digital Heritage and Humanities Collections Faculty and Staff Publications* 21. https://digitalcommons.usf.edu/dhhc_facpub/21.

Colwell-Chanthaphonh, Chip, T.J. Ferguson, Dorothy Lippert, Randall H. McGuire, George P. Nicholas, Joe E. Watkins, and Larry J. Zimmerman. 2010. "The Premise and Promise of Indigenous Archaeology." *American Antiquity* 75(2): 228-238. https://doi.org/10.7183/0002-7316.75.2.228.

Cooper, Eben. 2000. "Technological Advances in Rock Art Recording." *Eastern States Rock Art Research Association (ESRARA) Newsletter* 5(4): 15.

Darvill, Timothy, Julie Eklund, Andrew Fulton, Hannelle Hentula, Cornelia Kleinitz, Blaze V. O'Connor, Clifford Price, Nicholas Stanley-Price, and Peter Ucko. 2000. *Rock Art Pilot Project: Main Report; A Report on the Results of a Pilot Project to Investigate the Current State of Research, Conservation, Management and Presentation of Prehistoric Rock Art in England Commissioned by English Heritage from Archaeology Group, School of Conservation Sciences, Bournemouth University and the Institute of Archaeology, University College London*. Second edition [final report]. Bournemouth and London: Bournemouth University School of Conservation Sciences and University College of London Institute of Archaeology. https://eprints.bournemouth.ac.uk/9602/1/Rock_Art.pdf.

David, Bruno, and Meredith Wilson, eds. 2002. *Inscribed Landscapes: Marking and Making Place*. Honolulu, HI: University of Hawai'i Press.

David, Bruno, John M. Brayer, Ian J. McNiven, and Alan Watchman. 2001. "Why Digital Enhancement of Rock Paintings Works: Rescaling and Saturating Colours." *Antiquity* 75(290): 781-792. https://doi.org/10.1017/S0003598X00089286.

Davidson, Iain, and April Nowell, eds. 2021. *Making Scenes: Global Perspectives on Scenes in Rock Art*. New York, NY: Berghahn Books.

DeGayner, Jake, and Jeremy M. Moss. 2022. Personal communication to author via email, received November 3-4, 2022.

DeGayner, Jake, Iraida Rodriguez, and Jeremy M. Moss. 2019. "Pecos Petroglyphs: Documentation as Preservation." *Archaeology Southwest Magazine* 33(3): 40-41.

Delabarre, Edmund Burke. 1917. "Early Interest in Dighton Rock." In *Publications of the Colonial Society of Massachusetts, Volume 18: Transactions, 1915-1916*, edited by Albert Matthews, 235-300. Cambridge, MA: University Press.

Delabarre, Edmund Burke. 1919. *Recent History of Dighton Rock*. Cambridge, MA: University Press. Reprinted from the Publications of the Colonial Society of Massachusetts, Vol. 20.

Delabarre, Edmund Burke. 1928. *Dighton Rock: A Study of the Written Rocks of New England*. New York, NY: Walter Neale.

Diaz-Granados, Carol, and James R. Duncan, eds. 2004. *The Rock-Art of Eastern North America: Capturing Images and Insight*. Tuscaloosa, AL: University of Alabama Press.

Diaz-Granados, Carol, Jan F. Simek, George Sabo III, and Mark J. Wagner, eds. 2018. *Transforming the Landscape: Rock Art and the Mississippian Cosmos*. Oxford, UK: Oxbow Books.

Doering, Travis, and Lori Collins. 2012. *Terrestrial Laser Scanning, 3D and Reflective Imagery Documentation of a Newly Discovered Group of Prehistoric Native American Petroglyphs: Interim Report Revised 3/30/12*. Report prepared for the

National Park Service, National Capital Region, on behalf of the Alliance for Integrated Spatial Technologies, University of South Florida, under cooperative agreement through the Piedmont-South Atlantic Coast Cooperative Systems Studies Unit.

Doering, Travis, and Lori Collins. 2013. *Terrestrial Laser Scanning, 3D and Reflective Imagery Documentation of a Newly Discovered Group of Prehistoric Native American Petroglyphs: Phases I and II*. Report prepared for the National Park Service, National Capital Region, on behalf of the Alliance for Integrated Spatial Technologies, University of South Florida, under cooperative agreement through the Piedmont-South Atlantic Coast Cooperative Systems Studies Unit.

Dring, Katherine Sebastian, Stephen W. Silliman, Natasha Gambrell, Shianne Sebastian, and Ralph Sebastian Sidberry. 2019. "Authoring and Authority in Eastern Pequot Community Heritage and Archaeology." *Archaeologies: Journal of the World Archaeological Congress* 15(3): 352-370.

Dubelaar, Cees N. 1991. "Petroglyphs in the U.S. Virgin Islands: A Survey." In *Proceedings of the Thirteenth International Congress for Caribbean Archaeology*, edited by E.N. Ayubi and J.B. Haviser, 944-973. Curacao, Netherlands Antilles: Archaeological Institute of the Netherlands Antilles. Reports of the Archaeological Institute of the Netherlands Antilles No. 9, Part 2.

Fenenga, Franklin. 1949. *Methods of Recording and Present Status of Knowledge Concerning Petroglyphs in California*. Berkeley, CA: University of California, Berkeley, Department of Anthropology. Reports of the California Archaeological Survey, No. 3.

Fredlund, Glen, and Linea Sundstrom. 2007. "Digital Infra-Red Photography for Recording Painted Rock Art." *Antiquity* 81(313): 733-742. https://doi.org/10.1017/S0003598X00095697.

Galbreath, Charles B., ed. 1921. *Expedition of Celoron to the Ohio Country in 1749*. Columbus, OH: The F.J. Heer Printing Co.

Gil-Docampo, Mariluz, Simón Peña-Villasenín, and Juan Ortiz-Sanz. 2020. "An Accessible, Agile and Low-Cost Workflow for 3D Virtual Analysis and Automatic Vector Tracing of Engravings: Atlantic Rock Art Analysis." *Archaeological Prospection* 27(2): 153-168. https://doi.org/10.1002/arp.1760.

Gillette, Donna L., Mavis Greer, Michele Helene Hayward, and William Breen Murray, eds. 2014. *Rock Art and Sacred Landscapes*. New York, NY: Springer.

Green, Ashely, Christian Horn, Oscar Ivarsson, Cecilia Lindhé, Rich Potter, and Johan Ling. 2019. *Topography Visualisation Toolbox*. Computer software, ver. 2.1. Program created by the Department of Historical Studies and Centre for Digital Humanities, University of Gothenburg, for infrastructure project *Rock Carvings in Three Dimensions: Documentation, Research and Dissemination (IN18-0557:1)*, funded by Riksbankens Jubileumsfond. Last accessed online October 31, 2023. https://tvt.dh.gu.se/.

Hale, John Patrick. 2010. *Rock Art in the Public Trust: Managing Prehistoric Rock Art on Federal Land*. PhD dissertation. University of California, Riverside.

Hale, Richard W., Jr. 1971. "Dighton Rock." National Register of Historic Places Inventory Nomination Form. Form prepared March 30, 1971.

Hanna, Charles A. 1911. *The Wilderness Trail; or, the Ventures and Adventures of the Pennsylvania Traders on the Allegheny Path, with Some New Annals of the Old West, and the Records of Some Strong Men and some Bad Ones*. Vol. 2. New York, NY: G.P. Putnam's Sons.

Hanson, Kelsey E., Steven Baumann, Theresa Pasqual, Octavius Seowtewa, and T.J. Ferguson. 2022. "'This Place Belongs to Us': Historic Contexts as a Mechanism

for Multivocality in the National Register." *American Antiquity* 87(3): 439-456. https://www.doi.org/10.1017/aaq.2022.15.

Harman, Jon. 2005. *Using Decorrelation Stretch to Enhance Rock Art Images*. Paper presented at the 32nd Annual Meeting of the American Rock Art Research Association, Sparks, Nevada, May 28. Revised 2006. https://www.dstretch.com/AlgorithmDescription.pdf.

Horn, Christian, Derek Pitman, and Rich Potter. 2019. "An Evaluation of the Visualisation and Interpretive Potential of Applying GIS Data Processing Techniques to 3D Rock Art Data." *Journal of Archaeological Science: Reports* 27, art. 101971. https://doi.org/10.1016/j.jasrep.2019.101971.

Horn, Christian, Oscar Ivarsson, Cecilia Lindhé, Rich Potter, Ashely Green, and Johan Ling. 2022. "Artificial Intelligence, 3D Documentation, and Rock Art: Approaching and Reflecting on the Automation of Identification and Classification of Rock Art Images." *Journal of Archaeological Method and Theory* 29(1): 188-213. https://doi.org/10.1007/s10816-021-09518-6.

Hunter, Douglas. 2017. *The Place of Stone: Dighton Rock and the Erasure of America's Indigenous Past*. Chapel Hill, NC: University of North Carolina Press.

Jalandoni, Andrea, and Maria Kottermair. 2018. "Rock Art as Microtopography." *Geoarchaeology* 33(5): 579-593. https://doi.org/10.1002/gea.21677.

Jalandoni, Andrea, and Paul S.C. Taçon. 2018. "A New Recording and Interpretation of the Rock Art of Angono, Rizal, Philippines." *Rock Art Research* 35(1): 47-61.

Joutel, Henri. 1714. *A Journal of the Last Voyage Perform'd by Monsr. de La Sale, to the Gulph of Mexico, to Find Out the Mouth of the Mississippi River*. Translated anonymously. London: A. Bell, B. Lintott, and F. Baker. Originally published in 1713 as *Journal Historique du Dernier Voyage que Feu M. de la Sale Fit dans le Golfe de Mexique, Pour Trouver L'Embouchure & le Cours de la Riviere de Missicipi, Nommée à Present la Riviere de Saint Loüis, Qui Traverse la Louisiane*, edited by Monsier de Michel. Paris: Estienne Robinot.

Kazhdan, Michael M., Matthew Bolitho, and Hugues Hoppe. 2006. "Poisson Surface Reconstruction." In *Proceedings of the Fourth Eurographics Symposium on Geometry Processing, Cagliari, Sardinia, Italy, June 26-28, 2006*, edited by Konrad Polthier and Alla Sheffer, 61-70. Aire-la-Ville, Switzerland: Eurographics Association.

Kimball, Justin J.L. 2016. *3D Delineation: A Modernisation of Drawing Methodology for Field Archaeology*. Oxford, UK: Archaeopress Publishing Ltd.

Kirk, Deborah Lyn. 2013. *Visualizing the Cherokee Homeland through Indigenous Historical GIS: An Interactive Map of James Mooney's Ethnographic Fieldwork and Cherokee Collective Memory*. Master's thesis. University of Kansas.

Landon, George V., and W. Brent Seales. 2006. "Petroglyph Digitization: Enabling Cultural Heritage Scholarship." *Machine Vision and Applications* 17(6): 361-371. https://doi.org/10.1007/s00138-006-0044-0.

Lee, Georgia, and William D. Hyder. 2009. "Correcting the Rock Art Record." *Journal of California and Great Basin Anthropology* 29(2): 195-200.

Lenik, Edward J. 2002. *Picture Rocks: American Indian Rock Art in the Northeast Woodlands*. Hanover, NJ: University Press of New England.

Loendorf, Lawrence L., Linda A. Olson, and Stuart Conner. 1988. *A Recording Manual for Rock Art*. Report prepared for the National Park Service, Rocky Mountain Regional Office, Denver, Colorado.

Loendorf, Lawrence L., Linda A. Olson, Stuart Conner, and J. Claire Dean. 1998. *A Manual for Rock Art Documentation*. Minot, ND: Minot State University.

Loubser, Johannes H. N., and Joel Logan [joellogan]. 2017. "Judaculla Rock July 2017 –
 Terrestrial Model." *Sketchfab*. 3D Model. Published online July 25, 2017.
 https://sketchfab.com/3d-models/judaculla-rock-july-2017-terrestrial-model-
 2530b6766d2f46df8a4452a320adfa3c.

Loubser, Johannes H. N., Anthony Scott Ashcraft, and James Wettstaed. 2018. "Betwixt
 and Between: The Occurrence of Petroglyphs between Townhouses of the Living
 and Townhouses of Spirit Beings in Northern Georgia and Western North
 Carolina." In *Transforming the Landscape: Rock Art and the Mississippian
 Cosmos,* edited by Carol Diaz-Granados, Jan F. Simek, George Sabo III, and
 Mark J. Wagner, 200-244. Oxford, UK: Oxbow Books.

Mallery, Garrick. 1893. "Picture-Writing of the American Indians." In *Tenth Annual Report
 of the Bureau of Ethnology to the Secretary of the Smithsonian Institution: 1888-
 '89*, edited by J.W. Powell, 3-807. Washington, D.C.: Government Printing Office.

Mark, Robert. 2017. "Creating a Digital Rubbing from a 3D Model of Petroglyphs." *Rock
 Art Research* 34(2): 215-217.

Mark, Robert [rmark]. 2022. "Virgin Islands National Park Petroglyphs." *Sketchfab*. 3D
 Model. Published online April 28, 2022. https://sketchfab.com/3d-models/virgin-
 islands-national-park-petroglyphs-24b57b8ccaef41e5a0a38f69bc7afcf5.

Mark, Robert, and Evelyn Billo. 2021. "Use of Radiance Scaling to Enhance Visibility of
 Petroglyphs." In *American Indian Rock Art, Vol. 47*, edited by David A. Kaiser,
 Mavis Greer, and James D. Keyser, 221-226. Chula Vista, CA: Sunbelt
 Publications for American Rock Art Research Association.

McDonald, Jo, and Peter Veth, eds. 2012. *A Companion to Rock Art*. Chichester, UK:
 Blackwell Publishing.

McDonald, Jo, Andrea Catacora, Sarah de Koning, and Emily Middleton. 2016. "Digital
 Technologies and Quantitative Approaches to Recording Rock Art in the Great
 Basin." *Journal of Archaeological Science: Reports* 10:917-930.
 https://doi.org/10.1016/j.jasrep.2016.03.052.

Moore, Erwin W. 1894. "Sketchbook." Drawings of petroglyphs, 5 pgs. Charcoal and ink
 on paper. *Maine Historical Society Collections*, Object # GA175.2.
 https://mainehistory.catalogaccess.com/objects/2116.

Moro Abadía, Oscar, and Martin Porr, eds. 2021. *Ontologies of Rock Art: Images,
 Relational Approaches, and Indigenous Knowledges*. New York, NY: Routledge.

Morse, Jedidiah. 1802. *The American Universal Geography; or, A View of the Present
 State of All the Empires, Kingdoms, States, and Republics in the Known World,
 and of the United States in Particular*. 4th edition. Vol. 1. Boston, MA: Isaiah
 Thomas and Ebenezer T. Andrews.

Nash, George, and Aron Mazel, eds. 2019. *Narratives and Journeys in Rock Art: A
 Reader*. Oxford, UK: Archaeopress Publishing.

New England Antiquities Research Association [NEARA]. 2023. "Petroglyphs in Maine."
 Sketchfab. 3D Model. Published online April 4, 2023. https://sketchfab.com/3d-
 models/petroglyphs-in-maine-c3b4bf79ff5941fcab11d75a1b10a6d5.

Nicholas, George P. 2014. "Reconciling Inequalities in Archaeological Practice and
 Heritage Research." In *Transforming Archaeology: Activist Practices and
 Prospects*, edited by Sonya Atalay, Lee Rains Clauss, Randall McGuire, and
 John Welch, 133-158. Walnut Creek, CA: Left Coast Press.

Pereira Uzal, José Manuel. 2015. *Técnicas de Análise Multiespectral on Arte Rupestre
 Levantino*. Bachelor's dissertation. Escola Superior de Conservación e
 Restauración de Bens Culturais de Galicia, Pontevedra, Spain.

Research Labs of Archaeology [RLA Archaeology]. 2017. "Judaculla Rock." *Sketchfab*. 3D Model. Published online December 16, 2017. https://sketchfab.com/3d-models/judaculla-rock-04a8f3c8f00549c4a0f2b5fbb107c9b0.

Riveiro, Belén, Julia Armesto, Fernando Carrera, Pedro Arias, Mercedes Solla, and Susana Lagüela. 2011. "New Approaches for 3D Documentation of Petroglyphs in the Norwest of the Iberian Peninsula." *Proceedings of the International Scientific Committee for Documentation of Cultural Heritage (CIPA 2011) Symposium 23, September 12-16, 2011, Prague, Czech Republic*. Valencia, Spain: CIPA Heritage Documentation.

Robinson, David, Colin Rosemont, Devlin Gandy, and Brendan Cassidy. "When the Virtual Becomes Actual: Indigenous Ontologies within Immersive Reality Environments." In *Ontologies of Rock Art: Images, Relational Approaches, and Indigenous Knowledges*, edited by Oscar Moro Abadía and Martin Porr, 412-430. New York, NY: Routledge.

Rowan, Yorke M., and Austin Chad Hill. 2014. "Pecking at Basalt: Photogrammetric Documentation of Petroglyphs in the Black Desert, Jordan." In *Settlement, Survey, and Stone: Essays on Near Eastern Prehistory in Honour of Gary Rollefson*, edited by Bill Finlayson and Cheryl Makarewicz, 209-217. Berlin, Germany: Ex Oriente e.V.

Sanger, Kay Kenady, and Clement W. Meighan. 1990. *Discovering Prehistoric Rock Art: A Recording Manual*. Calabasas, CA: Wormwood Press.

Schiffer, Michael B. 1985. "Is There a 'Pompeii Premise' in Archaeology?" *Journal of Anthropological Research* 41(1): 18-41. http://www.jstor.org/stable/3630269.

Scofield, John, and Charles Allmon. 1956. "Virgin Islands: Tropical Playland, U.S.A." *National Geographic Magazine* 109(2): 201-232.

Seidl, Markus. 2016. *Computational Analysis of Petroglyphs*. PhD dissertation. Technische Universität Wien, Vienna, Austria.

Simek, Jan F., Joseph C. Douglas, Sarah C. Sherwood, and Alan Cressler. 2019. "Prehistoric Rock Art Research in Tennessee 2008." *Tennessee Archaeology* 10(1): 58-76. Revised and published from a paper presented at the conference for Current Research in Tennessee Archaeology (CRITA), Nashville, Tennessee, 2009.

Simek, Jan F., Stephen Alvarez, and Alan Cressler. 2022. "Discovering Ancient Cave Art Using 3D Photogrammetry: Pre-Contact Native American Mudglyphs from 19th Unnamed Cave, Alabama." *Antiquity* 96(387): 662-678. https://doi.org/10.15184/aqy.2022.24.

Simpson, Alice, Phil Clogg, Margarita Díaz-Andreu, and Brian Larkman. 2004. "Towards Three-Dimensional Non-Invasive Recording of Incised Rock Art." *Antiquity* 78(301): 692-698. https://doi.org/10.1017/S0003598X00113328.

Smith, Harlan I. 1926. "Cement Casts of Petroglyphs." *Science* 64(1669): 626.

Spake, Laure, George P. Nicholas, and Hugo F.V. Cardoso. 2020. "The Digital Lives of Ancestors: Ethical and Intellectual Property Considerations Surrounding the 3-D Recording of Human Remains." In *Working with and for Ancestors: Collaboration in the Care and Study of Ancestral Remains*, edited by Chelsea H. Meloche, Laure Spake, Katherine L. Nichols, 205-218. New York, NY: Routledge.

Steberglokken, Heidrun, Ragnhild Berge, Eva Lindgaard, and Helle Vangen Studeal, eds. 2015. *Ritual Landscapes and Borders within Rock Art Research: Papers in Honour of Professor Kalle Sognnes*. Oxford, UK: Archaeopress Publishing.

Steward, Julian H. 1937. "Petroglyphs of the United States." In *Annual Report of the Board of Regents of the Smithsonian Institution: Showing the Operations,*

Expenditures, and Condition of the Institution for the Year Ended June 30, 1936, 405-425. Washington, D.C.: Government Printing Office. Publication No. 3405.

Swartz, Benjamin K., Jr., comp. 1980. "Minimum Recording Standards Proposed by the American Committee to Advance the Study of Petroglyphs and Pictographs." *La Pintura* 7(2): 11-12.

Swartz, Benjamin K., Jr. 1981. "Standards for the Recording of Petroglyphs and Pictographs." *Current Anthropology* 22(1): 94-95.

Trinks, Immo, Margarita Díaz-Andrieu, Richard W. Hobbs, and Kate E. Sharpe. 2005. "Digital Rock Art Recording: Visualising Petroglyphs Using 3D Laser Scanner Data." *Rock Art Research* 22(2): 131-139.

Tufte, Edward R. 1990. *Envisioning Information*. Cheshire, CT: Graphic Press.

Urcia, Alberto, John C. Darnell, Colleen M. Darnell, and Sara E. Zaia. 2018. "From Plastic Sheets to Tablet PCs: A Digital Epigraphic Method for Recording Egyptian Rock Art and Inscriptions." *African Archaeological Review* 35(2): 169-189. https://doi.org/10.1007/s10437-018-9297-z.

Valdez-Tullett, Joana, and Sofia Figueiredo Persson. 2023. "Digital Rock Art: Beyond 'Pretty Pictures.'" *F1000Research* 12, art. 523. https://doi.org/10.12688/f1000research.127249.1.

Vilas-Estevez, Benito, Alia Vázquez-Martínez, and Miguel Carrero-Pazos. 2016. "Going Further: (Re)Discovering Rock Art Carvings with Photogrammetric Techniques in Galicia (North-West Iberian Peninsula)." In *Handbook of Research on Emerging Technologies for Digital Preservation and Information Modeling*, edited by Alfonso Ippolito and Michela Cigola, 175-200. Hershey, PA: IGI Global. https://doi.org/10.4018/978-1-5225-0680-5.ch008.

Wang, Shaohua, Yue Wang, Qingwu Hu, Jiayuan Li, and Mingyao Ai. 2019. "Unmanned Aerial Vehicle and Structure-from-Motion Photogrammetry for Three-Dimensional Documentation and Digital Rubbing of the Zuo River Valley Rock Paintings." *Archaeological Prospection* 26(3): 265-279. https://doi.org/10.1002/arp.1739.

Whitley, David S. 2013. *Department of Defense-Wide Inventory of Rock Art Sites and Assessment of Management Practices*. Report prepared for the Department of Defense Legacy Resource Management Program.

Wilkes, Stephen. 2015. "Dighton Rock." 3D Model. Created for Feldman Geospatial, published online by New England Antiquities Research Association. Last accessed online October 31, 2023. https://neara.org/chapters/Massachusetts/DightonRock.html.

Wojcicki, Piotr, Sylwester Korga, and Marek Milosz. 2022. "Preliminary Application of the Algorithm Highlighting Petroglyph Patterns." *Applied Science* 12(3), art. 1660. https://doi.org/10.3390/app12031660.

Zachar, Ján. 2017. "2D and 3D Visual Products: First Steps Towards Virtual Reconstruction." In *Virtual Reconstructions and Computer Visualisations in Archaeological Practice*, edited by Predrag Novaković, Nenad Tasić, and Milan Hornák, 87-95. Ljubljana, Slovenia: University of Ljubljana Press. https://doi.org/10.4312/9789612378998.

Zainuddin, K., Z. Majid, M. F. M. Ariff, K. M. Idris, M.A. Abbas, and N. Darwin. 2019. "3D Modeling for Rock Art Documentation using Lightweight Multispectral Camera." In *Int. Arch. Photogramm. Remote Sens. Spatial Inf. Sci., Volume XLII-2/W9*, edited by A. Cardaci, F. Fassi, and F. Remondino, 787-793. https://doi.org/10.5194/isprs-archives-XLII-2-W9-787-2019.

Zeppelzauer, Matthias, and Markus Seidl. 2015. "Efficient Image-Space Extraction and Representation of 3D Surface Topography." In *Proceedings of the 2015 IEEE*

International Conference on Image Processing (ICIP 2015), 2845-2849. Piscataway, NJ: Institute of Electrical and Electronics Engineers.